การออพติไมซ์พลังงานของกระบวนการไฮโดรทรีตติ้งสำหรับการผลิตกรีนดีเซลจากน้ำมันปาล์ม

นางสาวสุวิสา แซ่อึ่ง

วิทยานิพนธ์นี้เป็นส่วนหนึ่งของการศึกษาตามหลักสูตรปริญญาวิศวกรรมศาสตรมหาบัณฑิต
สาขาวิชาวิศวกรรมเคมี ภาควิชาวิศวกรรมเคมี
คณะวิศวกรรมศาสตร์ จุฬาลงกรณ์มหาวิทยาลัย
ปีการศึกษา 2557

ENERGY OPTIMIZATION OF A HYDROTREATING PROCESS FOR GREEN DIESEL PRODUCTION FROM PALM OIL

Miss Suwisa Sae-ueng

A Thesis Submitted in Partial Fulfillment of the Requirements
for the Degree of Master of Engineering Program in Chemical Engineering
Department of Chemical Engineering
Faculty of Engineering
Chulalongkorn University
Academic Year 2014

Thesis Title	ENERGY OPTIMIZATION OF A HYDROTREATING PROCESS FOR GREEN DIESEL PRODUCTION FROM PALM OIL
By	Miss Suwisa Sae-ueng
Field of Study	Chemical Engineering
Thesis Advisor	Professor Dr. Paisan Kittisupakorn

Accepted by the Faculty of Engineering, Chulalongkorn University in Partial Fulfillment of the Requirements for the Master's Degree

.....Dean of the Faculty of Engineering
(Professor Dr. Bundhit Eua-arporn)

THESIS COMMITTEE

.....Chairman
(Assistant Professor Dr. Kasidit Nootong)
.....Thesis Advisor
(Professor Dr. Paisan Kittisupakorn)
.....Examiner
(Dr. Pimporn Ponpesh)
.....External Examiner
(Dr. Wachira Daosud)

สุวิสา แซ่อึ่ง : การออพติไมซ์พลังงานของกระบวนการไฮโดรทรีตติ้งสำหรับการผลิตกรีนดีเซลจากน้ำมันปาล์ม (ENERGY OPTIMIZATION OF A HYDROTREATING PROCESS FOR GREEN DIESEL PRODUCTION FROM PALM OIL) อ.ที่ปรึกษาวิทยานิพนธ์หลัก: ศ. ดร. ไพศาล กิตติศุภกร, 132 หน้า.

งานวิจัยนี้ได้ศึกษาการผลิตกรีนดีเซลจากน้ำมันปาล์มด้วยกระบวนการไฮโดรทรีตติ้งและการออพติไมซ์พลังงานในกระบวนการ โดยการจำลองกระบวนการด้วยโปรแกรมแอสเพน พลัส ในส่วนแรกจะศึกษากระบวนการผลิตกรีนดีเซลจากน้ำมันปาล์มโดยใช้ตัวเร่งปฏิกิริยานิเกิลโมลิบดินัมซัลไฟด์ที่มีแกมมาอะลูมินาเป็นตัวรองรับ จากการจำลองกระบวนการที่เสนอขึ้นนี้พบว่า ค่าผลได้ของกรีนดีเซล ความบริสุทธ์ของกรีนดีเซล การกระจายตัวของผลิตภัณฑ์ที่เป็นของเหลว และอัตราการเกิดปฏิกิริยาไฮโดรดีออกซิจีเนชัน ปฏิกิริยาดีคาร์บอนิลเลชัน และปฏิกิริยาดีคาร์บอกซิลเลชัน มีแนวโน้มเป็นไปตามผลการทดลอง โดยมีความคลาดเคลื่อนจากผลการทดลองไม่เกิน 2% นอกจากนี้ยังมีการศึกษาการใช้พลังงานอย่างเหมาะสมของกระบวนการผลิตกรีนดีเซล การลดพลังงานในกระบวนการผลิตกรีนดีเซลนั้นสามารถทำได้โดยการใช้เครือข่ายเครื่องแลกเปลี่ยนความร้อน โดยในการวิจัยนี้ได้ศึกษาการออกแบบเครือข่ายเครื่องแลกเปลี่ยนความร้อนออกเป็นสามกลยุทธ์ โดยในกลยุทธ์ที่หนึ่งสามารถลดพลังงานที่ต้องการใช้ไปได้ 81.79% และกลยุทธ์ที่สองสามารถลดพลังงานไปได้ 80.73% เมื่อเทียบกับกระบวนการที่ไม่มีการใช้เครือข่ายเครื่องแลกเปลี่ยนความร้อน ทั้งสองกลยุทธ์นี้ลดการใช้พลังงานลงแตกต่างกัน 1.07% แสดงให้เห็นว่าลำดับของการแลกเปลี่ยนความร้อนนั้นมีผลต่อการลดการใช้พลังงานเนื่องจากขอบเขตของความแตกต่างของอุณหภูมิน้อยสุดที่จะสามารถแลกเปลี่ยนความร้อนระหว่างกันได้ เมื่อเทียบกับกลยุทธ์ที่สามซึ่งมีการแยกสายร้อนออกเป็นสามสายก่อนการแลกเปลี่ยนพลังงาน ทำให้พลังงานที่ต้องการใช้ในกระบวนการลดลงไปถึง 89.35% เมื่อเทียบกับกระบวนการที่ไม่มีการใช้เครื่องแลปเปลี่ยนความร้อน จากผลการจำลองกระบวนการที่กล่าวมาข้างต้น แสดงให้เห็นว่ากลยุทธ์การใช้พลังงานที่สามที่นำเสนอในงานวิจัยนี้เป็นกระบวนการที่มีประสิทธิภาพสำหรับการผลิตกรีนดีเซล เมื่อทำการเปรียบเทียบราคาค่าก่อสร้างเครือข่ายเครื่องแลกเปลี่ยนความร้อนและหน่วยสาธารณูปโภคแล้ว พบว่ากลยุทธ์ที่สามนั้นมีค่าใช้จ่ายต่อปีน้อยที่สุด ดังนั้นกลยุทธ์ที่สามจึงถือเป็นกลยุทธ์ที่คุ้มค่าต่อการลงทุนมากที่สุด ในกรณีที่เกิดความดันลดในกระบวนการ จะส่งผลให้กระบวนการต้องการพลังงานเพิ่มขึ้นโดยพลังงานที่เพิ่มขึ้นส่วนใหญ่มาจากการใช้เครื่องอัดความดัน

ภาควิชา วิศวกรรมเคมี ลายมือชื่อนิสิต .....

สาขาวิชา วิศวกรรมเคมี ลายมือชื่อ อ.ที่ปรึกษาหลัก .....

ปีการศึกษา 2557

5570568521 : MAJOR CHEMICAL ENGINEERING
KEYWORDS: ENERGY SAVING / HYDRITREATING PROCESS / SIMULATION / GREEN DIESEL PRODUCTION / HEAT INTEGRATION

SUWISA SAE-UENG: ENERGY OPTIMIZATION OF A HYDROTREATING PROCESS FOR GREEN DIESEL PRODUCTION FROM PALM OIL. ADVISOR: PROF. DR. PAISAN KITTISUPAKORN, 132 pp.

This work focus on the hydrotreating process for green diesel production from palm oil and the energy optimization of the process. The process simulations were performed by using Aspen plus program. The green diesel production process from palm oil by using $NiMoS_2/\gamma\text{-}Al_2O_3$ is considered. The results show that the green diesel yield, green diesel purity, liquid product distribution, hydrodeoxygenation (HDO) and decarbonylation (DCO)/decarboxylation (DCO_2) reactions occurring in the process are good agreement with the experimental data. The tolerance allowed is not more than 2%. In addition, the energy optimization for green diesel production process by using the heat exchanger network is studied. To minimize the energy consumption of the process, the energy optimization is divided into 3 strategies. From the energy optimization strategy 1 and 2, the energy consumption of 81.79% and 80.73% are decreased, respectively. The difference of energy saving of strategy 1 and 2 is 1.07%. Thus, the exchanged heat sequence affects on the energy saving due to the boundary of minimum temperature difference of exchanged hot and cold streams. Based on the energy optimization strategy 3, split hot stream, the energy consumption of 89.36% is decreased when compared with the original process. The results suggest that the energy optimization strategy 3 is very promising process for green diesel production. When comparing the cost of heat exchanger network construction and cost of utilities, the energy optimization strategy 3 has the lowest annual cost. Therefore, the energy optimization strategy 3 is the most worthwhile investment. In case of the pressure drop over the process, the compressor is used to increase the pressure that results in the increasing energy requirement.

Department:	Chemical Engineering	Student's Signature	.....
Field of Study:	Chemical Engineering	Advisor's Signature	.....
Academic Year:	2014		

ACKNOWLEDGEMENTS

I would like to express my deepest gratitude to advisor, Professor Dr. Paisan Kittisupakorn, for his excellent guidance, caring, patience, and providing me with an excellent atmosphere for doing research. I would like to thank Assistant Professor Dr. Kasidit Nootong as the chairman, Dr. Pimporn Ponpesh and Dr. Wachira Daosud as the members of the thesis committee for their kind.

Moreover, I would like to acknowledge The Institutional Research Fund (The Thailand Research Fund), Contract No. IRG5780014 and Chulalongkorn University, Contract No. RES_57_411_21_076 for financial supports.

I take this opportunity to record our sincere thanks to Mr. Jutipong Poosumas and all the faculty members of the Department of Chemical Engineering, Chulalongkorn University for their help and encouragement.

Most of all, I am fully indebted to my parents and family for their love, patience, enthusiasm and for pushing me farther than I thought I could go.

CONTENTS

Page

Page

Page

LIST OF TABLES

Page

LIST OF FIGURES

Page

CHAPTER 1

INTRODUCTION

1.1 Rationale

The growing demand for fuel results in the development of various alternative energy production. A number of countries are looking for alternative energy production. Many types of clean and renewable energy such as solar, wind, geothermal, hydroelectric and biofuels have been proposed to replace the fossil fuel which has limited supply.

Biofuels, one of a clean and renewable fuel, become more and more important in the past 5-10 years and this tendency is expected to continue (Raldov 2005). Therefore, the development of biofuels, is essential for energy production in the future. Biodiesel or fatty acid methyl esters (FAMEs), a first generation of biofuels, can be produced by the transesterification of triglycerides combined with methanol at a temperature range of 65-100°C (Chen, Gong et al. 2013). However, biodiesel has some downsides compared to petroleum diesel as follows (Jain and Sharma 2010, Liu, Sotelo-Boyás et al. 2011, Shin, Lim et al. 2011):

- Sludge formation after long storage.
- Sensitive to hydrolysis.
- Low thermal and oxidation stability because of its high oxygen content.
- High viscosity.
- Low heating value.

All of the disadvantages mentioned above show that biodiesel is still limited in its use. Therefore, an alternative energy that produced from triglycerides has been developed in various methods.

Green diesel, a second generation of biofuel, has similar molecular structure as petroleum diesel. Green diesel overcome the drawbacks of biodiesel and provide a

better diesel properties. In comparison with biodiesel, the advantages of green diesel are (Mikkonen 2008):

- The green diesel product is compatible with existing engines.
- Flexibility with the feedstock.
- Higher cetane number.
- Higher energy density.
- Higher oxidation stability.
- By-products of the process not require additional treatment.
- Better performance in cold weather.

The green diesel has been produced by a hydrotreating of triglycerides in vegetable oils with hydrogen. The hydrotreating process consists of 3 main reactions which are hydrodeoxygenation (HDO), decarbonylation (DCO) and decarboxylation (DCO_2) (Kubička and Kaluža 2010, Faungnawakij and Suriye 2013). Hydrodeoxygenation (HDO) is an exothermic reaction that removes oxygen in the form of water. Decarbonylation (DCO) and decarboxylation (DCO_2) are endothermic reactions that remove oxygen in form of carbonmonoxide, water and carbondioxide, respectively (Snåre, Kubičková et al. 2006, Gong, Shinozaki et al. 2012).

The hydrotreating process of vegetable oils leads to C_{15}-C_{18} primary hydrocarbon products. The range of reactions' temperature is 300-450 °C and pressure above 30 bar (Huber and Corma 2007, Donnis, Gottschalck et al. 2009). The by-products of process are carbonmonoxide, carbondioxide, propane, ethane, methane and water. The catalyst used in the hydrotreating of triglycerides can be divided in two types (Srifa, Faungnawakij et al. 2014):

(1) Metal catalysts: nickel (Ni), ruthenium (Ru), rhodium (Rh), platinum (Pt), palladium (Pd). These type are favorable to decarbonylation (DCO) and decarboxylation (DCO_2).

(2) Bimetallic sulfide catalysts: nickel-molybdenum-sulfide ($NiMoS_2$) supported on alumina (Al_2O_3), cobalt-molybdenum-sulfide ($CoMoS_2$) supported on alumina (Al_2O_3), nickel-tungstan-sulfide ($NiWS_2$) supported on alumina (Al_2O_3). They are favorable to hydrodeoxygenation (HDO).

According to the reasons given above, simulation study is needed to predict a result of the process and improve a process efficiency. The main objective of this work aims to simulate and optimize an energy of a hydrotreating process for green diesel production from palm oil.

1.2 Objective

To design and optimize energy of an efficient hydrotreating process for green diesel production from palm oil.

1.3 Scope of Work

1.3.1 Design a green diesel production process.

1.3.1.1 Design a green diesel production from palm oil by using aspen plus simulator. The purity of product, product composition, product yield, amount of hydrogen excess and energy consumption are considered.

1.3.2 Energy optimization of a green diesel production process.

1.3.2.1 Apply the heat exchanger network to the green diesel production process to minimize the overall energy consumption.

1.3.2.3 Compare the developed hydrotreating process with heat exchanger network with an original process.

1.4 Expected Outputs

An efficient energy optimization for a green diesel production process by using the heat integration is expected.

CHAPTER 2

THEORY

2.1 Green diesel

Green diesel, one of the renewable diesels, is produced from biomass such as vegetable oils and fats via catalytic hydrotreating. The green diesel is called as a second generation fuel. The differences between petroleum refinery, first generation fuel and second generation fuel are presented in Table 2.1 (Naik, Goud et al. 2010).

Table 2.1 The differences between petroleum refinery, first generation fuel and second generation fuel.

	Petroleum refinery	**First generation fuel**	**Second generation fuel**
Feedstock	Crude petroleum	- Vegetable oils - Corn - Sugar	- Edible oil - Non-edible oil - Cheap and abundant waste biomass (Agricultural & forest residue, grass, aquatic biomass and waste hyacinth etc.)
Product	- CNG - LNG - Diesel	- Biodiesel (FAMEs) - Corn ethanol - Sugar alcohol	- Hydrotreating oil - Bio-oil - Lignocellulosic ethanol

Table 2.1 The differences between petroleum refinery, first generation fuel and second generation fuel. (Continued)

	Petroleum refinery	**First generation fuel**	**Second generation fuel**
Product	- Petrol - Kerosene - Jet fuel		- Butanol - Mixed alcohols
Problem	- Declining of petroleum reserve. - Environmental pollution - Economics and ecological problems.	- Limited feedstock (food versus fuel) - Blended partly with conventional fuel.	- Advance technology still under development to reduce the cost of conversion. - High cost of production. - Hardly to produce in larger scale.
Benefit	- Economical technology. - Fit with mostly present diesel engine.	- Environmental friendly. - Economics & social security	- Non competing with food. - Environmental friendly. - Economics & social security

The green diesel can be produced from various vegetable oil such as palm oil, jatropha oil, soybean oil, rapeseed oil via catalytic hydrotreating reaction. The hydrotreating process for green diesel production differences from biodiesel because biodiesel is produced via esterification or transesterification reaction. A green diesel also has a difference physical properties as shown in Table 2.2 (Bezergianni and Dimitriadis 2013).

Table 2.2 Properties of the difference types of renewable diesel.

Analysis	Units	White diesel	FAME diesel	Green diesel	Fossil diesel	Diesel standard Min/Max	
Density	g/ml	0.79	0.855 – 0.9	0.77 – 0.83	0.85	Min 0.8	Max 0.845
Sulfur	mg/kg (ppmwt)	1.54	0 – 0.012	<10	12		Max 10
Cetane Index		77.23	58.3	50 - 105	54.57	Min 46	
Cetane number			45 -72.7	80 – 99	50	Min 51	
Flash point	^{o}C	116	96 - 188	68- 102	52 – 136	Min 60	Max 170
Water	mg/kg	13	28.5 – 500	42 – 95	0.5		200
MCRT carbon residue	(wt%) %m/m	0.0066	0.02 – 0.3				Max 0.3
Viscosity at 40^{o}C	cSt	3.5	3.89 – 7.9	2.5 – 4.15	2.71	Min 2	Max 4.5
Copper strip corrosion	(3 h in 50 ^{o}C)	1b	1		<3	Class 1	-
Color	(ASTM)	0		2			-

Table 2.2 Properties of difference types of renewable diesel. (Continued)

Analysis	Units	White diesel	FAME diesel	Green diesel	Fossil diesel	Diesel standard Min/Max	
HPLC	%wt (%m/m)			<0.1		<11	
Induction time (oxidation time) at 110ºC	h	>22	0.9 – 10.9	>22		Min 6	
Distillation 90 vol%	ºC	302.6		298 - 342	341	85 – 360	-
Net heating value	MJ/kg	49	37.1 – 40.4	42 – 44	34.97	Min 35	-
CFPP	ºC	20	(-13) – 15	>20	-6	-5	+5
Cloud point	ºC		(-3) – 17	(-25) – 30	-5	Min -5	Max 12
Pour point	ºC	23	(-15) - 16	(-3) – 29	-21	Min -13	Max 10

Green diesel mainly consists of C_{15} – C_{18} n-paraffins and free of aromatics, oxygen and sulfur. A green diesel not only has higher cetane index and cetane number than biodiesel (Figure 2.1) but heating value also higher than conventional diesel (Figure 2.2) (Bezergianni and Dimitriadis 2013).

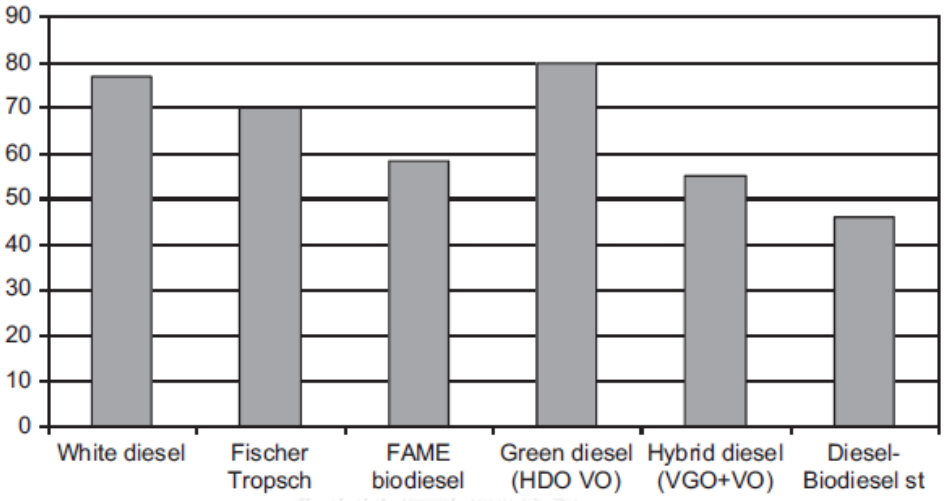

Figure 2.1 Cetane index of the difference types of renewable diesel.

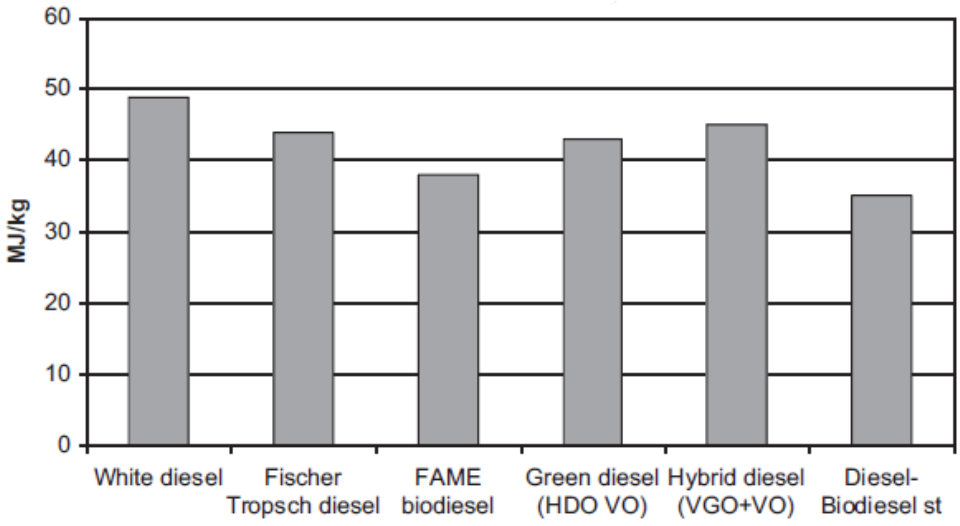

Figure 2.2 Net heating value of difference types of renewable diesel.

The advantages of green diesel are (Mikkonen 2008):

- The product is compatible with existing engines.
- Flexibility with the feedstock.
- Higher cetane number.
- Higher energy density.
- Higher oxidation stability (zero O_2 content).
- It does not increase the emissions of NO_x.
- It does not require water.
- There are not byproducts that require additional treatment (e.g. glycerol).
- The distribution of the renewable diesel does not cause additional pollution since it can be transported through the same pipelines that are currently used for distribution of petrodiesel.
- Better performance in cold weather.

2.2 Green diesel feedstock

2.2.1 Triglycerides

The main structure of vegetable oils and animal fats found in nature makes up from triglycerides. The triglycerides are high molecular weight compound (around 550 to 1050 g/mol) that composed of long chains of fatty acid esters. The side chains of triglyceride consist of saturated, monounsaturated and polyunsaturated. A structure of triglyceride commonly presents in vegetable oils and fats as shown in Figure 2.3 and a structure of fatty acid commonly presents in vegetable oils and fats as shown in Figure 2.4.

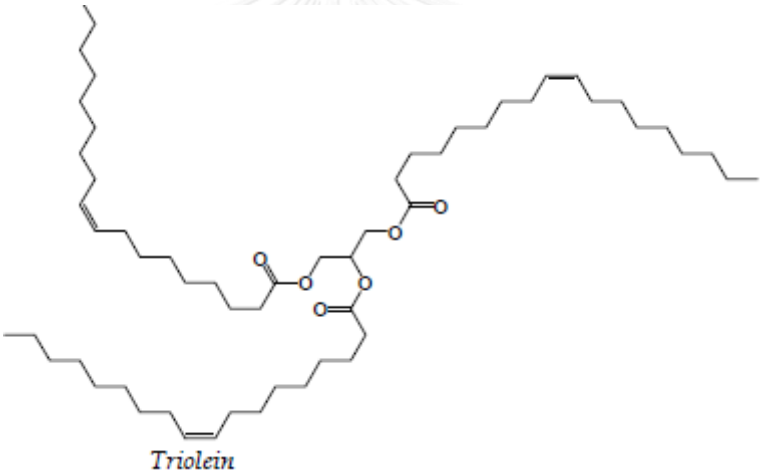

Figure 2.3 Basic structure of triglyceride (Triolein).

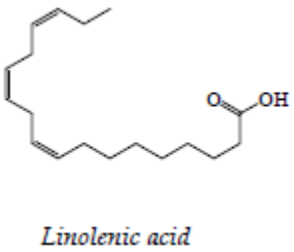

Figure 2.4 Basic structure of fatty acid (Linolenic acid).

Triglycerides can be classified by saturation degree of their side chains. One of the difference point between fats and oils is a melting point. Fats are solid at an ambient temperature but oils are liquid. Fats and oils have many forms of triglycerides such as saturated, unsaturated acids or isomeric. Saturated oils have higher melting point than unsaturated oils and also have better oxidation stability (Alí, El–Alí et al. 2005).

The composition of triglyceride and fatty acid depends on a type of vegetable oil. Typical composition of various vegetable oils can be summarized in Table 2.3 (Sotelo-Boyás, Trejo-Zarraga et al. 2012).

Table 2.3 Typical composition of various vegetable oils.

Source	Struc-ture	Molecular weight (MW)		Typical composition, wt%				
		Fatty acid	Trigly-ceride	Jatro pha	Palm	Canola	Soy bean	Sun flower
Capric	$C_{10:0}$	172.3	554.8	0.0	0.0	0.6	0.0	0.0
Lauric	$C_{12:0}$	200.3	639.0	0.0	0.0	0.0	0.0	0.0
Myristic	$C_{14:0}$	228.4	723.2	0.0	2.5	0.1	0.0	0.0
Palmitic	$C_{16:0}$	256.4	807.3	15.9	40.8	5.1	11.5	6.5
Palmi-toleic	$C_{16:1}$	254.4	801.3	0.9	0.0	0.0	0.0	0.2
Stearic	$C_{18:0}$	284.5	891.5	6.9	3.6	2.1	4.0	5.8
Oleic	$C_{18:1}$	282.5	885.4	41.1	45.2	57.9	24.5	27.0
Linoleic	$C_{18:2}$	280.4	879.4	34.7	7.9	24.7	53.0	60.0
Linolenic	$C_{18:3}$	278.4	873.3	0.3	0.0	7.9	7.0	0.2
Arachidic	$C_{20:0}$	312.5	975.6	0.0	0.0	0.2	0.0	0.3
Eicosenoic	$C_{20:1}$	310.5	969.6	0.2	0.0	1.0	0.0	0.0
Behenic	$C_{22:0}$	340.6	1059.8	0.0	0.0	0.2	0.0	0.0
Erucic	$C_{22:1}$	338.6	1053.8	0.0	0.0	0.2	0.0	0.0
			Estimated MW:	869.7	847.0	876.9	871.9	876.7

Note: $C_{n:m}$ describes a fatty acid with n carbon atoms and m double bonds.

2.3 Fundamentals of hydroconversion processes

Hydroprocessing is an important processes in a refinery scheme that contains a set of reactions in which hydrogen is passed through a bifunctional catalyst. This process is used to convert a variety of petroleum fractions into environmental friendly fuel. The reactions that occur in hydroprocessing can be derived in two main types: hydrocracking and hydrotreating.

2.3.1 Hydrocracking

Hydrocracking is a chemical process that used to convert the high-boiling point hydrocarbons from petroleum fractions to more valuable lower-boiling point hydrocarbons such as gasoline, kerosene, jet fuel and diesel fuel. From a catalytic viewpoint, hydrocracking is carried out on acid supports such as amorphous supports (alumino-silicates), silicoaluminophosphates (SAPO) and crystalline supports (zeolites) (Ancheyta, Trejo et al. 2009). For example, a hydrocracking of gas oil component ($C_{26}H_{54}$) into gasoline (C_8H_{18}) and diesel ($C_{18}H_{38}$) is shown in Figure 2.5.

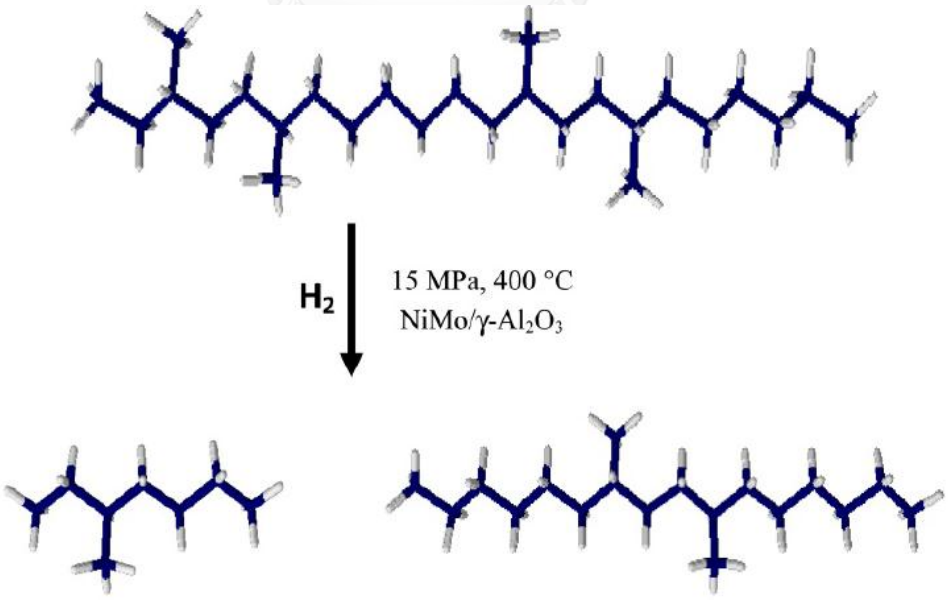

Figure 2.5 Hydrocracking of gas oil into gasoline and diesel on a bifunctional catalyst.

2.3.2 Hydrotreating

Hydrotreating is used to remove about 90% of impurities such as nitrogen, sulfur, oxygen and metals from liquid petroleum fractions. The hydrotreating can be improved the quality of petroleum distillates without significant alteration of the boiling range. This reactions take place on the metal active sites of a catalyst such as NiMo or CoMo in sulfide state supported on γ-Al_2O_3 (Ancheyta, Trejo et al. 2009). Other catalysts have been used in hydrotreating such as supported noble metal catalysts (Lestari, Ma¨ki-Arvela et al. 2009) and NiMo/γ-Al_2O_3 catalyst. The NiMo/γ-Al_2O_3 is generally used in the hydroprocessing process at petroleum refineries. This catalyst has a high hydrogenation activity and mild acidity and this catalyst also appropriate for the hydroconversion of triglycerides into diesel hydrocarbons (Sotelo-Boyás, Liu et al. 2011).

2.4 The reaction of a hydrotreating of vegetable oils

The hydrotreating process (or hydroprocessing process) is used to increase a hydrogen to carbon ratio. This process reduces the boiling point of petroleum fractions and eliminates metal impurities. For green diesel production, the hydrotreating process is focused to produce an alternative diesel that has the properties like a conventional diesel from petroleum refinery.

The green diesel production can be produced by a hydrotreating of triglycerides through three main reactions: hydrodeoxygenation (HDO), decarboxylation (DCO_2) and decarbonylation (DCO). The triglycerides are converted into primary hydrocarbon products (n-paraffins) and by-products (carbonmonoxide, carbondioxide and water). The reactions occurring in the hydrotreating of triglycerides are shown in Figure 2.6.

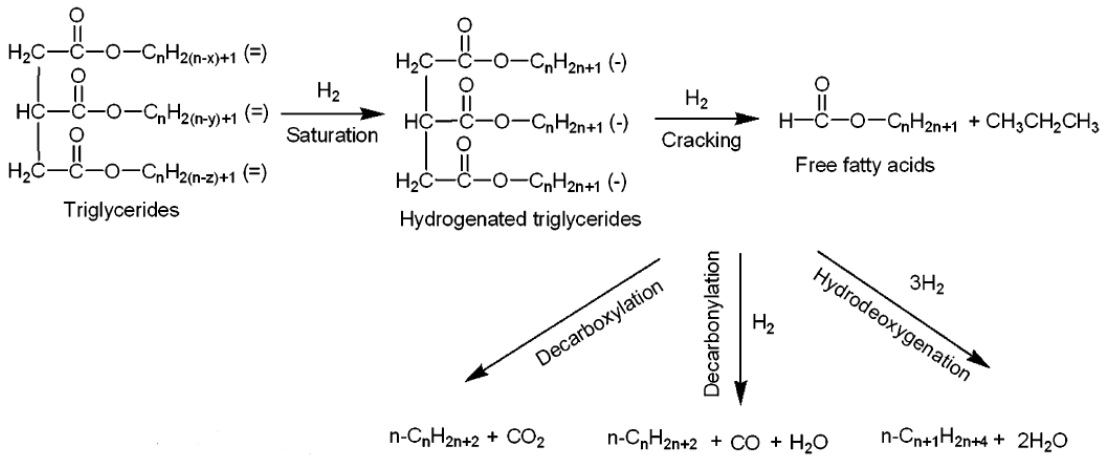

Figure 2.6 The reactions occurring in the hydrotreating of triglycerides. (adapted from (Veriansyah, Han et al. 2012))

Where:

n	:	Odd number
x, y, z	:	Number of double bonds
=	:	Double bond
-	:	Single bond

2.4.1 Hydrodeoxygenation

Hydrodeoxygenation (HDO) is a hydrogenolysis process for removing oxygen in the form of water from oxygen organic compounds. The carbon atom number of n-alkanes that produced from this reaction are corresponding with fatty acids composition in oil source. Equation (2.1) shows a sample of hydrodeoxygenation that relate on green diesel production process.

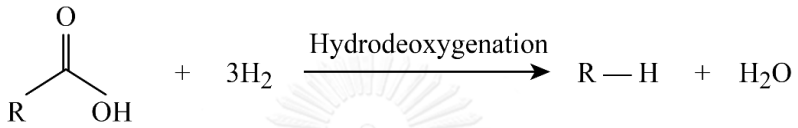

(2.1)

The thermodynamics data at 300°C for linear C_{17} hydrocarbons from stearic acid ($C_{17}H_{35}COOH$) indicate that a Gibbs free energy (ΔG) is -86.1 kJ/mol and a standard enthalpy of reaction (ΔH) is -115.0 kJ/mol. The negative value of standard enthalpy of a reaction is indicated that the hydrodeoxygenation is an exothermic reaction. The hydrodeoxygenation reaction for linear C_{17} hydrocarbons from stearic acid is shown in Equation (2.2).

$$C_{17}H_{35}COOH + 3H_2 \xrightarrow{Hydrodeoxygenation} C_{18}H_{38} + 2H_2O \quad (2.2)$$

2.4.2 Decarboxylation

Decarboxylation (DCO_2) is a chemical reaction that removes a carboxyl group and produces carbondioxide as a by-product. Equation (2.3) shows a sample of decarboxylation that relate on green diesel production process.

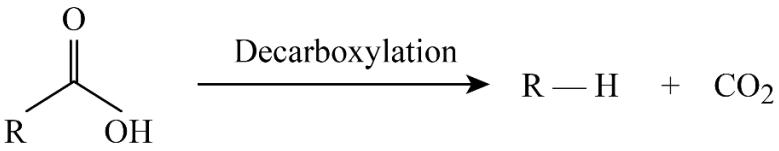

(2.3)

Equation (2.4) shows the decarboxylation reaction of a stearic acid. Thermodynamics data at 300°C for linear C_{17} hydrocarbons from stearic acid ($C_{17}H_{35}COOH$) indicate that a Gibbs free energy (ΔG) is -83.5 kJ/mol and a standard enthalpy of reaction (ΔH) is 9.2 kJ/mol. The positive value of standard enthalpy of a reaction is indicated that the decarboxylation is an endothermic reaction.

$$C_{17}H_{35}COOH \xrightarrow{Decarboxylation} C_{17}H_{36} + CO_2 \quad (2.4)$$

2.4.3 Decarbonylation

Decarbonylation (DCO) is a chemical reaction that leads to elimination of oxygen to form alkanes and produces CO and water as by-product. The mechanism of a decarbonylation reaction is shown in Equation (2.5).

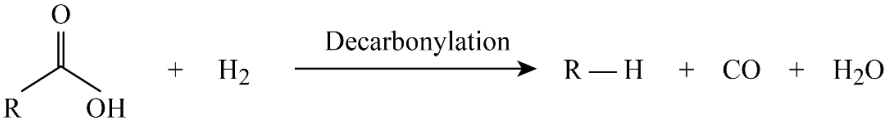

(2.5)

Thermodynamics data at 300ºC for linear C_{17} hydrocarbons from stearic acid ($C_{17}H_{35}COOH$) indicate that a Gibbs free energy (ΔG) is -7.0 kJ/mol and a standard enthalpy of reaction (ΔH) is 179.1 kJ/mol. The positive value of standard enthalpy of a reaction is indicated that the decarbonylation is an endothermic reaction. The decarbonylation reaction for linear C_{17} hydrocarbons from stearic acid is shown in Equation (2.6).

$$C_{17}H_{35}COOH + H_2 \xrightarrow{Decarbonylation} C_{17}H_{36} + CO + H_2O \qquad (2.6)$$

All of hydrotreating reactions: hydrodeoxygenation, decarboxylation and decarbonylation have a negative value of a Gibbs free energy at the specified conditions. Thus, all three reactions can be occurred under the thermodynamics principle. However, without catalyst presence in the process, the rate of reactions will be low and reactions may take a longer reaction time (Sotelo-Boyás, Trejo-Zarraga et al. 2012). The catalyst is a substance that increases the rate of chemical reaction. For green diesel production, the catalyst is usually presented in the solid phase that packed inside the reactor. The catalyst plays the important role for a hydrotreating process that specifies the state of main condition in the process (such as temperature, pressure, reaction phase, hydrogen to oil ratio etc).

The general condition for hydrotreating process are 300 to 450ºC, pressure above 30 bar. Figure 2.7 shows a probable mechanism in which triglycerides are converted into linear n-paraffins. In this case, the palm oil is considered to be composed by triolein, tripalmitin and trilinolein (Guzman, Torres et al. 2010).

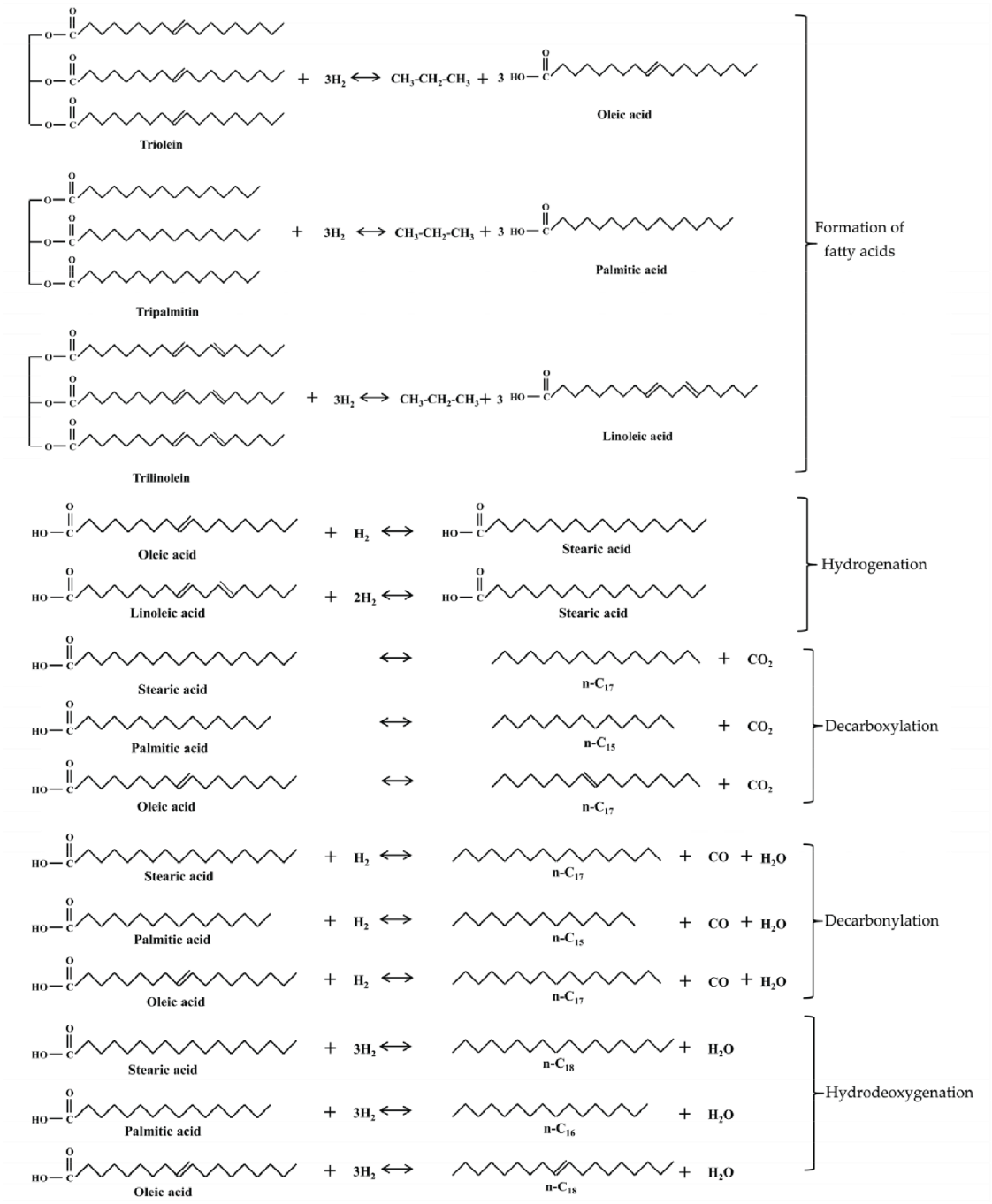

Figure 2.7 The reaction pathways during a hydrotreating of triglycerides in palm oil.

2.5 Heat Exchanger Network

2.5.1 What is heat exchanger network?

A heat exchanger network is one of the method that conserve an energy in the process and minimize an energy requirement from external sources or utilities. A heat exchanger network can transfer heat between the hot and cold streams. The objectives of heat exchanger network can be described as follows:

- To heat and cool process streams from initial temperatures to specified target temperatures.
- To reduce an energy from utilities such as heater and cooler.
- To minimize the number of heating and cooling unit.

The additional heat exchangers for recovering heat from the hot or cold streams would invariably increase the capital cost but it reduce the cost of utilities. Figure 2.8a shows the maximum operating cost and the maximum utility cost. On the other hand, if all the hot and cold streams are used for heating and cooling duties and the utilities take care of only those extreme duties that cannot be met by mutual exchange of heat from the streams as presented in Figure 2.8b, this structure causes the maximum heat recovery at a minimum energy cost, having minimum hot and cold utility requirements. However, this structure has some drawbacks such as higher capital cost, higher process complexity and complicated process start-up.

There is an actual optimum that lies between these two extreme design of heat exchanger network, and the total annual cost should be minimized (total annual cost are the sum of annual utility cost and annualized capital cost such as an annual deterioration, plus interest).

The driving forces and the effects of heat load are two basic thermodynamic effects that influence capital costs, as depicted in Figure 2.9. The capital cost increases with reduced driving forces, but decreases with reduced heat load.

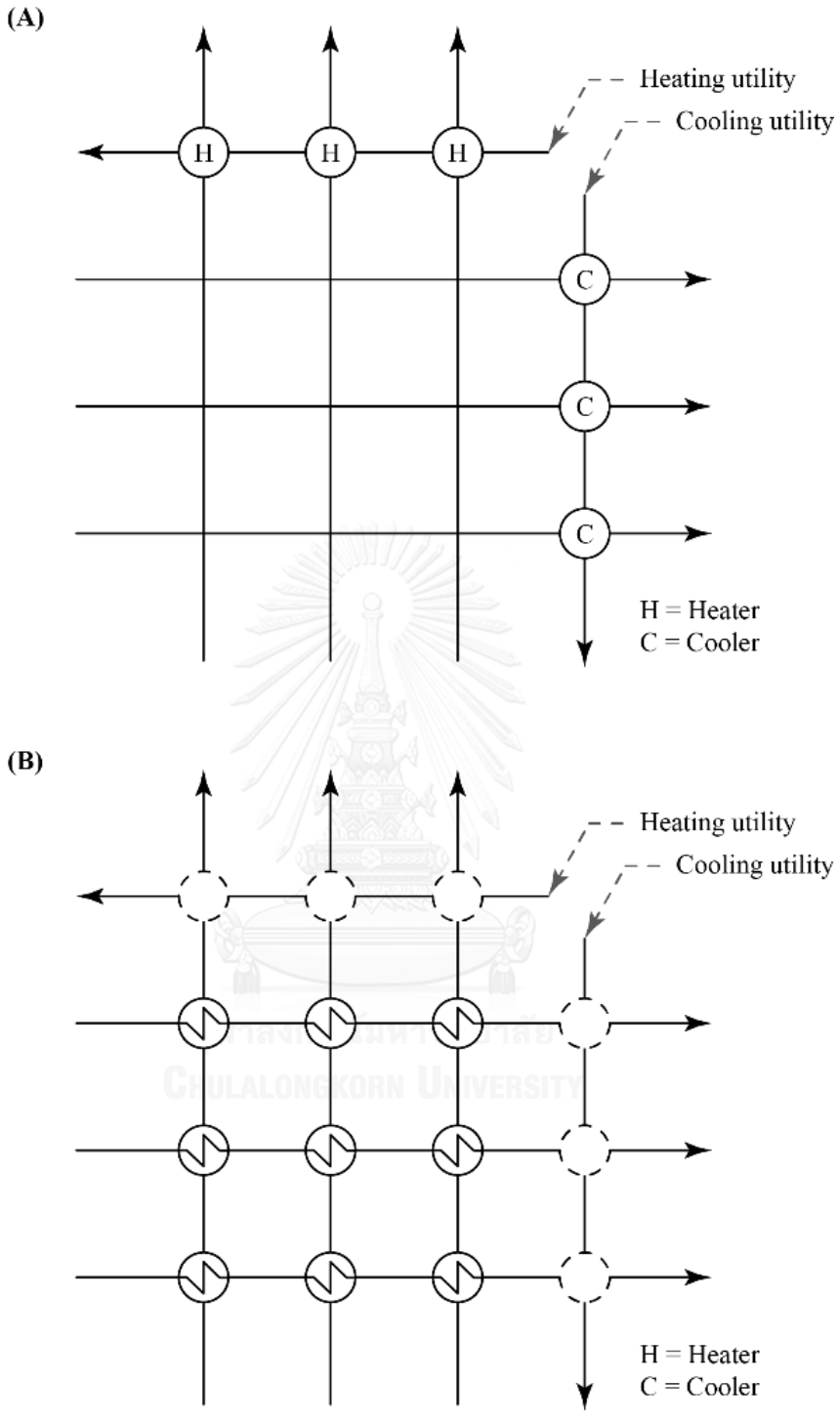

Figure 2.8 Two extreme designs of heat exchanger network
(a) Maximum capital cost (b) Maximum heat recovery.

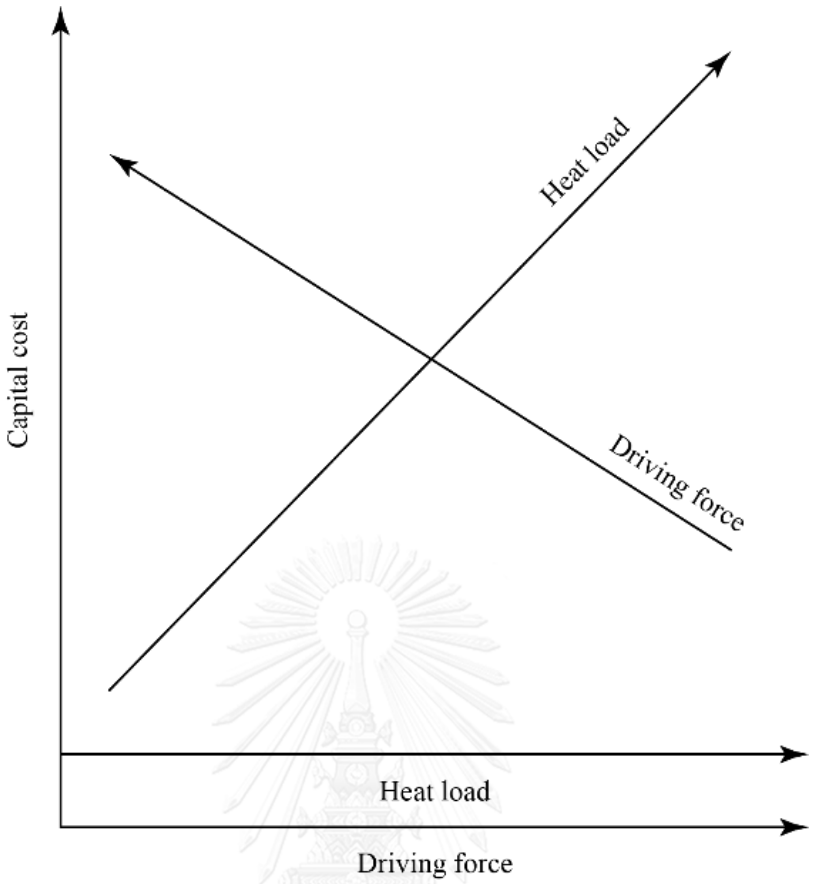

Figure 2.9 The effect of driving force and heat load on a capital cost.

A heat exchanger network is designed to handle the heat available. The hot process streams can be used to meet heating demand and the cold process streams can be used to meet cooling demand. Matching heating and cooling duties in the process streams consequently reduce the hot and cold utilities usage.

The recovery of energy not only improve economy by reducing the energy cost, but also reduce the operating costs. Thus, the heat exchanger network design is a key aspect of chemical process that should be considered to save the energy (Coker 2015).

2.5.2 The temperature–enthalpy diagram (T–H)

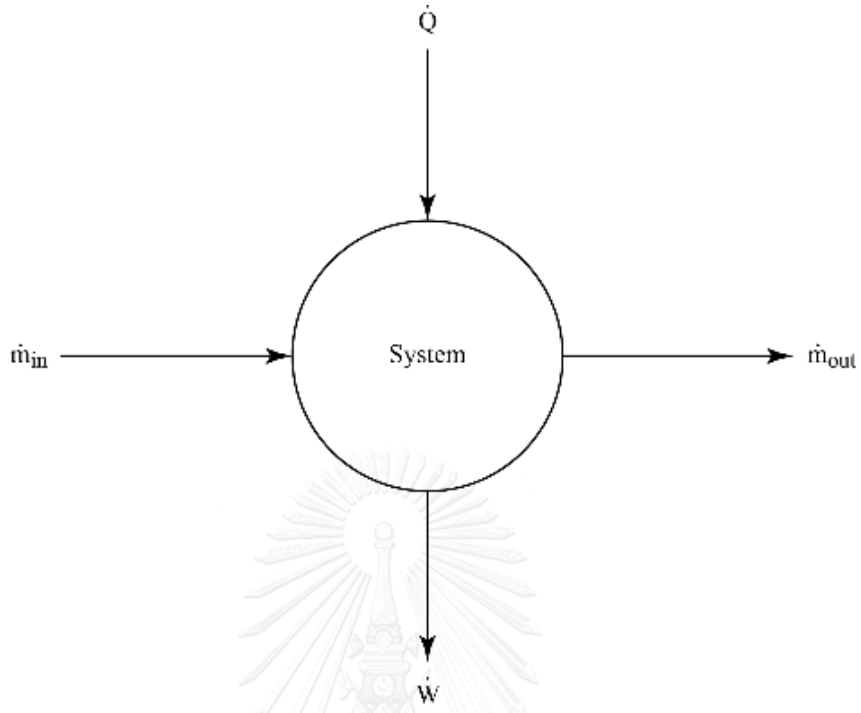

Figure 2.10 General flow system

From a general flow system as shown in Figure 2.10, this is one inlet and one outlet stream. The total energy, mass inlet ($\dot{m}_{in}$) and mass outlet ($\dot{m}_{out}$) of the system, the general energy balance is:

$$\frac{dE_{sys}}{dt} = \dot{Q} - \dot{W} + \dot{m}_{in}\left(u + \frac{P}{\rho} + \frac{1}{2}V^2 + gz\right)_{in} - \dot{m}_{out}\left(u + \frac{P}{\rho} + \frac{1}{2}V^2 + gz\right)_{out} \quad (2.7)$$

Where:

ρ = Fluid density (mass/volume)

The specific enthalpy (energy/mass), h is:

$$h = u + \frac{P}{\rho} \tag{2.8}$$

The energy balance equation becomes:

$$\frac{dE_{sys}}{dt} = \dot{Q} - \dot{W} + \dot{m}_{in}\left(h + \frac{1}{2}V^2 + gz\right)_{in} - \dot{m}_{out}\left(h + \frac{1}{2}V^2 + gz\right)_{out} \tag{2.9}$$

For steady state operation,

$$\frac{dE_{system}}{dt} = 0 \quad , \; \dot{m} = \dot{m}_{in} = \dot{m}_{out}$$

So, the Equation (2.9) after re-arranging becomes:

$$\dot{Q} = \dot{W} + \dot{m}\left[\left(h + \frac{1}{2}V^2 + gz\right)_{out} - \left(h + \frac{1}{2}V^2 + gz\right)_{in}\right] \tag{2.10}$$

Assuming work done, w, kinetic energy and potential energy of the streams are negligible:

$$\dot{Q} = \dot{m}[h_{out} - h_{in}] = \Delta\dot{H} \tag{2.11}$$

Where:

$$\Delta\dot{H} = \dot{m}CpdT \tag{2.12}$$

and

$$CP = \dot{m}Cp \tag{2.13}$$

The heat flow through the system is:

$$\dot{Q} = \Delta\dot{H} = CP \cdot dT \tag{2.14}$$

Where:

$\Delta\dot{H}$ = Heat content (kW).

CP = Heat capacity flow rate (KW/°C).

dT = Temperature change for stream (°C) = $(T_{out} - T_{in})$, $(T_{target} - T_{supply})$.

Where CP is assumed to be constant for a stream that requires heating from a supply temperature (T_s) to a target temperature (T_t). The total heat added will be equal to the stream enthalpy change as shown in Equation (2.15).

$$Q = CP \int_{T_s}^{T_t} dT = CP(T_t - T_s) = \Delta H \tag{2.15}$$

The differentiation of Equation (2.15) provides the slope of the line representing the stream that shows in Equation (2.16).

$$\frac{dT}{dQ} = \frac{1}{CP} \tag{2.16}$$

The CP can also be calculated from:

$$CP = \frac{dQ}{dT} = \frac{dH}{dT} = \frac{\Delta H}{(T_t - T_s)} \tag{2.17}$$

In the heat exchanger, the heat flow is defined by:

$$Q = UA\Delta T_{LMTD} \tag{2.18}$$

Where:

U = Overall heat transfer coefficient (kW/m^2K).

A = Heat transfer area (m^2).

ΔT_{LMTD} = Log mean temperature difference (K).

Figure 2.11 shows that the T-H diagram can be used to represent heat exchange. Where the phase transition occurs, the latent heat is used instead of CP to calculate the stream duties. The energy in term of the latent heat is:

$$\dot{Q} = \dot{m}\lambda \tag{2.19}$$

Where:

$\dot{m}$ = Mass flow rate (kg/s)

λ = Latent heat (kJ/kg)

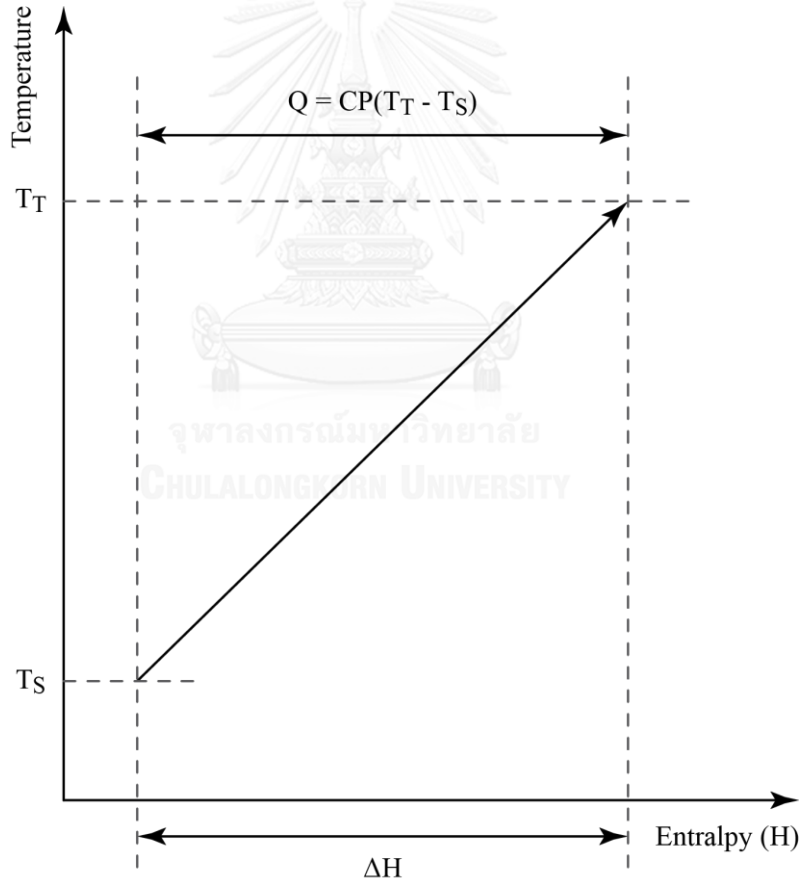

Figure 2.11 A process stream in the T-H diagram.

2.5.3 Heat exchanger network design

2.5.3.1 Minimum temperature difference (ΔT_{min})

For the design of heat exchanger network, the temperature difference between hot and cold stream must greater than ΔT_{min} in every contact point along the length of heat exchanger. ΔT_{min} can be shown in Equation (2.20) and the typical ΔT_{min} values from experience-based (Linnhoff 1998) are shown in Table 2.4.

$$T_H - T_C \geq \Delta T_{min} \tag{2.20}$$

Where:

T_H = Hot stream temperature.

T_C = Cold stream temperature.

Table 2.4 The typical ΔT_{min} values for various types of processes.

No.	Industrial Sector	Experience ΔT_{min} values
1	Oil refining	20-40℃
2	Petrochemical	10-20℃
3	Chemical	10-20℃
4	Low temperature processes	3-5℃

Figure 2.12 shows the hot stream and cold stream in term of temperature and enthalpy. The minimum temperature difference between hot and cold streams is defined as ΔT_{min}.

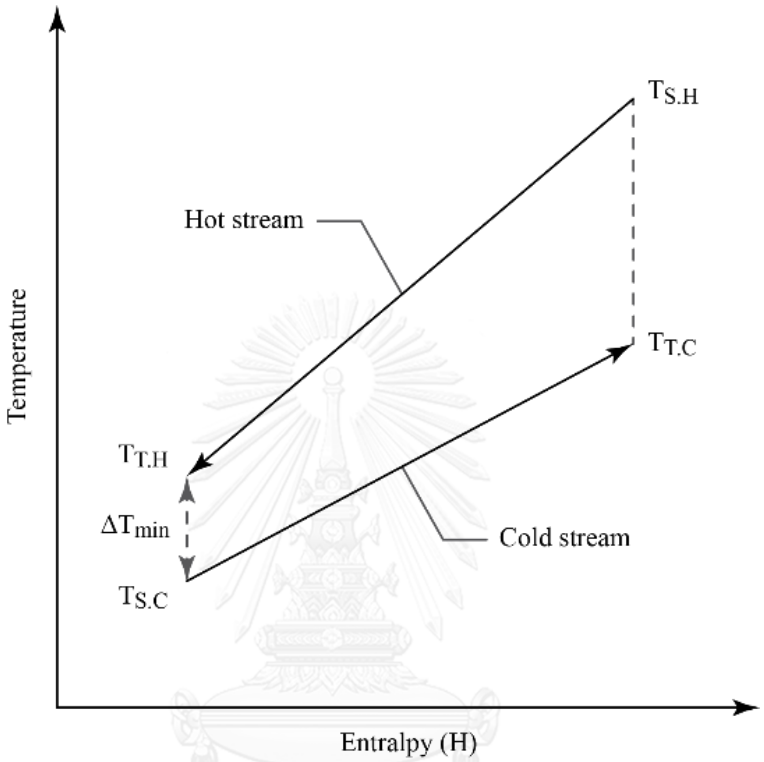

Figure 2.12 T-H diagram in a single heat exchanger unit.

2.5.3.2 Construction of composite curves

The composite curves show the relation between temperature and enthalpy (T-H) that include the enthalpy of hot streams in a process and the enthalpy of cold streams in a process. The enthalpy of hot and cold stream are plotted in the same diagram. Figure 2.13 shows the composite curve in a process. The hot and cold pinch temperature is defined by the closest point between hot and cold composite curve and a middle of hot and cold pinch temperature is called pinch temperature. The $\Delta T_{\min}$ can be evaluated by the temperature difference between hot pinch temperature and cold pinch temperature. The interception enthalpy of hot composite curve and cold composite curve represent the possibility range that can be recoverd the heat in a process. $Q_{H,min}$ and $Q_{C,min}$ are

the minimum heat required from external utilities. The composite curves can be guided a target of energy recovery and energy added in the process.

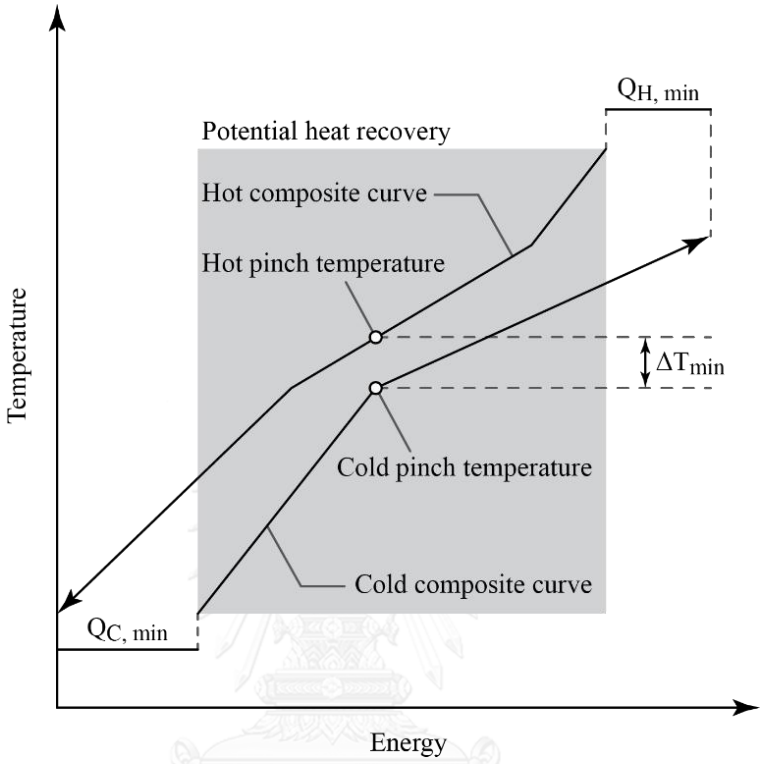

Figure 2.13 The composite curves of a process.

CHAPTER 3

LITERATURE REVIEWS

This chapter showed the review of research that related to the hydrotreating of vegetable oils process with various catalysts.

3.1 The hydrotreating of vegetable oils

The first study about a hydrotreating of vegetable oils was presented by (Nunes 1984). He used rhodium and ruthenium supported catalysts in a batch reactor with soybean oil feedstock. Two years later, (Nunes, Brodzki et al. 1986) reported that the temperature of the hydrotreating of soy bean oil was observed to begin at about 400^{o}C. They used bifunctional catalyst at this temperature and observed the decarbonylation/decarboxylation of fatty acids to take place with a marked hydrogenolysis on a catalyst. The overall conversion is 83 wt% including the gas fraction of carbonmonoxide, carbondioxide, methane, ethane, propane, butane and yielding mainly normal paraffins under favorable conditions of pressure and temperature. Since then, many types of catalysts have been used to crack the long chain of hydrocarbons of vegetable oils to produce short chain of hydrocarbons.

(Charusiri and Vitidsant 2005) worked at a temperature range of 400 to 430^{o}C in a 70 cm^{3} batch micro-reactor with reaction time from 30 to 90 min over sulfated zirconia catalyst and the range of hydrogen pressures between 10 and 30 bar. They reported that a maximum conversion to gasoline occurred at a lower limit (10 bar). They found that the longer reaction times (than 90 min) favored a light gases and aromatics production. The production of liquid hydrocarbons consisting of gasoline was occurred at high temperature. The conclusion of this research, they found that the initial hydrogen pressure was responsible for the catalytic cracking step. The hydrocracking and hydrogenation were possible for the cracking and rearrangement to yield light

hydrocarbon molecules. In the next year, (Charusiri, Yongchareon et al. 2006) studied about the catalytic conversion of waste cooking vegetable oil at the temperature range of 380 to 430^{o}C and hydrogen pressure about 10 to 20 bar with reaction time from 45 to 90 min. In this case, they used zeolite HZSM-5, sulfated zirconia and a hybrid catalyst HZSM-5-sulfated zirconia. The result showed that the hybrid catalyst provided a higher conversion to gasoline fuel with a yield of 26.57 wt% at 430^{o}C. In the hydrotreating process, the three parallel reactions consisted of hydrogenation, hydrodeoxygenation and decarboxylation of carboxylic acids. The hydrodeoxygenation produced n-paraffins with an even number of carbon atom such as n-C_{16} and n-C_{18}. The carbon atom number of n-paraffins corresponded to the side chains of the fatty acids in the triglycerides.

(Hancsók, Krár et al. 2007) studied the isomerization of pre-hydrogenated sunflower oil for diesel production. In this case, they used Pt/HZSM-22/γ-Al_2O_3 catalysts over catalysts containing 0.25–1.1% platinum on HZSM-22. They worked at temperatures of 280 to 370^{o}C, total pressures of 35 to 80 bar and liquid hourly space velocities (LHSV) of 1.0 to 4.0 h^{-1}. They found a yield of liquid products higher than 90% with cold filter plugging point (CFPP) in between -18 and -14^{o}C, the range of cetane number between 81–84 and the ratio of iso-paraffins to n-paraffins was in the range of 3.7:1–4.7:1 under favorable conditions. This catalyst provided a good quality of green diesel fuel. The green diesel from this experiment not only provided a high cetane number, but also provided a low freezing point.

Some studies conducted by (Nasikin, Susanto et al. 2009), the production of biogasoline from palm oil by simultaneous cracking and hydrogenation reactions over NiMo/zeolite catalyst. The experiment used a batch reactor with atmospheric pressure in presence of hydrogen, temperature at 300 and 320^{o}C, a feed per catalyst ratio of 75 wt/wt with the reaction times were 1, 1.5 and 2 hours for each temperature. The experimental result produced biogasoline that contained C_8 to C_{10} with a volumetric yield of 11.93%. The green diesel was obtained with 13.1% volumetric yield. In the same year, (Simacek, Kubicka et al. 2009) worked at various temperature between 260 to 340^{o}C, pressure under 70 bar in a laboratory continuous flow reactor. The hydrotreating of rapeseed oil can be converted into diesel fuel with using a different

concentrations of NiO and MoO_3 of three NiMo/alumina catalysts (such as A (3.8 and 15.7 wt%), B (2.6 and 15.7 wt%) and C (2.6 and 8.8 wt%)), respectively. An organic liquid product was obtained only hydrocarbons as same as diesel fuel compositions that found in the nature.

In 2010, (Kikhtyanin, Rubanov et al. 2010) tested siliconaluminophosphates materials (SAPO) in the hydroconversion of sunflower oil on Pd/SAPO-31 catalysts. They used a bifunctional catalysts for single-stage production of hydrocarbons in the diesel fuel range. A sunflower oil transformed to hydrocarbons product at a temperature between 320 to 360^{o}C. The main product components were identified as C_{17} and C_{18} n-paraffins and iso-paraffins. The catalyst exhibited a high initial activity for the hydroconversion of the feed and provided a good isomerization activity, but this catalyst deactivation occurred after several hours of operation.

(Murata, Liu et al. 2010) studied a renewable green diesel (alkanes type) by hydrotreated a jatropha oil at standard hydrotreating conditions (temperature of 270 to 300^{o}C and pressure of 20 bar) with Pt/H-ZSM-5 and rhenium-modified Pt/H-ZSM-5 catalysts. The production of hydrocarbons (C_{15}–C_{18} paraffins) cannot produced by the non-modified Pt/H-ZSM-5 catalysts at a high oil per catalyst ratio but the rhenium-modified Pt/H-ZSM-5 catalysts were found more effective for a hydrotreating of jatropha oil process at a high oil per catalyst ratio of 10. The conversion was up to 80% and the selectivity of C_{18} was up to 70%. The deoxygenation activity of a catalyst was improved with the addition of rhenium.

(Sotelo-Boyás, Liu et al. 2011) worked about the hydrocracking of rapeseed oil on three different types of a bifunctional catalysts are Pt/H-Y, Pt/H-ZSM-5 and sulfide NiMo/γ-Al_2O_3. They worked at a temperature range of 300 to 400^{o}C and an initial hydrogen pressure from 50 to 110 bar in a batch reactor. To prevent a high degree of cracking, the reaction time was limited to 3 hours. Among the three catalysts, NiMo/γ-Al_2O_3 gave a highest yield of liquid hydrocarbons in the boiling range of diesel fraction and provided mainly n-paraffins from C_{15} to C_{18}. Therefore, this catalyst produced a diesel with high cetane number but poor cold flow properties. The both zeolitic catalysts produced more iso-paraffins than n-paraffins in the boiling range of C_5 to C_{22}. The Pt-

zeolite catalysts had a strong catalytic activity for cracking and hydrogenation reactions.

(Liu, Sotelo-Boyás et al. 2011) studied about the production of bio-hydrogenated diesel from a hydrotreating of vegetable oils using Ni-Mo based catalysts in a high pressure fixed bed flow reactor at the temperature of 350^{o}C under hydrogen pressure at 40 bar. They used a jatropha curcas L. oil as a feedstock and converted into paraffins by one step hydrotreatment process. The production of hydrocarbons had a high melting point and poor cold properties (a pour point higher than 20^{o}C). The Ni-Mo based catalysts supported on zeolites (such as Ni-Mo/H-Y or Ni-Mo/H-ZSM5) produced a large amount of gasoline hydrocarbons. The Ni-Mo/SiO_2 catalyst favored n-$C_{18}H_{38}$, n-$C_{17}H_{36}$, n-$C_{16}H_{34}$ and n-$C_{15}H_{32}$ production.

In the next year, (Liu, Sotelo-Boyás et al. 2012) worked on the production of bio-hydrogenated diesel by hydrotreatment of high-acid-value waste cooking oil over ruthenium catalyst supported on Al-polyoxocation-pillared montmorillonite at the temperature of 350^{o}C and hydrogen pressure at 20 bar. The triglycerides and free fatty acids in waste cooking oil concurrently deoxygenated. The main products were n-$C_{18}H_{38}$, n-$C_{17}H_{36}$, n-$C_{16}H_{34}$ and n-$C_{15}H_{32}$ with a conversion of 98.9 wt%

A cleaner process for hydrocracking of jatropha oil into green diesel was presented by (Liu, Liu et al. 2013). They used a new green Ni-HPW/Al_2O_3 catalyst in a fixed-bed reactor. They worked on the reaction conditions at 360^{o}C, pressure of 33 bar, liquid hourly space velocity (LHSV) of 1 h^{-1} and hydrogen per oil ratio of 600 Nm^3/m^3. The experiment observed that the higher reaction temperatures favored the decarboxylation and decarbonylation reactions in a hydrotreating process and favored an oxygen removal from the products. A jatropha oil was transformed into hydrocarbons with a conversion of 99.85% and a selectivity of 85.52% of n-C_{15} to n-C_{18} fractions. The new Ni-HPW/Al_2O_3 catalyst had great potential for green diesel production.

A commercially-viable, one-step process for green diesel production from soybean oil on Pt/SAPO-11 catalyst was conducted by (Herskowitz, Landau et al. 2013). In this experiment a trickle-bed reactor was used. They worked on the

temperature of 375 to 380°C, hydrogen pressure of 30.4 bar (30 atm) and liquid hourly space velocities (LHSV) of 1 h^{-1}. The steady-state operation was reached after about 150 hours. The renewable diesel fuel (isodiesel) that produced in this study was improved the properties. The catalyst performed a hydrodeoxygenation to water, decarboxylation to carbondioxide and decarbonylation to carbonmonoxide. The result of this study were measured over the period of 150 to 650 hours. The organic liquid and water yield varied over a narrow range of 85–86 wt% and 7–8 wt%, respectively.

(Srifa, Faungnawakij et al. 2014) studied the production of bio-hydrogenated diesel by catalytic hydrotreating of palm oil over $NiMoS_2/\gamma\text{-}Al_2O_3$ catalyst in continuous flow fixed bed reactor. They found the optimal hydrotreating conditions from the temperature of 270 to 420°C, hydrogen pressure of 15 to 80 bar, liquid hourly space velocity (LHSV) of 0.25 to 5 h^{-1} and hydrogen per oil ratio of 250 to 2000 Nm^3/m^3. The greatest of hydrotreating conditions were: temperature at 300°C, pressure of 30 to 50 bar, liquid hourly space velocity (LHSV) of 1 to 2 h^{-1} and hydrogen per oil ratio of 750 to 1000 Nm^3/m^3. The result of this experiment provided 90.0% of product yield and more than 95.5% of n-alkanes content. The main compositions of liquid product were the n-alkane of C_{16} and C_{18}. The $NiMoS_2/\gamma\text{-}Al_2O_3$ catalyst had a high selective hydrodeoxygenation reaction. They found that the temperature strongly affected to the reaction pathways while the higher hydrogen pressure favored a hydrodeoxygenation reaction.

In addition, there are many research about a hydrotreating of vegetable oil in the different oil sources, reactor type, reaction conditions, catalysts, main products and performance were summarized in Table 3.1.

Table 3.1 The type of oil, reactor, reaction conditions, catalyst, main products and performance of a hydrotreating of vegetable oil
(Adapted from several references).

Oil source	Reactor type	Reaction conditions	Catalyst	Main products	Performance	Ref.
Soybean	Batch	T=400°C P=9.2MPa t=1 h Cat./oil weight ratio = 0.044, 0.088	NiMo/ γ-Al_2O_3	C_{15}-C_{18} n-paraffins	Conversion:92.9% Yield C_{15}-C_{18}: 64.45 wt %	(Veriansyah, Han et al. 2012)
			Pd/γ-Al_2O_3	C_{15}-C_{17} n-paraffins	Conversion:91.9% Yield C_{15}-C_{17}: 79.22 wt%	
			CoMo/ γ-Al_2O_3	C_{15}-C_{17} n-paraffins	Conversion:78.9% Yield C_{15}-C_{17}: 33.67 wt%	
			Ni/ Al_2O_3-SiO_2	C_{15}-C_{17} n-paraffins	Conversion:60.8% Yield C_{15}-C_{17}: 39.24 wt%	
			Pt/γ-Al_2O_3	C_{15}-C_{17} n-paraffins	Conversion:39.7% Yield: 32.00 wt%	
			Ru/γ-Al_2O_3	C_{15}-C_{17} n-paraffins	Conversion:39.7% Yield: 32.00 wt%	
	Batch	T=350°C P=0.7 MPa t=4 h Stirring rate = 1000 rpm	Ni/Al_2O_3	$\geq C_{18}$	Conversion: 68% Yield $\geq C_{18}$: 51.20 wt%	(Morgan, Santillan-Jimenez et al. 2012)
			NiAl/LDH	C_8-C_{17}	Conversion :74% Yield C_8-C_{17}: 52.90 wt%	
			MgAl/LDH	C_8-C_{17}	Conversion: 72% Yield C_8-C_{17}: 47.80 wt%	

Table 3.1 The type of oil, reactor, reaction conditions, catalyst, main products and performance of a hydrotreating of vegetable oil
(Adapted from several references). (Continued)

Oil source	Reactor type	Reaction conditions	Catalyst	Main products	Performance	Ref.
Rapeseed	Fixed bed	T=340°C P=4.0 MPa LHSV=1 h^{-1} H_2/oil ratio = 500-1000 Nm^3/m^3	NiMo/ γ-Al_2O_3	C_{15}-C_{18} n-paraffins	Conversion:93% Yield C_{15}-C_{18} n-paraffins: 54.52 wt%	(Mikulec, Cvengroš et al. 2010)
Sun-flower	Fixed bed	T=350-370°C P=2-4 MPa LHSV=1.0 h^{-1} H_2/oil ratio= 500 Nm^3/m^3	NiMo/ Al_2O_3-F	C_{15}-C_{18} n-paraffins	Yield: 73.2-75.6 wt%	(Kovacs, Kasza et al. 2011)
	Fixed bed	T=380°C P=4-6 MPa LHSV=1.0 h^{-1} H_2/oil ratio= 500-600 Nm^3/m^3	CoMo/Al_2O_3	C_{14}-C_{19} n-paraffins	Conversion: 100% Yield: 73.7-73.9%	(Krár, Kovacs et al. 2010)
Palm	Fixed bed (pilot plant)	T=350°C P=4-9 MPa LHSV=2 h^{-1} TOS=0-14 days	NiMo/Al_2O_3	C_{16}-C_{18} n-paraffins	Molar yield: 100%	(Guzman, Torres et al. 2010)

CHAPTER 4

SIMULATION

The simulation of green diesel production was performed using Aspen Plus program. The procedures of the process simulation consist in defining chemical components and thermodynamical models, selecting and specifying operating equipment and operating conditions. The pseudo simulating components were created by UNIFAC thermodynamic properties. The UNIFAC model was used to predict some binary interaction parameters that were not available in a databank of the simulation.

The simulation study is divided into two main parts. Firstly, the green diesel production process from palm oil by using $NiMoS_2/\gamma\text{-}Al_2O_3$ catalyst will be designed. Second, the energy optimization of a green diesel production process will be designed.

4.1 Green diesel production process by using $NiMoS_2/\gamma\text{-}Al_2O_3$ catalyst

In this work, we studied the green diesel production from the hydrotreating of palm oil and hydrogen with $NiMoS_2/\gamma\text{-}Al_2O_3$ catalyst. Mass and energy balance for each unit, as well as operating conditions, were obtained. The existing pressure drop in different equipment was neglected in the present study.

4.1.1 Experimental studies supporting the process simulation

The simulation study was based on an experimental of (Srifa, Faungnawakij et al. 2014). They investigated the catalytic hydrotreating of palm oil over $NiMoS_2/\gamma\text{-}Al_2O_3$ catalyst at various temperatures (270, 300, 330, 360, 390, 420°C), pressures (15, 30, 50, 80 bar), and hydrogen per oil ratios (250, 500, 750, 1000, 1500, 2000 $N(cm^3/cm^3)$). The continuous flow fixed bed reactor was used to produce a green diesel. Their results showed that a good quality green diesel was produce at 300°C, with pressure of 30 bar, a 1000 $N(cm^3/cm^3)$ of hydrogen per oil ratio. The effect of dominant

hydrotreating parameters (temperature, pressure, hydrogen per oil ratio) can be described as follows:

(1) Effect of hydrotreating temperature

The reaction temperature has been identified as one of dominant parameters on the catalyst performance and catalyst deactivation (Yang, Wang et al. 2013). In this section, they studied the effect of temperature in the range of 270 to 420°C with a fixed other operating condition. At the temperature of 270°C, the organic liquid product became solidified at room temperature. Their result was consistent to those of (Simacek, Kubicka et al. 2009). The increasing temperature from 270 to 300°C increased the product yield. On the other hand, the promotion of isomerization, cracking and cyclization reactions were occurred at the temperature of 330 to 420°C. At 330 to 420°C, the product yield was decreased. The results confirmed that the hydrotreating temperature of 300°C was successful to convert triglyceride to n-alkane for palm oil via $NiMoS_2/\gamma\text{-}Al_2O_3$ catalyst.

(2) Effect of hydrotreating pressure

The pressure was strong effect to deoxygenation, isomerization and cracking reactions. At the pressure of 15 bar, the liquid product remained small amount of fatty acids that indicated the incomplete transformation of free fatty acids to n-alkane. The low conversion was observed at the pressure of 20 bar similarly to (Kubicˇka, Šimácˇek et al. 2009) and (Anand and Sinha 2012). The increasing pressure from 15 to 80 bar slightly increased the product yield. The pressure did not significant effect on the conversion of triglycerides.

(3) Effect of hydrogen per oil ratio

The hydrogen per oil ratio defines to the ratio of hydrogen feed to the liquid feed. The hydrogen per oil ratio showed a small impact on the conversion. The increasing hydrogen per oil ratio from 250 to 1500 $N(cm^3/cm^3)$ improved the product yield. At the hydrogen per oil ratio of 250 $N(cm^3/cm^3)$, the product was separated into two layer at room temperature. However, the hydrogen per oil ratio of 2000 $N(cm^3/cm^3)$

reduced the product yield due to the decreasing of decarbonylation (DCO) and decarboxylation (DCO_2) reactions.

Hydrodeoxygenation (HDO) was a major reaction pathway, whereas decarbonylation (DCO) and decarboxylation (DCO_2) were minor reaction pathways. The palm oil use in their experiment was composed mainly C_{16} and C_{18} fatty acids. Therefore, the main composition of liquid products were C_{16} and C_{18} n-alkane due to high selective hydrodeoxygenation reaction of $NiMoS_2/\gamma\text{-}Al_2O_3$ catalyst.

4.1.2 Description of process simulation

The green diesel production process will be designed under the theoretical concepts and computational methods that describe, represent and simulate the functioning of real-world process.

The green diesel production is produced by the hydrotreating process of palm oil with hydrogen via $NiMoS_2/\gamma\text{-}Al_2O_3$ catalyst. The hydrotreating process for green diesel production is shown in Figure 4.1.

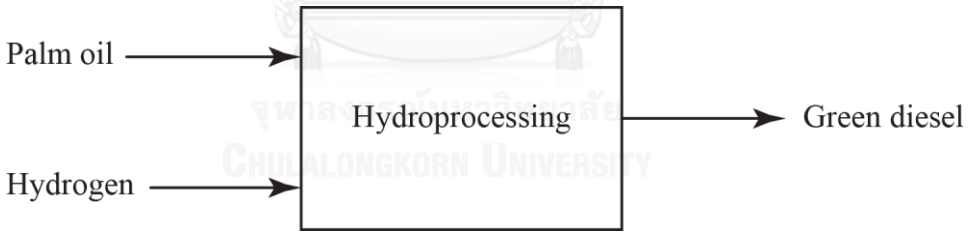

Figure 4.1 The green diesel production process

The simulation study can be divided into four main parts that consists of reactor feed preparation system, reactor system, phase separation system and recycle system. Figure 4.2 shows the process structure of green diesel production (Turton, Bailie et al. 2009).

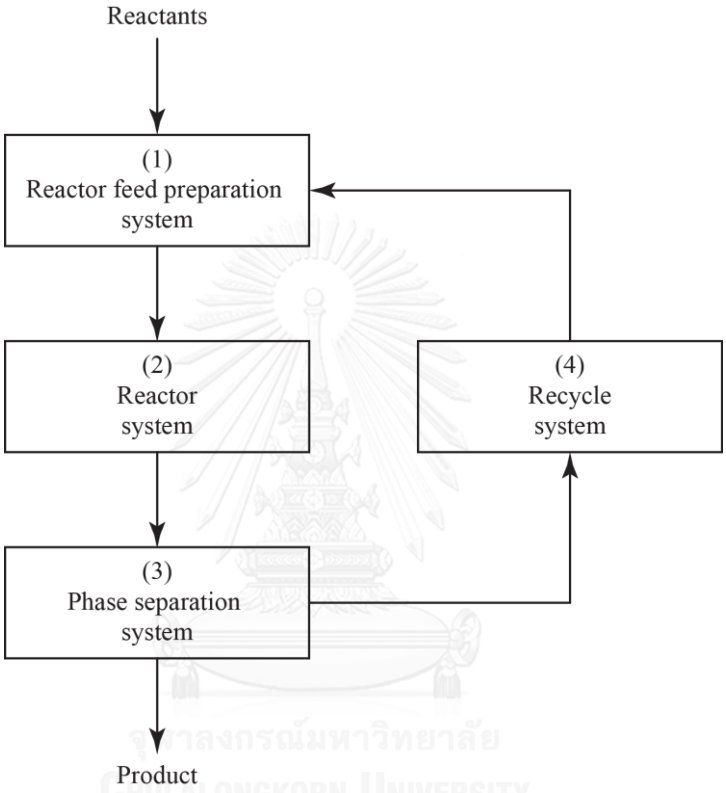

Figure 4.2 The process structure of green diesel production

(1) Reactor feed preparation system

The reactor feed preparation system provides the suitable operating conditions (temperature, pressure, phase etc.). This section also mix the multiple feed streams and/or recycle streams before feeding to the reactor. The green diesel production process is produced by palm oil and hydrogen. The palm oil and hydrogen used in this process are adjusted temperature and pressure as required in the reactor. The palm oil composition used in this simulation is described by its content of fatty acids as it is shown in Table 4.1.

Table 4.1 The palm oil composition used in the simulation study

Component		Name of component	Mass fraction
FFA	FFA1 C16:0	Palmitic acid	42.2%
	FFA2 C18:1	Oleic acid	46.3%
	FFA3 C18:2	Linoleic acid	11.5%

(2) Reactor system

The palm oil and hydrogen from the reactor feed preparation system are mixed and fed into a fixed bed reactor with the suitable operating conditions. In this section, the reaction temperature, pressure and hydrogen per oil ratio will be considered.

The reactions occurred in the reactor are divided into two parts. Firstly, the triglycerides are converted to fatty acids. Second, the fatty acids are converted to n-alkanes. In this work, the palm oil is considered to be composed by trilinolein, tripalmitin and triolein. As first step, free fatty acids are formed by scission of propane from the glycerol backbone of the triglyceride molecules in presence of hydrogen. The three moles of linoleic acid, palmitic acid and oleic acid are formed. In the second step, the unsaturated fatty acids are converted to saturated fatty acids by the hydrogenation. Then, the hydrodeoxygenation (HDO), decarbonylation (DCO) and decarboxylation (DCO_2) are occurred to eliminate oxygen. The hydrodeoxygenation (HDO) removes the oxygen. This reaction keeps the same carbon atoms as in the original fatty acids whereas the decarbonylation (DCO) and decarboxylation (DCO_2) form n-alkane that have one carbon atom less than the original fatty acids. All of reactions for the green diesel production process are shown in Equations (4.1) to (4.12).

$$C_{57}H_{98}O_6 \; + \; 3\,H_2 \leftrightarrow \; 3\,C_{17}H_{31}COOH \; + \; C_3H_8 \tag{4.1}$$

$$(\text{Trilinolein} \; + \; \text{Hydrogen} \; \leftrightarrow \; \text{Linoleic acid} \; + \; \text{Propane})$$

$$C_{51}H_{98}O_6 + 3\,H_2 \leftrightarrow 3\,C_{15}H_{31}COOH + C_3H_8 \quad (4.2)$$

(Tripalmitin + Hydrogen ↔ Palmitic acid + Propane)

$$C_{57}H_{104}O_6 + 3\,H_2 \leftrightarrow 3\,C_{17}H_{33}COOH + C_3H_8 \quad (4.3)$$

(Triolein + Hydrogen ↔ Oleic acid + Propane)

$$C_{17}H_{31}COOH + 2\,H_2 \leftrightarrow C_{17}H_{35}COOH \quad (4.4)$$

(Linoleic acid + Hydrogen ↔ Stearic acid)

$$C_{17}H_{33}COOH + H_2 \leftrightarrow C_{17}H_{35}COOH \quad (4.5)$$

(Oleic acid + Hydrogen ↔ Stearic acid)

$$C_{15}H_{31}COOH + 3\,H_2 \leftrightarrow C_{16}H_{34} + 2\,H_2O \quad (4.6)$$

(Palmitic acid + Hydrogen ↔ Hexadecane + Water)

$$C_{17}H_{35}COOH + 3\,H_2 \leftrightarrow C_{18}H_{38} + 2\,H_2O \quad (4.7)$$

(Stearic acid + Hydrogen ↔ Octadecane + Water)

$$C_{15}H_{31}COOH + H_2 \leftrightarrow C_{15}H_{32} + H_2O + CO \quad (4.8)$$

(Palmitic acid + Hydrogen ↔ Pentadecane + Water + Carbonmonoxide)

$$C_{17}H_{35}COOH + H_2 \leftrightarrow C_{17}H_{36} + H_2O + CO \quad (4.9)$$

(Stearic acid + Hydrogen ↔ Heptadecane + Water + Carbonmonoxide)

$$C_{15}H_{31}COOH \leftrightarrow C_{15}H_{32} + CO_2 \quad (4.10)$$

(Palmitic acid ↔ Pentadecane + Carbondioxide)

$$C_{17}H_{35}COOH \leftrightarrow C_{17}H_{36} + CO_2 \quad (4.11)$$

(Stearic acid ↔ Heptadecane + Water + Carbonmonoxide)

$$C_3H_8 + H_2 \leftrightarrow CH_4 + C_2H_6 \quad (4.12)$$

(Propane + Hydrogen ↔ Methane + Ethane)

Where:

Equations (4.1) to (4.3) are the hydrogenolysis reaction.

Equations (4.4) to (4.5) are the hydrogenation reaction.

Equations (4.6) to (4.7) are the hydrodeoxygenation reaction (HDO).

Equations (4.8) to (4.9) are the decarbonylation reaction (DCO).

Equations (4.10) to (4.11) are the decarboxylation reaction (DCO_2).

Equation (4.12) is the side reaction.

(3) Phase separation system

All of components from the reactor are separated by phase separation system. In this section, the various compounds can be separated from each other by phase separator. In the green diesel production process, all of product from the reactor can be defined as a gases (carbonmonoxide, carbondioxide, methane, ethane, propane, hydrogen), a polar liquid (water) and non-polar liquid (green diesel). As the first step, the gases and liquids will be separated. In the second, the polar and non-polar liquid will be separated. The purity of green diesel, the product yield and the distribution of hydrodeoxygenation (HDO), decarbonylation (DCO) and decarboxylation (DCO_2) are defined in Equations (4.13) to (4.16), respectively.

$$Purity\ (\%) = \frac{Mass\ of\ n{-}alkane\ (n{-}C_{15}to\ n{-}C_{18})\ in\ product\ stream}{Total\ mass\ in\ product\ stream} \times 100 \quad (4.13)$$

$$Product\ yield\ (\%) = \frac{Total\ mass\ of\ n{-}alkane\ (n{-}C_{15}to\ n{-}C_{18})\ in\ product}{Total\ mass\ of\ fatty\ acid\ (C_{15}to\ C_{18})\ in\ feed} \times 100 \quad (4.14)$$

$$HDO\ (\%) = \frac{Total\ mol\ of\ n{-}alkane\ (n{-}C_{16}and\ n{-}C_{18})\ in\ product}{Total\ mol\ of\ fatty\ acid\ (C_{15}to\ C_{18})\ in\ feed} \times 100 \quad (4.15)$$

$$DCO/DCO_2\ (\%) = \frac{Total\ mol\ of\ n{-}alkane\ (n{-}C_{15}and\ n{-}C_{17})\ in\ product}{Total\ mol\ of\ fatty\ acid\ (C_{15}to\ C_{18})\ in\ feed} \times 100 \quad (4.16)$$

(4) Recycle system

The recycle system is used to recycle the excess hydrogen. In this work, the recycle system increases a hydrogen volume that corresponding with hydrogen per oil ratio required in the green diesel production process.

In some case, the unit operations such as heater, cooler, pump and compressor are required to recondition the recycle stream before feeding to the reactor feed preparation system.

4.2 The energy optimization of a green diesel production process

The energy consumption is one of the key factor in various industrial process that affects to operating cost. Thus, the energy optimization must be considered.

4.2.1 The energy optimization by using heat exchanger network (HEN)

In this section, the heat exchanger network (HEN) is used to minimize the energy consumption. A heat exchanger network is designed to handle the heat available. The hot process streams can be used to meet heating demand and the cold process streams can be used to meet cooling demand. Matching heating and cooling duties in the process streams consequently reduce the hot and cold utilities usage. A heat exchanger network can improve the energy efficiency of green diesel production process.

4.2.2 Energy comparison between the original process and heat-integrated processes

This section will compare the energy consumption of the original process and heat-integrated processes. The energy consumption of each processes will be summarized and analyzed the energy saving efficiency.

4.2.3 Effect of the minimum temperature difference (ΔT_{min})

The minimum temperature difference (ΔT_{min}) affects to the heat recovery, cold utility requirement and hot utility requirement of the process. This section will compare the minimum temperature difference (ΔT_{min}) from 10°C to 30°C.

4.2.4 The cost estimation for heat exchanger network

A number of heat exchanger affect to the investment of the process. This section will compare the construction and operation cost of original process, energy optimization strategy 1, 2 and 3.

4.2.5 Pressure drop consideration for the green diesel production process

The pressure drop affects to the required energy of the process. The comparison between the green diesel production process with and without pressure drop will be considered.

CHAPTER 5

RESULTS AND DISCUSSION

In this chapter, the results and discussion of simulation studies of green diesel production is presented. The processes were simulated by using Aspen Plus program. From this simulation studies, the results of product purity, product composition, product yield and energy requirement are interested. This simulation study is divided into two main parts that consist of the green diesel production process by using NiMoS2/γ-Al_2O_3 catalyst and the energy optimization of a green diesel production process by heat exchanger network (HEN).

5.1 Green diesel production process by using $NiMoS_2/\gamma$-Al_2O_3 catalyst

5.1.1 Process description

The process flow diagram for a green diesel production process is shown in Figure 5.1, in which 200,000 metric tons per year of green diesel is produced. Due to the simplicity of the process, an operating factor greater than 0.91 (8,000 hours per year) is used.

A palm oil, Stream 1, which consists of trilinolein 11.5 wt%, tripalmitin 42.2 wt% and triolein 46.3 wt% is pumped to 30 bar by P-101 and heated to 300°C by H-101, respectively. A hydrogen, Stream 4, is reduced pressure to 30 bar by V-101 and heated to 300°C by H-102. Both stream (palm oil and fresh hydrogen) are mixed with recycled hydrogen, Stream 18. The hydrogen per oil ratio before fed to the reactor is 1000:1 by volume. After that, the palm oil and hydrogen is fed to the reactor, R-201.

The reactor, R-201, is fixed bed reactor that operated isothermally at the temperature of 300°C and pressure of 30 bar. The hydrogenolysis, hydrogenation, hydrodeoxygenation (HDO), decarbonylation (DCO), decarboxylation (DCO_2) and

side reaction are occurred. The product from reactor is cooled by H-301 before fed to flash drum, D-301.

The flash drum, D-301, is used to separate gases and liquid product. The gases, Stream 10, consist of unreacted hydrogen and light gas (methane, ethane, carbonmonoxide, carbondioxide). The gases of 99.5 wt% are recycled back to the front end of the process. The liquid product, Stream 11, is degased by expansion, EP-301, before sent to flash drum, D-302, to remove trace amounts of light gases. The liquid product from flash drum, D-302, is sent to decanter to separate primary product (non-polar liquid phase) and water (polar liquid phase).

Stream summaries, equipment summaries are presented in Tables 5.1 to 5.2, respectively.

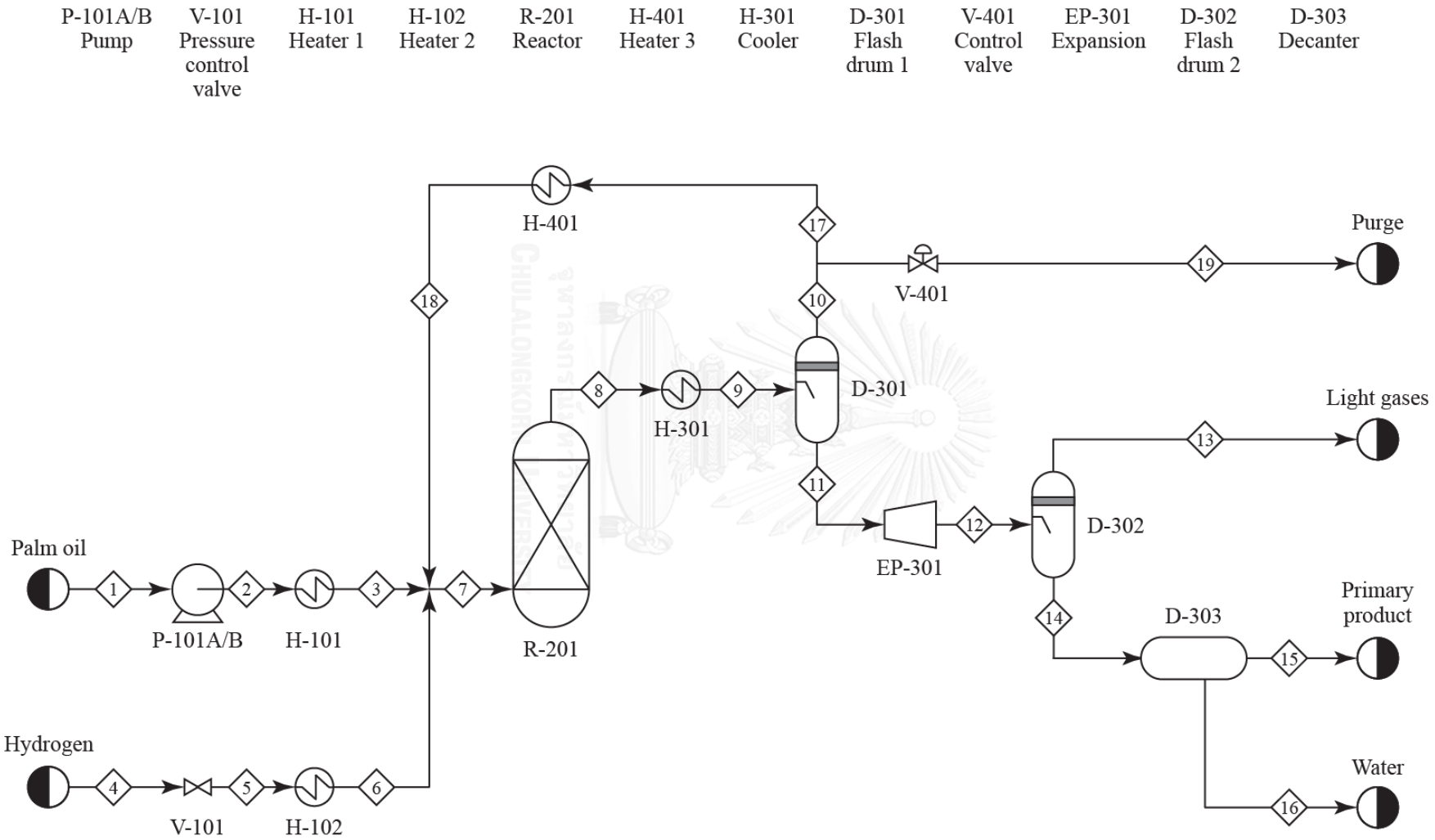

Figure 5.1 The process flow diagram for green diesel production process.

Table 5.1 Simulation results of the original process.

	1	2	3	4	5	6	7
Temperature (°C)	30.00	31.00	300.00	30.00	34.40	300.00	300.10
Pressure (bar)	1.01	30.00	30.00	138.00	30.00	30.00	30.00
Vapor fraction	0.00	0.00	0.00	1.00	1.00	1.00	0.998
Mass flow (kg/hr)	29399.70	29399.70	29399.70	1067.37	1067.37	1067.37	253535.38
Volume flow (cum/hr)	17.95	17.96	23.35	105.03	459.30	850.05	35800.44
Enthalpy (Gcal/hr)	-18.16	-18.14	-13.73	0.04	0.04	1.02	-177.01
Mass flow (kg/hr)							
H_2	0	0	0	1067.37	1067.37	1067.37	29486.76
CO	0	0	0	0	0	0	54129.93
CH_4	0	0	0	0	0	0	46494.93
C_2H_6	0	0	0	0	0	0	61958.94
CO_2	0	0	0	0	0	0	30217.67
C_3H_8	0	0	0	0	0	0	0
H_2O	0	0	0	0	0	0	1844.03
$C_{15}H_{32}$	0	0	0	0	0	0	1.20
$C_{16}H_{34}$	0	0	0	0	0	0	1.63
$C_{17}H_{36}$	0	0	0	0	0	0	0.24
$C_{18}H_{38}$	0	0	0	0	0	0	0.35
$C_{16}H_{32}O_2$	0	0	0	0	0	0	0
$C_{18}H_{32}O_2$	0	0	0	0	0	0	0
$C_{18}H_{34}O_2$	0	0	0	0	0	0	0
TG2	12409.79	12409.79	12409.79	0	0	0	12409.79
TG1	3379.39	3379.39	3379.39	0	0	0	3379.39
TG3	13610.52	13610.52	13610.52	0	0	0	13610.52

Table 5.1 Simulation results of the original process. (Continued)

	8	9	10	11	12	13	14
Temperature (°C)	300.00	50.00	50.00	50.00	39.90	39.90	39.90
Pressure (bar)	30.00	30.00	30.00	30.00	1.01	1.01	1.01
Vapor fraction	1.00	0.985	1.00	0.00	0.156	1.00	0.00
Mass flow (kg/hr)	253535.38	253535.38	224145.18	29390.20	29390.20	1369.29	28020.91
Volume flow (cum/hr)	35623.49	19732.09	19689.40	42.70	1360.18	1323.42	36.76
Enthalpy (Gcal/hr)	-182.30	-237.10	-212.17	-24.93	-24.93	-1.676	-23.31
Mass flow (kg/hr)							
H_2	0	0	0	0	0	0	0
CO	28558.61	28558.61	28558.61	< 0.001	< 0.001	< 0.001	trace
CH_4	54456.88	54456.88	54395.38	61.50	61.50	60.36	1.14
C_2H_6	47049.77	47049.77	46716.43	333.34	333.34	297.30	36.04
CO_2	62998.92	62998.92	62264.11	734.81	734.81	615.33	119.48
C_3H_8	30731.38	30731.38	30354.17	377.21	377.21	315.17	62.04
H_2O	0	0	0	0	0	0	0
$C_{15}H_{32}$	4951.57	4951.57	1853.04	3098.53	3098.53	81.02	3017.51
$C_{16}H_{34}$	2205.18	2205.18	1.21	2203.98	2203.98	0.04	2203.94
$C_{17}H_{36}$	8094.41	8094.41	1.64	8092.78	8092.78	0.05	8092.74
$C_{18}H_{38}$	3119.06	3119.06	0.24	3118.82	3118.82	0.01	3118.82
$C_{16}H_{32}O_2$	11369.59	11369.59	0.35	11369.24	11369.24	0.01	11369.25
$C_{18}H_{32}O_2$	0	0	0	0	0	0	0
$C_{18}H_{34}O_2$	0	0	0	0	0	0	0
TG2	0	0	0	0	0	0	0
TG1	0	0	0	0	0	0	0
TG3	0	0	0	0	0	0	0

Table 5.1 Simulation results of the original process. (Continued)

	15	16	17	18	19
Temperature (°C)	39.90	39.90	50.00	300.00	50.00
Pressure (bar)	1.01	1.01	30.00	30.00	30.00
Vapor fraction	0.00	0.00	1.00	1.00	1.00
Mass flow (kg/hr)	25000.38	3020.53	223068.31	223068.31	1076.87
Volume flow (cum/hr)	33.66	3.10	19594.81	34924.58	94.59
Enthalpy (Gcal/hr)	-11.88	-11.43	-211.15	-164.31	-1.02
Mass flow (kg/hr)					
H_2	0	0	0	0	0
CO	trace	trace	28421.41	28419.40	137.21
CH_4	0.90	0.24	54134.05	54129.93	261.33
C_2H_6	35.10	0.94	46491.99	46494.93	224.44
CO_2	118.34	1.14	61964.97	61958.94	299.14
C_3H_8	56.53	5.51	30208.34	30217.67	145.83
H_2O	0	0	0	0	0
$C_{15}H_{32}$	4.77	3012.74	1844.14	1844.03	8.90
$C_{16}H_{34}$	2203.94	< 0.001	1.20	1.20	0.01
$C_{17}H_{36}$	8092.74	< 0.001	1.63	1.63	0.01
$C_{18}H_{38}$	3118.82	trace	0.24	0.24	0.00
$C_{16}H_{32}O_2$	11369.25	trace	0.35	0.35	0.00
$C_{18}H_{32}O_2$	0	0	0	0	0
$C_{18}H_{34}O_2$	0	0	0	0	0
TG2	0	0	0	0	0
TG1	0	0	0	0	0
TG3	0	0	0	0	0

Table 5.2 Equipment summary for the original process.

Pump	**P-101A/B**			
Flow (kg/hr)	29399.70			
Volumetric flow (m^3/hr)	17.95			
Power (shaft) (kW)	28.66			
Efficiency	0.50			
Temperature (in) (°C)	30.00			
Temperature (out) (°C)	31.00			
Pressure (in) (bar)	1.01			
Pressure(out) (bar)	30.00			
Pressure reducing unit	**V-101**	**EP-301**		
Pressure (in) (bar)	138.00	30.00		
Pressure (out) (bar)	30.00	1.01		
Power (kW)		-60.40		
Reactor	**R-201**			
Temperature (°C)	300.00			
Pressure (bar)	30.00			
Duty (kW)	-6142.59			
Orientation	Vertical			
Type	Fixed bed isothermal reactor			
Heaters	**H-101**	**H-102**	**H-301**	**H-401**
Temperature (in) (°C)	31.00	34.40	300.00	50.00
Temperature (out) (°C)	300.00	300.00	50.00	300.00
Pressure (bar)	30.00	30.00	30.00	30.00
Duty (kW)	5128.93	1142.43	-63741.28	54496.92

Table 5.2 Equipment summary for the original process. (Continued)

Vessels	**D-301**	**D-302**	**D-303**
Temperature (°C)	50.00	42.84	42.84
Pressure (bar)	30.00	1.01	1.01
Vapor fraction	0.99	0.16	-
Orientation	Vertical	Vertical	Horizontal

Under this condition, the purity of green diesel and green diesel yield are 99.2% and 88.3%, respectively. For the $NiMoS_2/\gamma\text{-}Al_2O_3$ catalyst, the hydrodeoxygenation (HDO) is favorer than decarbonylation (DCO) and decarboxylation (DCO_2). Therefore, the main composition of liquid product is n-C_{16} and n-C_{18} due to high selective hydrodeoxygenation (HDO) reaction. The comparison between original process and experimental data is shows in Table 5.3. The overall energy requirement of the original process is 124,509.56 kW. However, the overall energy requirement for green diesel production process can be reduced by using heat exchanger network (HEN).

Table 5.3 Comparison between the original process and experimental data.

	Experimental Data (Srifa, Faungnawakij et al. 2014)	**This work**	**Difference**
Raw material	Palm oil	Palm oil	-
Liquid product composition (%)			
$C_{15}H_{32}$	7.98	8.90	0.92
$C_{16}H_{34}$	30.78	32.65	1.87
$C_{17}H_{36}$	13.45	12.58	-0.87
$C_{18}H_{38}$	47.79	45.87	-1.92
Product purity (%)	-	99.20	-
Product yield (%)	89.80	88.25	-1.55
HDO (%)	77.78	77.50	-0.28
DCO/DCO_2 (%)	22.22	22.50	0.28

Table 5.3 shows the details of the original process compared with experimental data. The tolerance allowed is not more than 2% and the results of original process correspond with the experimental data.

5.2 The energy optimization of a green diesel production process

Efficiency energy utilization can reduce the cost of the process. To minimize the energy consumption of the green diesel production process, the heat exchanger network (HEN) is considered. In the original process, the product stream from the reactor is used to pre-heat palm oil feed stream, hydrogen feed stream and recycled hydrogen stream. Table 5.4 shows the heat exchange stream data for the green diesel production process.

Table 5.4 Heat exchange stream data for the green diesel production process.

Stream	Type	Supply temperature (°C)	Target temperature (°C)	Input Q (kW)	Heat capacity flow rate, CP* (kW/°C)
Hot	H-1	300.00	50.00	-63741.30	254.97
Cold	C-1	31.00	300.00	5128.93	19.07
Cold	C-2	34.40	300.00	1142.43	4.30
Cold	C-3	50.00	300.00	54496.90	217.99

* Heat capacity flow rate in this table not depend on the temperature.

From Table 5.4, the hot stream has a CP of 255 kW/°C and is cooled from 300°C to 50°C and losses of 63,741.30 kW. The cold streams are heated from 31°C to 300°C, 34.4°C to 300°C and 50°C to 300°C with the CP of 19 kW/°C, 4 kW/°C and 218 kW/°C and loss of 5,129 kW, 1,142 kW and 54,496.9 kW, respectively. The grid diagram of interval temperature versus heat capacity flow rate of hot and cold streams is presented in Figure 5.2. The construction of the hot composite curve and cold composite curve are shown in Figure 5.3 and Figure 5.4.

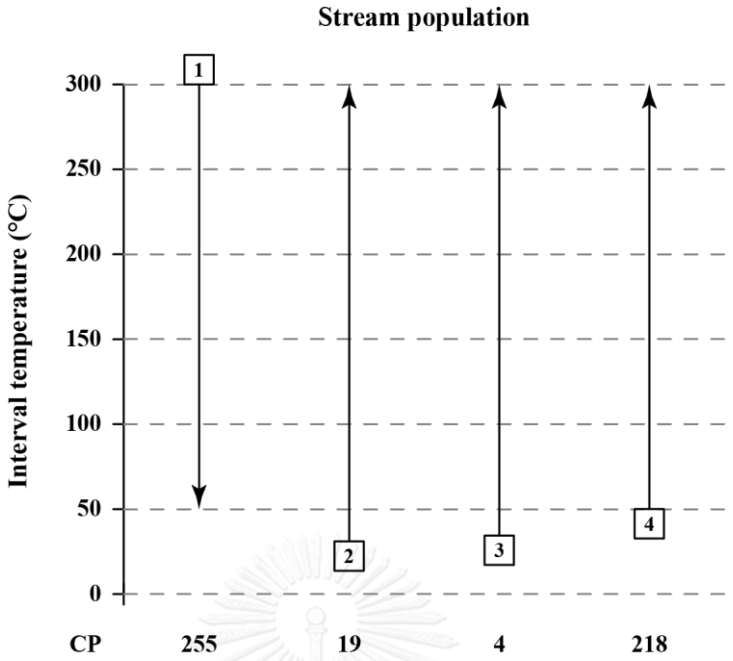

Figure 5.2 Grid diagram of hot and cold streams.

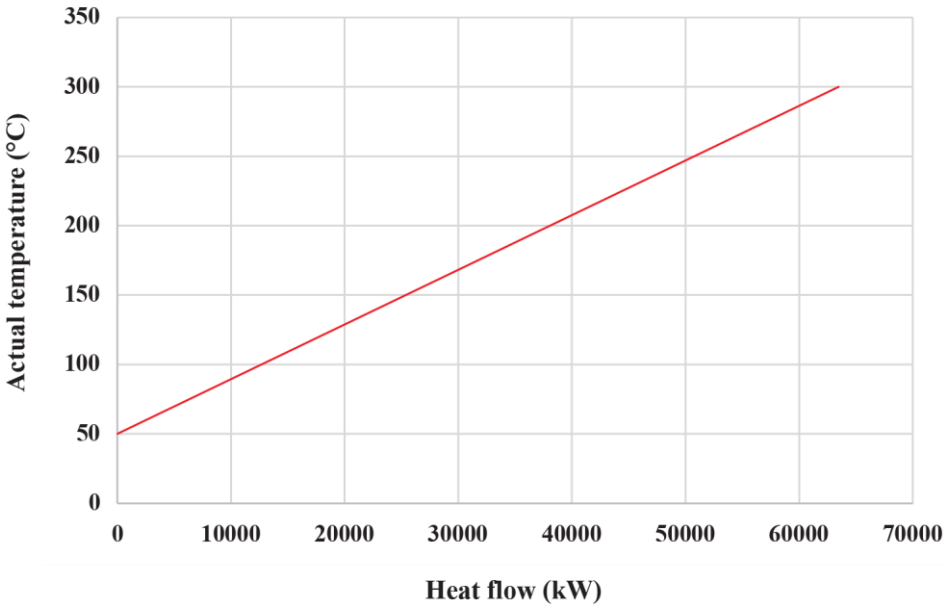

Figure 5.3 The hot composite curve of the process.

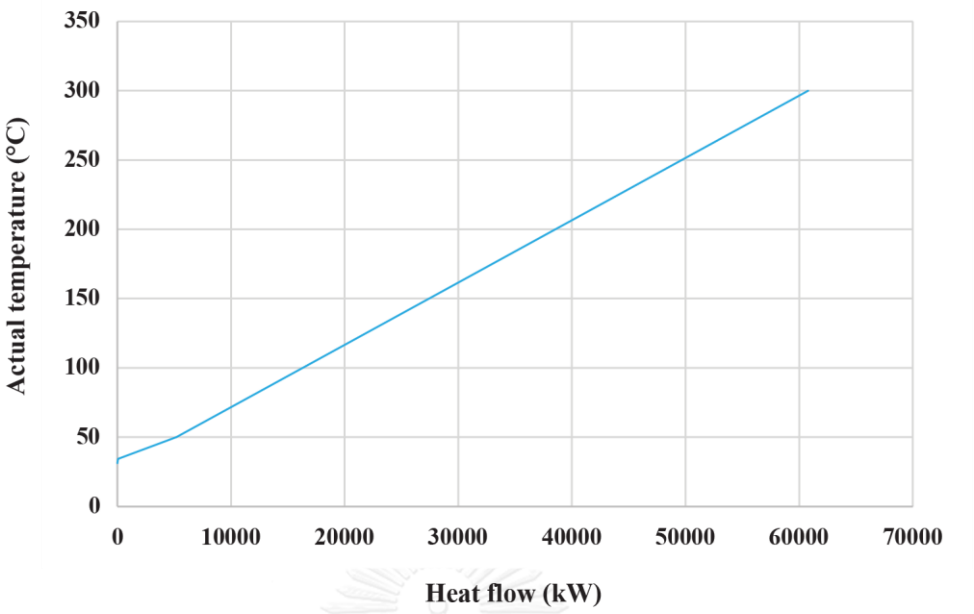

Figure 5.4 The cold composite curve of the process.

The composite curves can be used to illustrate the minimum energy target of the process. The composite curves of hot and cold streams with the minimum temperature difference (ΔT_{min}) of 20°C is presented in Figure 5.5.

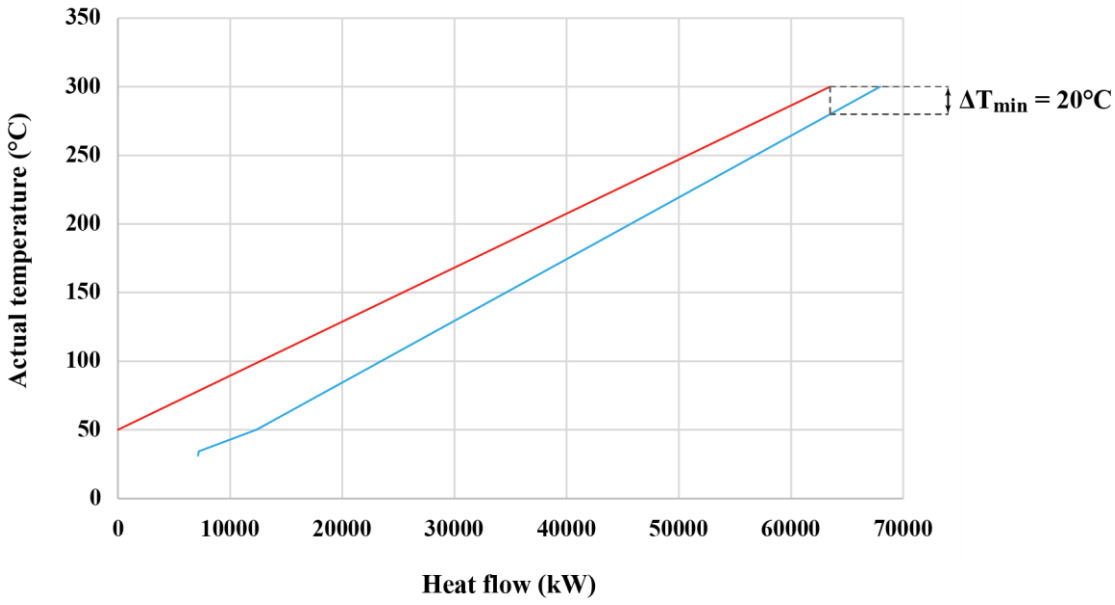

Figure 5.5 The composite curves for hot and cold streams at ΔT_{min} of 20°C.

As illustrated in Figure 5.5, the maximum heat recovery, minimum cold utility requirement and minimum hot utility requirement are around 56,269, 7,137 and 4,461 kW, respectively.

In this section, the energy optimization of a green diesel production process is divided into 3 strategies.

5.2.1 Energy optimization strategy 1

In this strategy, the product, Stream 10, is used to exchange the energy with recycled hydrogen stream, hydrogen feed stream and palm oil feed stream, respectively. The minimum temperature difference is set at 20°C.

Through this strategy, 25,000 kg/h of green diesel with purity of 99.2% are obtained with the total energy consumption of 22,654.65 kW. The yield of the process is 88.25%. The unit operation consists of pump, valve, reactor, heat exchanger, expansion, flash drum and decanter.

The process flow diagram of energy optimization strategy 1 is shown in Figure 5.6. The grid diagram of the heat exchanger network for energy optimization strategy 1 and the energy requirement of the original process and optimization strategy 1 are presented in Figures 5.7 and 5.8, respectively. From this strategy, the heat of 81.80% is saved when compares with the original process. The equipment of this strategy is summarized in Table 5.5.

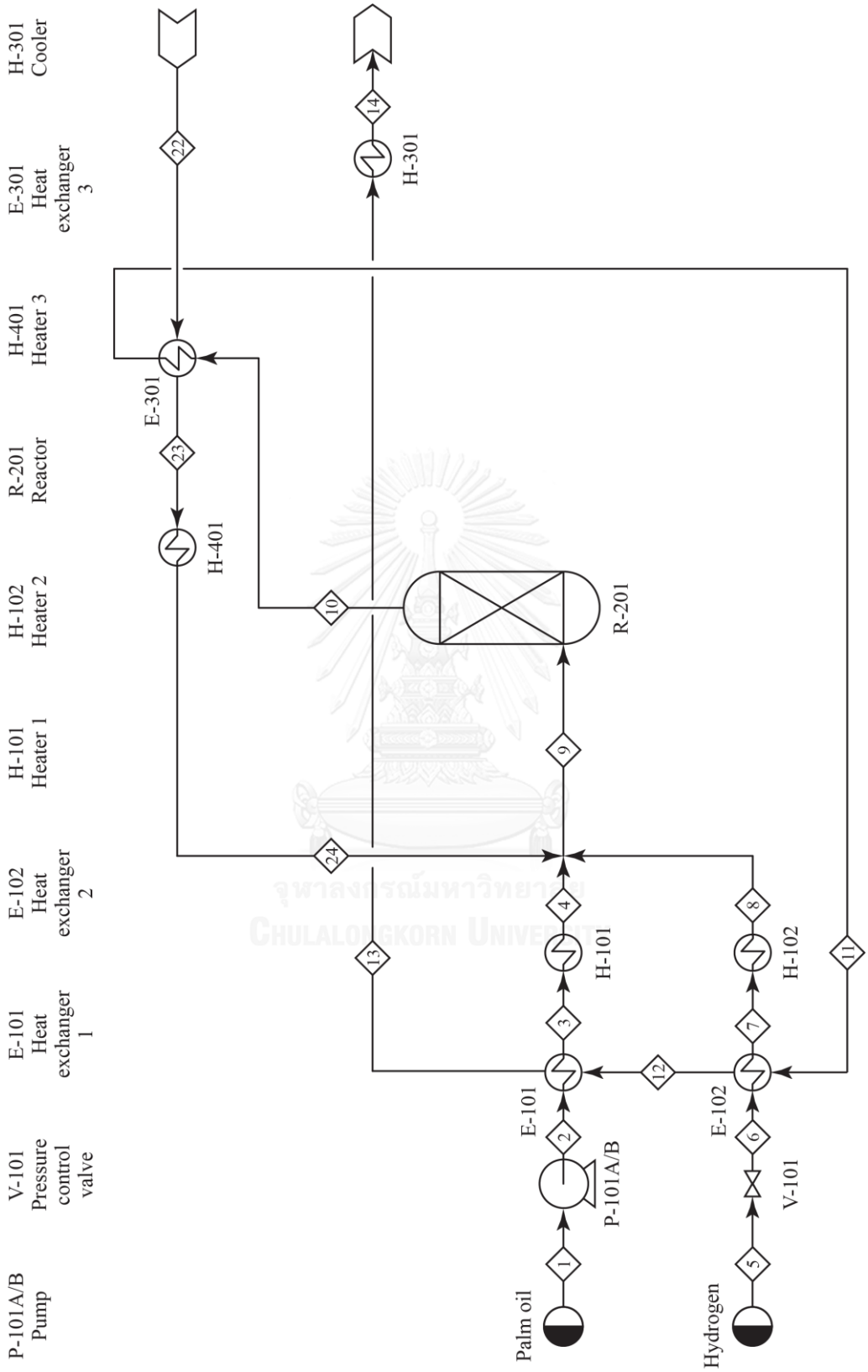

Figure 5.6 The process flow diagram for energy optimization strategy 1.

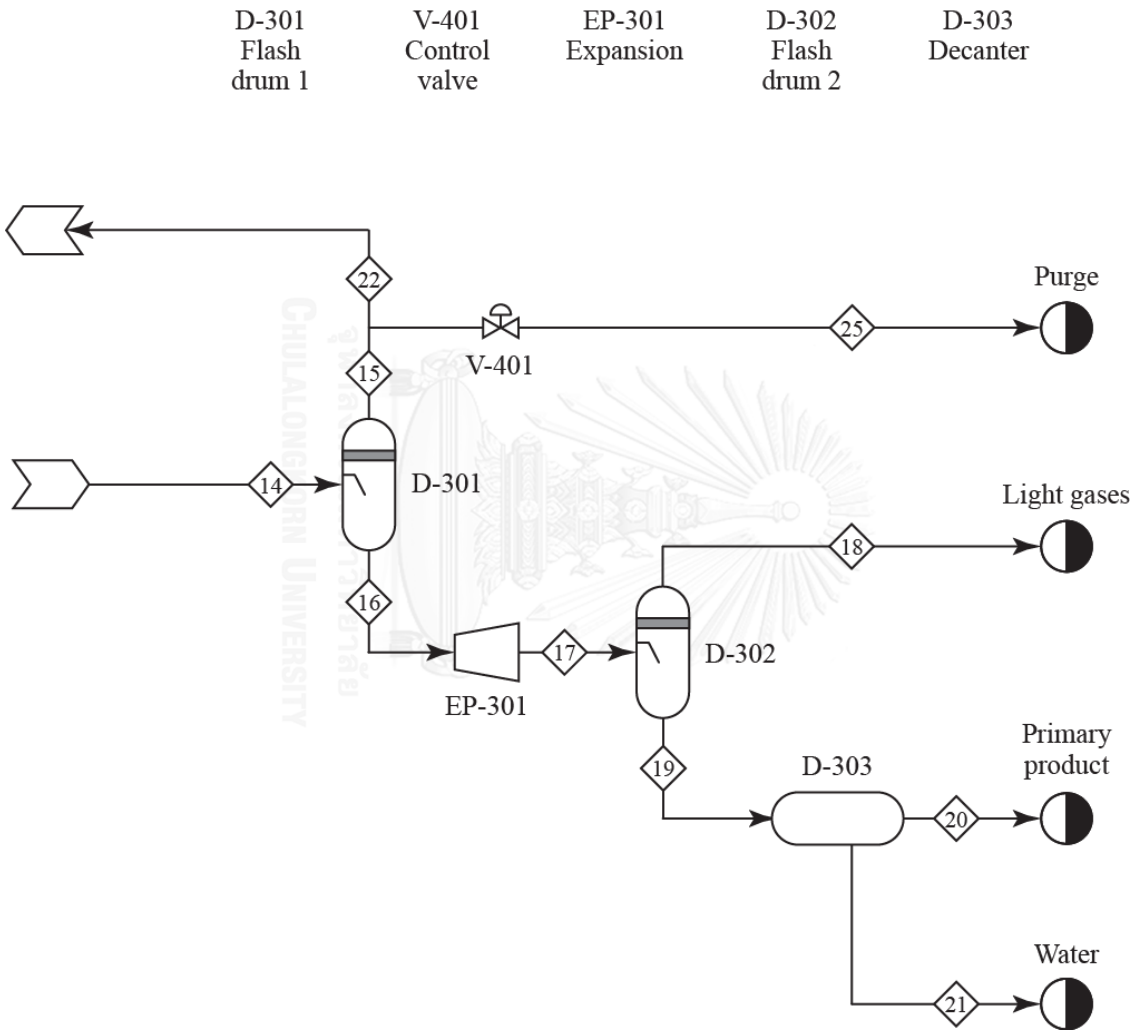

Figure 5.6 The process flow diagram for energy optimization strategy 1. (Continued)

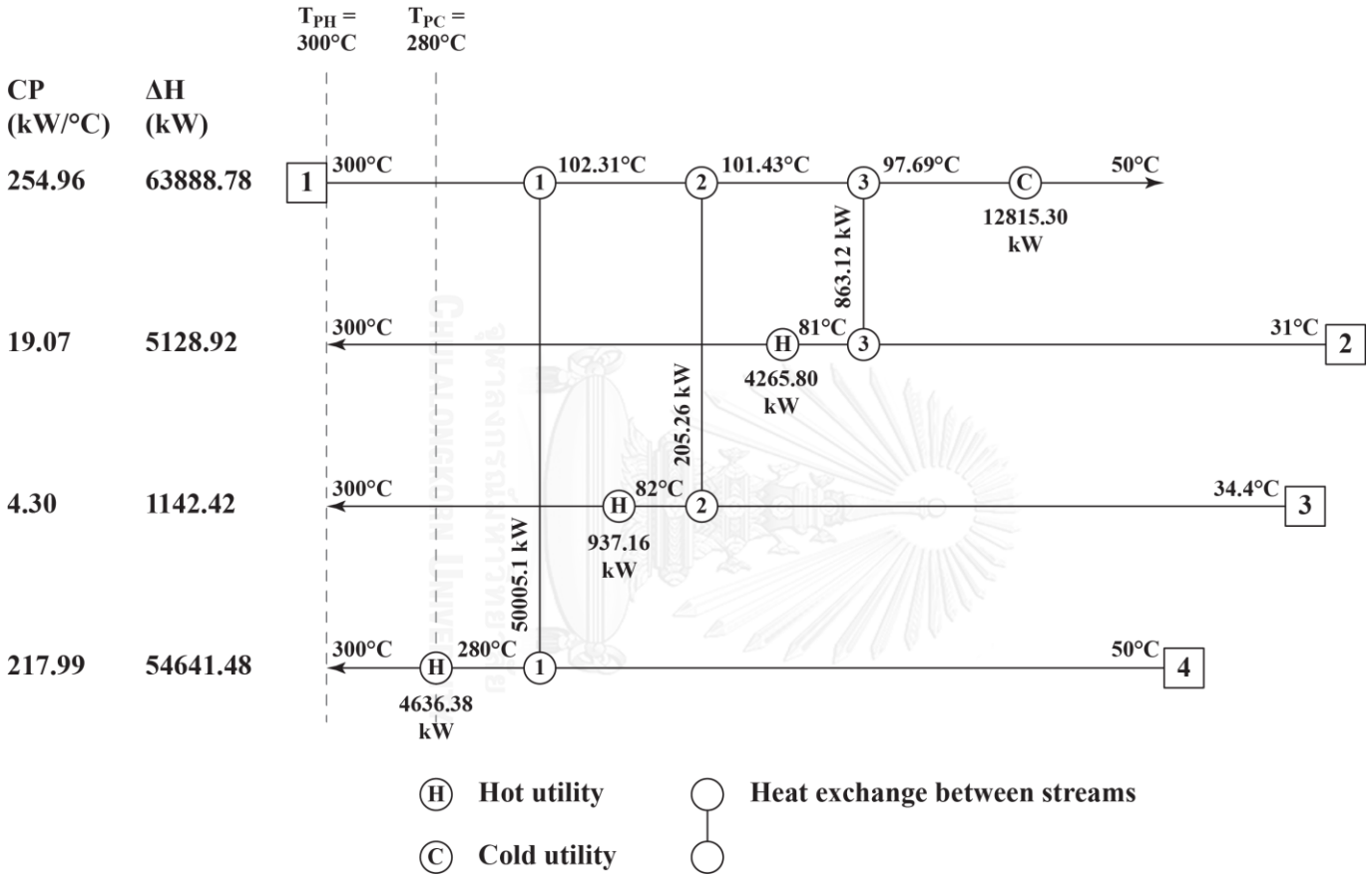

Figure 5.7 The grid representation of the heat exchanger network for energy optimization strategy 1.

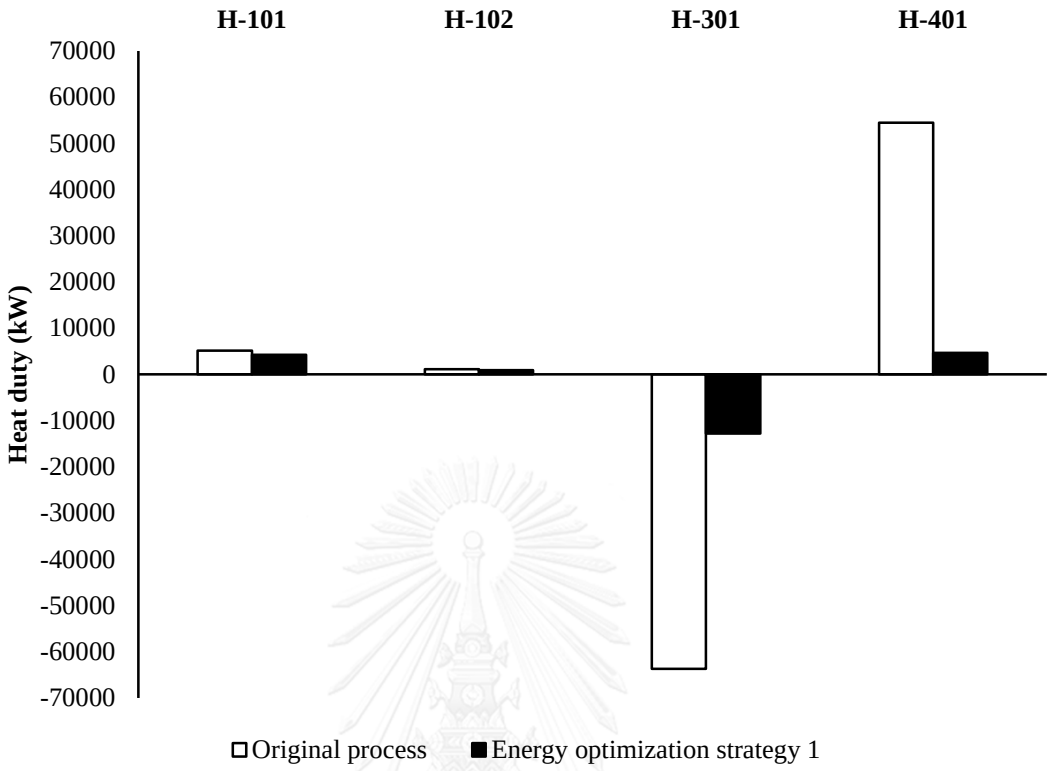

Figure 5.8 The energy requirement of
the original process and optimization strategy 1.

Table 5.5 Equipment summary for the energy optimization strategy 1.

Pump	**P-101A/B**	
Flow (kg/hr)	29399.70	
Volumetric flow (m^3/hr)	17.95	
Power (shaft) (kW)	28.66	
Efficiency	0.50	
Temperature (in) (°C)	30.00	
Temperature (out) (°C)	31.00	
Pressure (in) (bar)	1.01	
Pressure(out) (bar)	30.00	
Pressure reducing unit	**V-101**	**EP-301**
Pressure (in) (bar)	138.00	30.00
Pressure (out) (bar)	30.00	1.01
Power (kW)		-60.40
Reactor	**R-201**	
Temperature (°C)	300.00	
Pressure (bar)	30.00	
Duty (kW)	-6142.38	
Orientation	Vertical	
Type	Fixed bed isothermal reactor	

Table 5.5 Equipment summary for the energy optimization strategy 1. (Continued)

Heat exchanger	**E-101**	**E-102**	**E-301**	
Type	Shell and tube	Shell and tube	Shell and tube	
Area (m^2)	26.18	6.21	1869.64	
Duty (kW)	863.12	205.26	50005.10	
Temperature (°C)				
Hot stream (in)	101.43	102.31	300.00	
Hot stream (out)	97.69	101.43	102.31	
Cold stream (in)	30.96	34.36	50.00	
Cold stream (out)	81.43	82.31	280.00	
Heaters	**H-101**	**H-102**	**H-301**	**H-401**
Temperature (in) (°C)	81.43	82.31	97.70	280.00
Temperature (out) (°C)	300.00	300.00	50.00	300.00
Pressure (bar)	30.00	30.00	30.00	30.00
Duty (kW)	4265.80	937.16	-12815.30	4636.38
Vessels	**D-301**	**D-302**	**D-303**	
Temperature (°C)	50.00	42.84	42.84	
Pressure (bar)	30.00	1.01	1.01	
Vapor fraction	0.99	0.16	-	
Orientation	Vertical	Vertical	Horizontal	

5.2.2 Energy optimization strategy 2

This strategy is similar to the optimization strategy 1 but the sequence of heat exchanger is changed. The product, Stream 10, is used to exchange the energy with palm oil feed stream, hydrogen feed stream and recycled hydrogen stream, respectively. The minimum temperature difference is set at 20°C.

In this process, 25,000 kg/h of green diesel with purity of 99.2% is produced. The product yield of this process is the same as for energy optimization strategy 1. The unit operation of this strategy consists of pump, valve, reactor, heat exchanger, expansion, flash drum and decanter. The energy consumption of this process is 23,987.54 kW. The heat of 80.73% is saved when compares with the original process. The difference of energy saving of strategy 1 and strategy 2 is 1.07%. The heat recovery of energy optimization strategy 1 is better than energy optimization strategy 2 due to the boundary of minimum temperature difference of hot and cold streams. Thus, the exchanged heat sequence affects on the energy saving.

The process flow diagram for energy optimization strategy 2 is shown in Figure 5.9. The grid diagram of the heat exchanger network for energy optimization strategy 2 and the energy requirement of the original process and optimization strategy 2 are presented in Figures 5.10 and 5.11, respectively. The equipment of this strategy is summarized in Table 5.6.

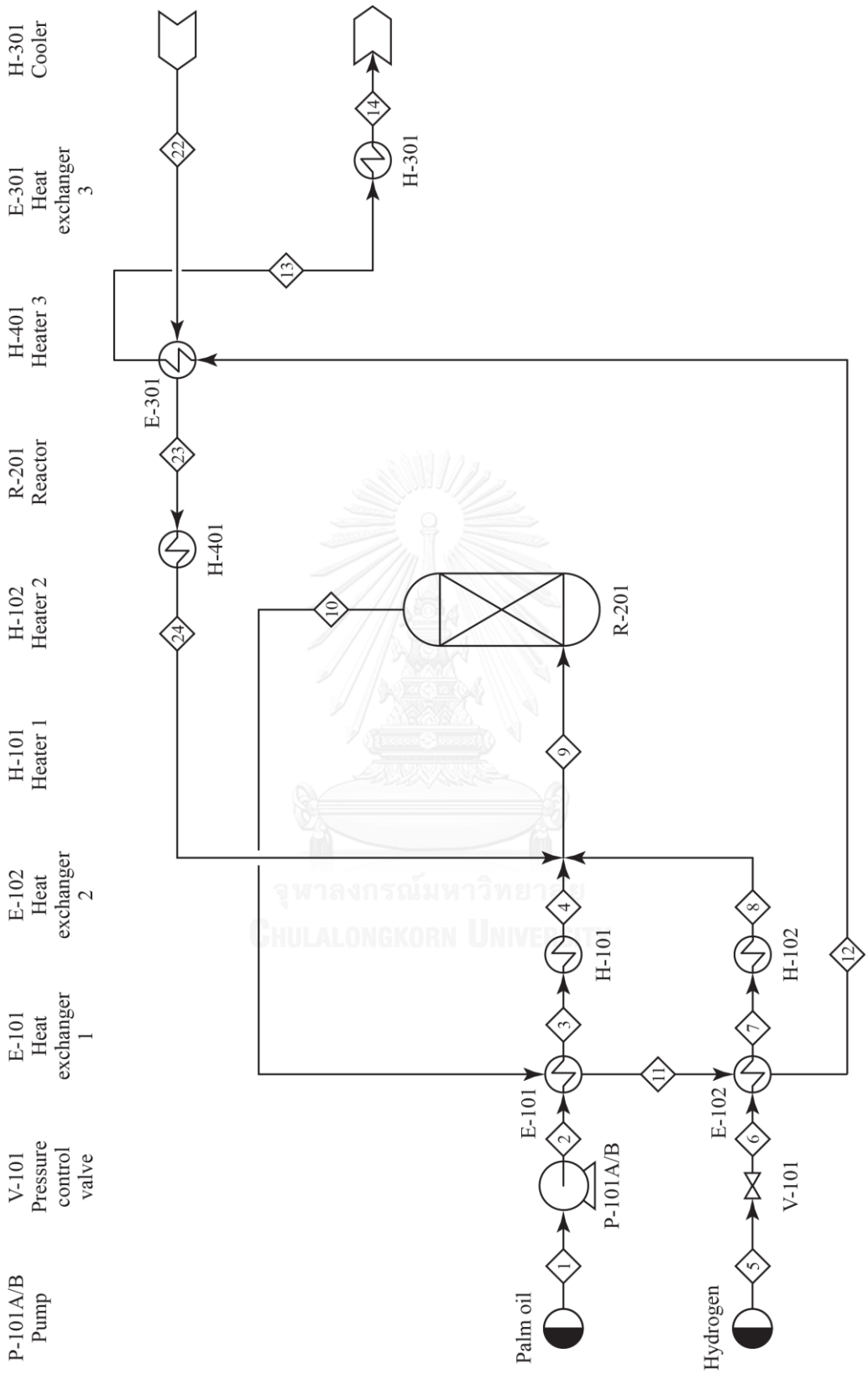

Figure 5.9 The process flow diagram for energy optimization strategy 2.

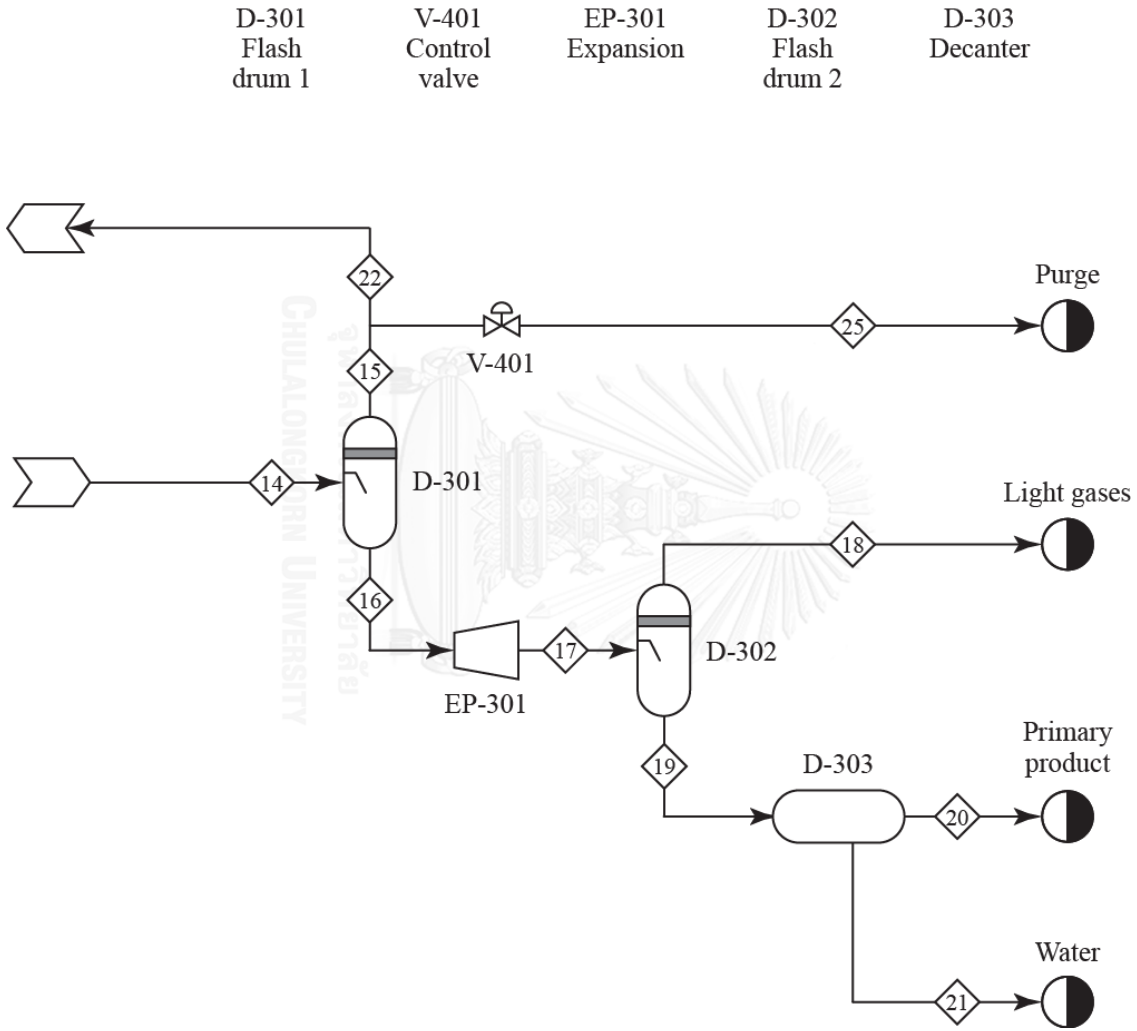

Figure 5.9 The process flow diagram for energy optimization strategy 2. (Continued)

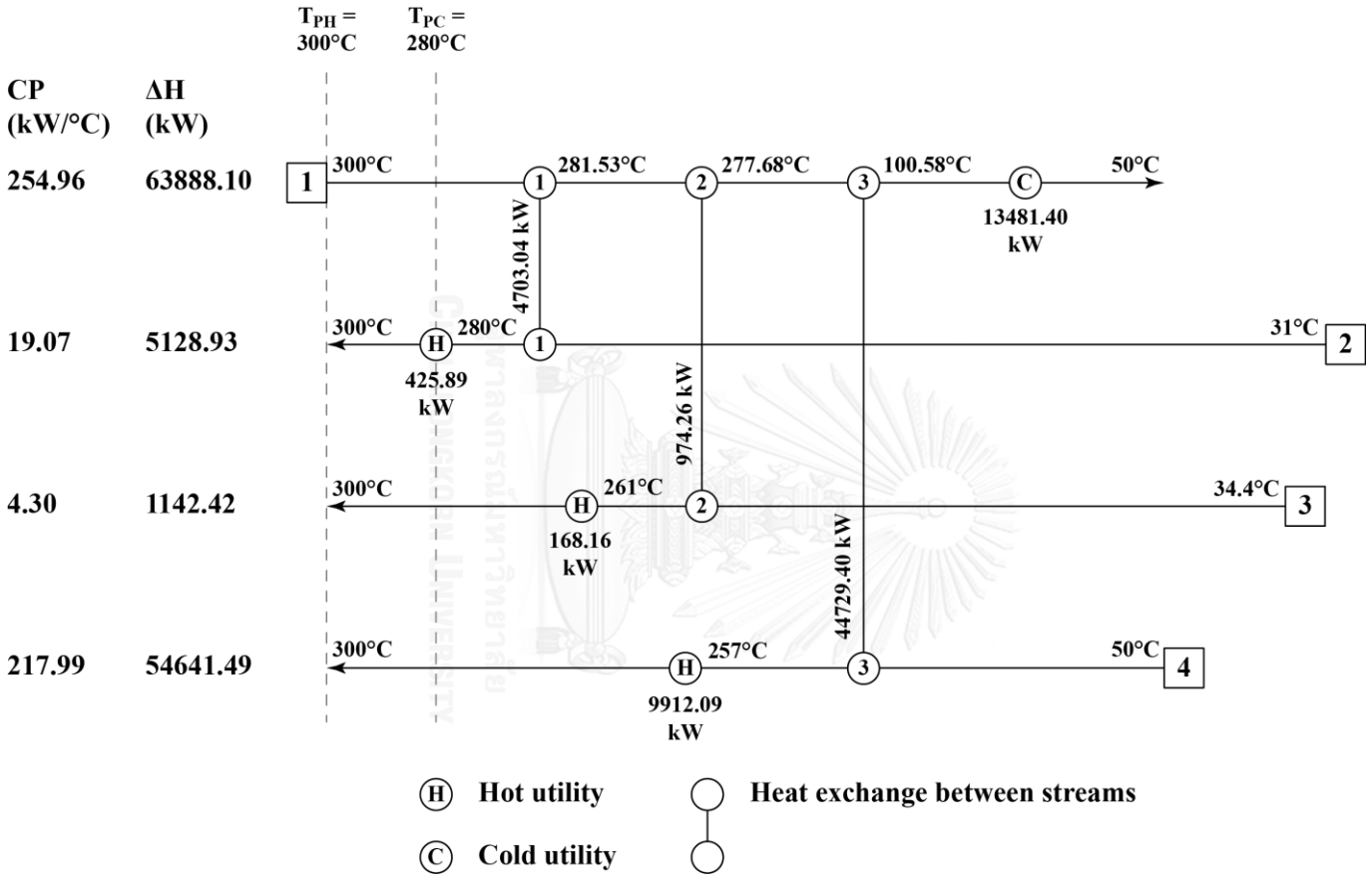

Figure 5.10 The grid representation of the heat exchanger network for energy optimization strategy 2.

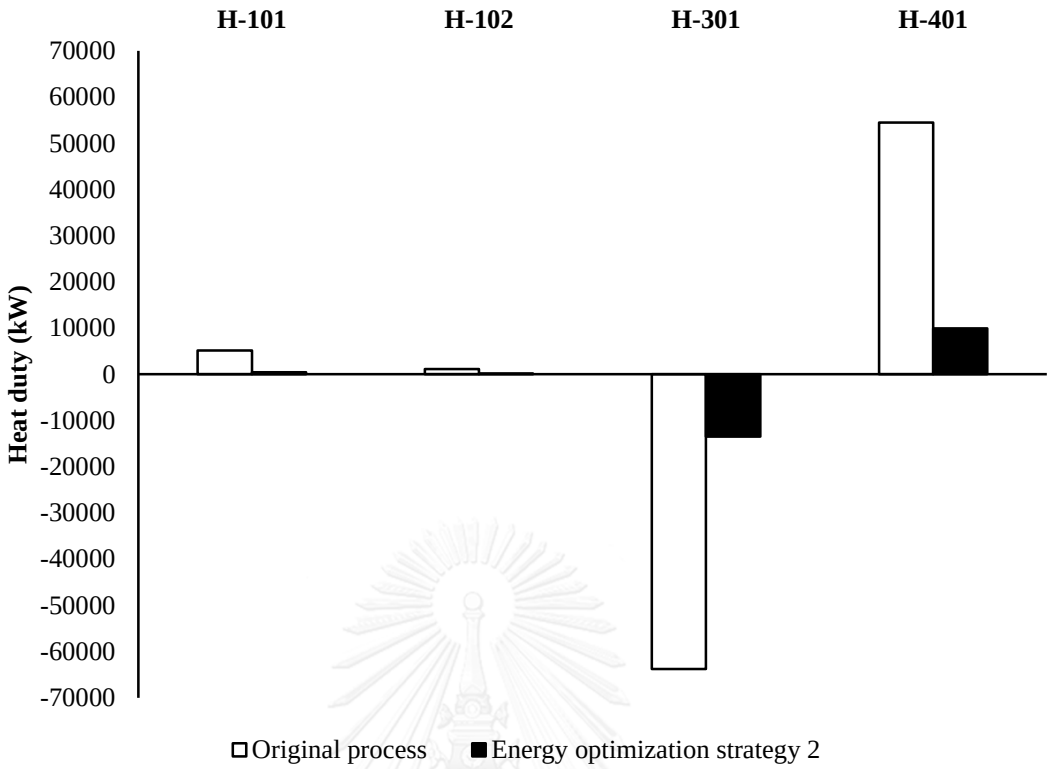

Figure 5.11 The energy requirement of
the original process and optimization strategy 2.

Table 5.6 Equipment summary for the energy optimization strategy 2.

Pump	**P-101A/B**	
Flow (kg/hr)	29399.70	
Volumetric flow (m^3/hr)	17.95	
Power (shaft) (kW)	28.66	
Efficiency	0.50	
Temperature (in) (°C)	30.00	
Temperature (out) (°C)	31.00	
Pressure (in) (bar)	1.01	
Pressure(out) (bar)	30.00	
Pressure reducing unit	**V-101**	**EP-301**
Pressure (in) (bar)	138.00	30.00
Pressure (out) (bar)	30.00	1.01
Power (kW)		-60.40
Reactor	**R-201**	
Temperature (°C)	300.00	
Pressure (bar)	30.00	
Duty (kW)	-6142.38	
Orientation	Vertical	
Type	Fixed bed isothermal reactor	

Table 5.6 Equipment summary for the energy optimization strategy 2. (Continued)

Heat exchanger	**E-101**	**E-102**	**E-301**	
Type	Shell & tube	Shell & tube	Shell & tube	
Area (m^2)	60.66	12.72	1662.11	
Duty (kW)	4703.04	974.26	44729.40	
Temperature (°C)				
Hot stream (in)	300.00	281.53	277.68	
Hot stream (out)	281.53	277.68	100.58	
Cold stream (in)	30.96	34.36	50.00	
Cold stream (out)	280.00	261.00	257.00	
Heaters	**H-101**	**H-102**	**H-301**	**H-401**
Temperature (in) (°C)	280.00	261.00	100.58	257.00
Temperature (out) (°C)	300.00	300.00	50.00	300.00
Pressure (bar)	30.00	30.00	30.00	30.00
Duty (kW)	425.89	168.16	-13481.40	9912.09
Vessels	**D-301**	**D-302**	**D-303**	
Temperature (°C)	50.00	42.84	42.84	
Pressure (bar)	30.00	1.01	1.01	
Vapor fraction	0.99	0.16	-	
Orientation	Vertical	Vertical	Horizontal	

5.2.3 Energy optimization strategy 3

To minimize the energy consumption in the process, the heat exchanger network is used to exchange the heat from hot and cold streams. In this strategy, the product, Stream 10, is split to three streams in order to exchange with cold stream. The first stream, Stream 11, is used to exchange the energy with palm oil feed stream. The second stream, Stream 13, is used to exchange the energy with hydrogen feed stream and the last stream, Stream 15, is used to exchange the energy with recycled hydrogen stream. The minimum temperature difference is set at 20°C.

In this process, 25,000 kg/h of green diesel with purity of 99.2% is produced. The product yield of this process is 88.25%. The energy consumption of this process is 13,253.88 kW. When compare with the original process, 89.36% of energy is saved. In this process, the unit operation consists of pump, valve, reactor, heat exchanger, expansion, flash drum and decanter.

Comparison of strategy 3 with the strategy 1 and 2, the highest energy saving efficiency is energy optimization strategy 3 due to each split hot streams can be exchanged the energy at a maximum temperature of hot stream. The driving forces of the strategy 3 is high due to the great temperature difference between hot and cold streams in this process.

In the energy optimization strategy 1 and 2, the driving forces of the strategy 1 and 2 are lower than the strategy 3 due to the lower temperature difference between hot and cold streams in this process. The hot stream temperature is decreased rapidly when the hot stream is used to meet heating demand with minimum temperature difference (ΔT_{min}) of 20°C. Therefore, the energy exchange is limited under the minimum temperature difference between hot and cold stream that results in the energy cannot be fully exchanged even if the streams have a sufficient energy.

The process flow diagram for energy optimization strategy 3 is shown in Figure 5.12. The grid diagram of the heat exchanger network for energy optimization strategy 3 and the energy requirement of the original process and optimization strategy 3 are presented in Figures 5.13 and 5.14, respectively. The equipment summary of this strategy is presented in Table 5.7 and the comparison of performance for a green diesel production process with heat-integrated, energy optimization strategy 1, 2 and 3, is presented in Table 5.8.

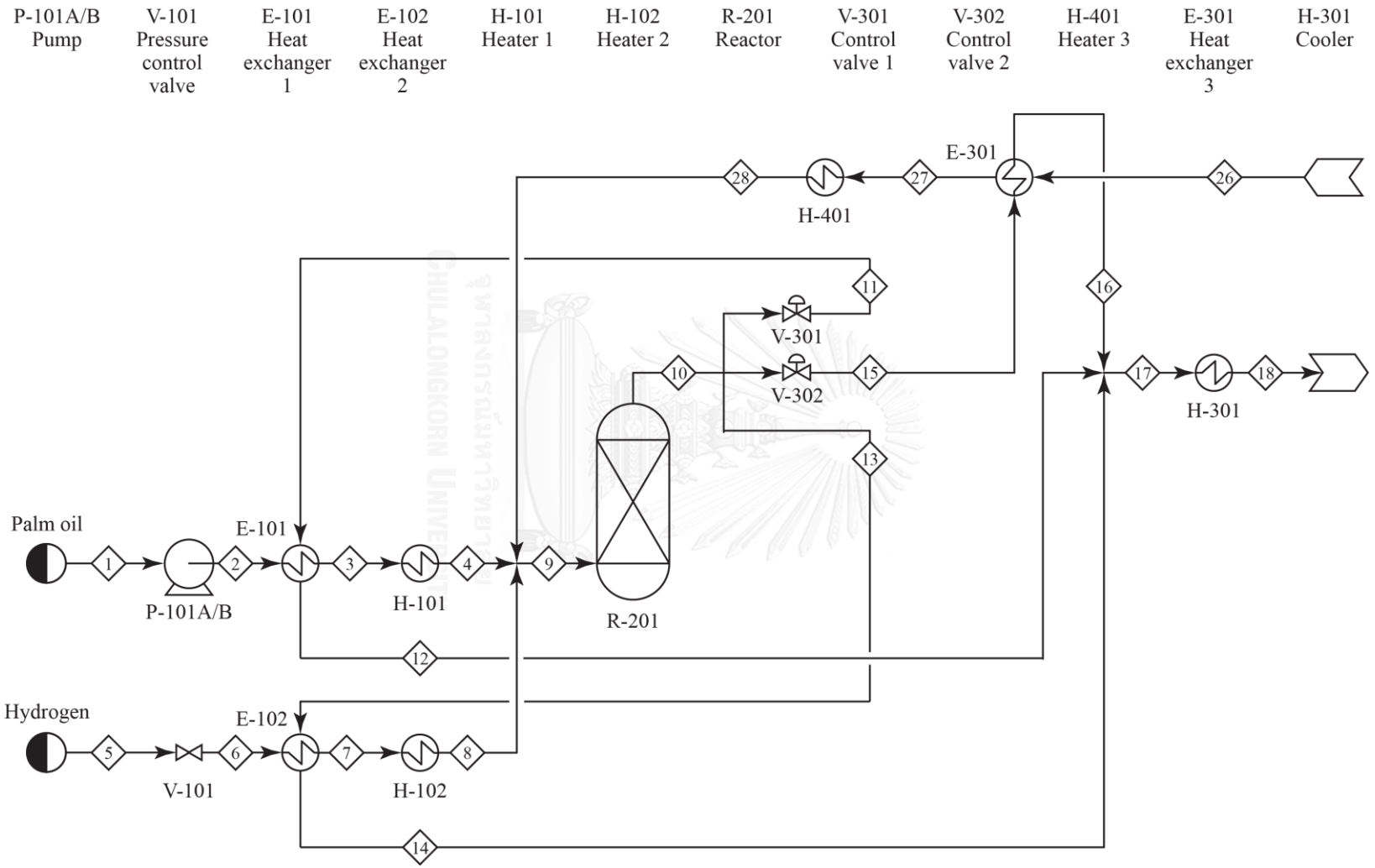

Figure 5.12 The process flow diagram for energy optimization strategy 3.

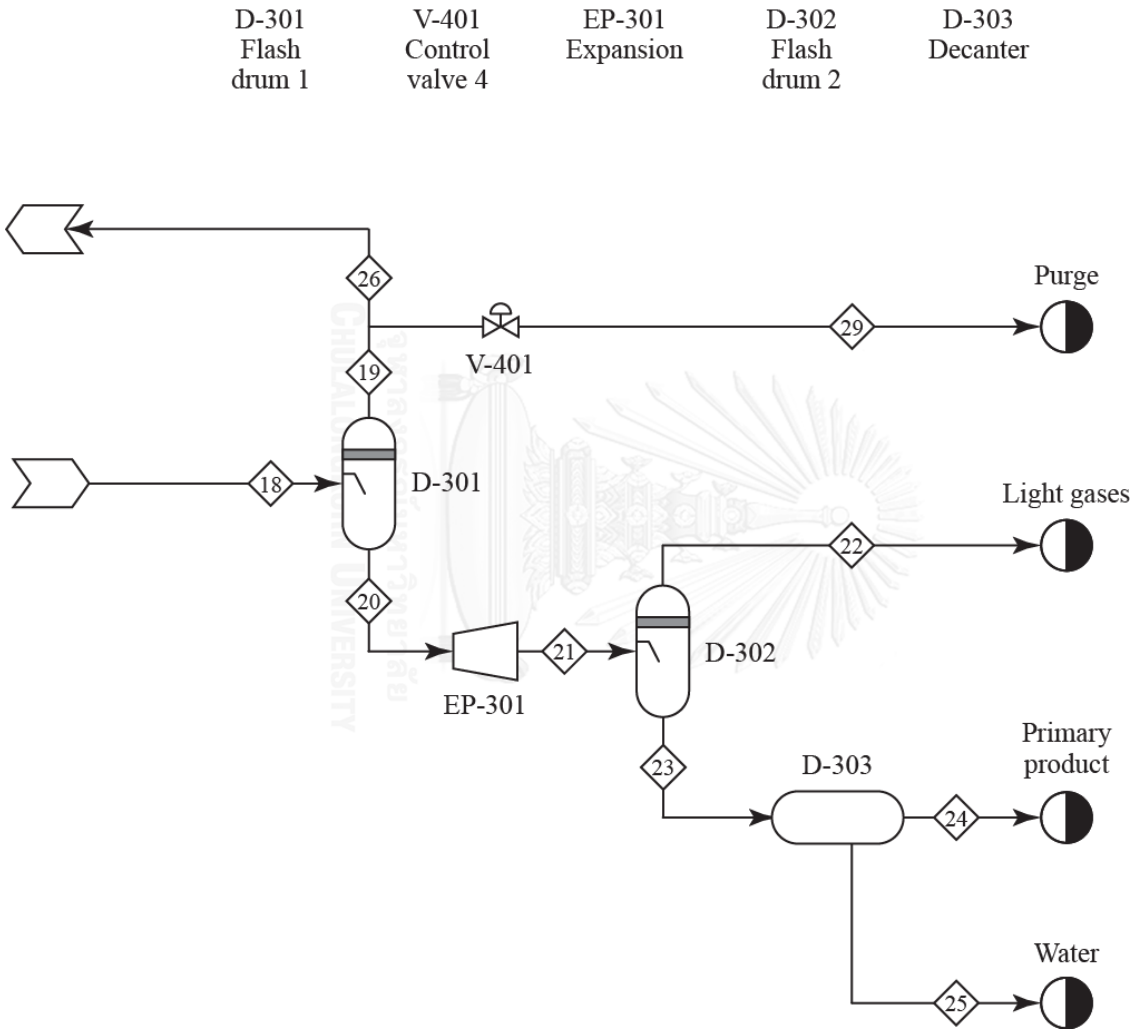

Figure 5.12 The process flow diagram for energy optimization strategy 3. (Continued)

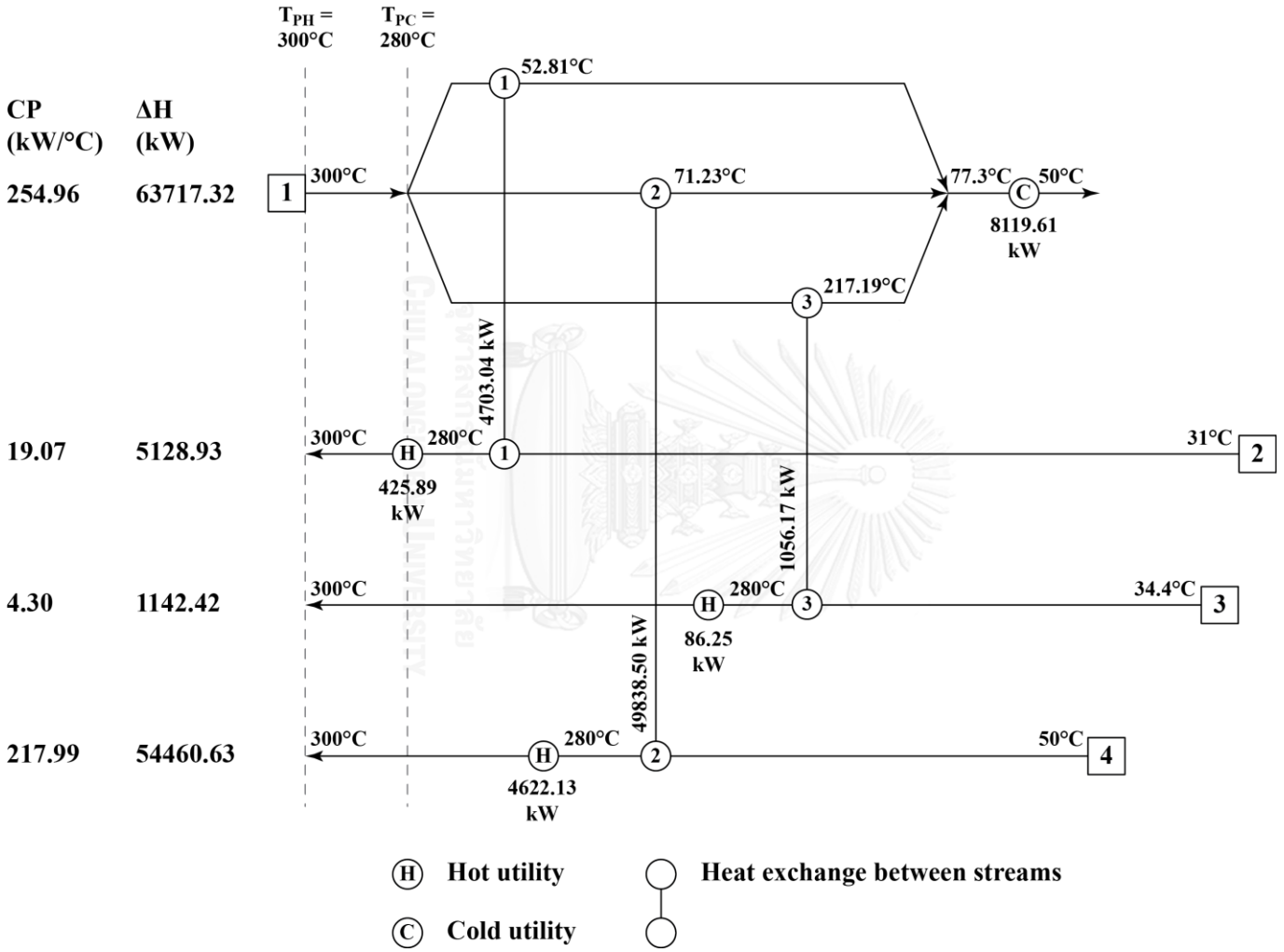

Figure 5.13 The grid representation of the heat exchanger network for energy optimization strategy 3.

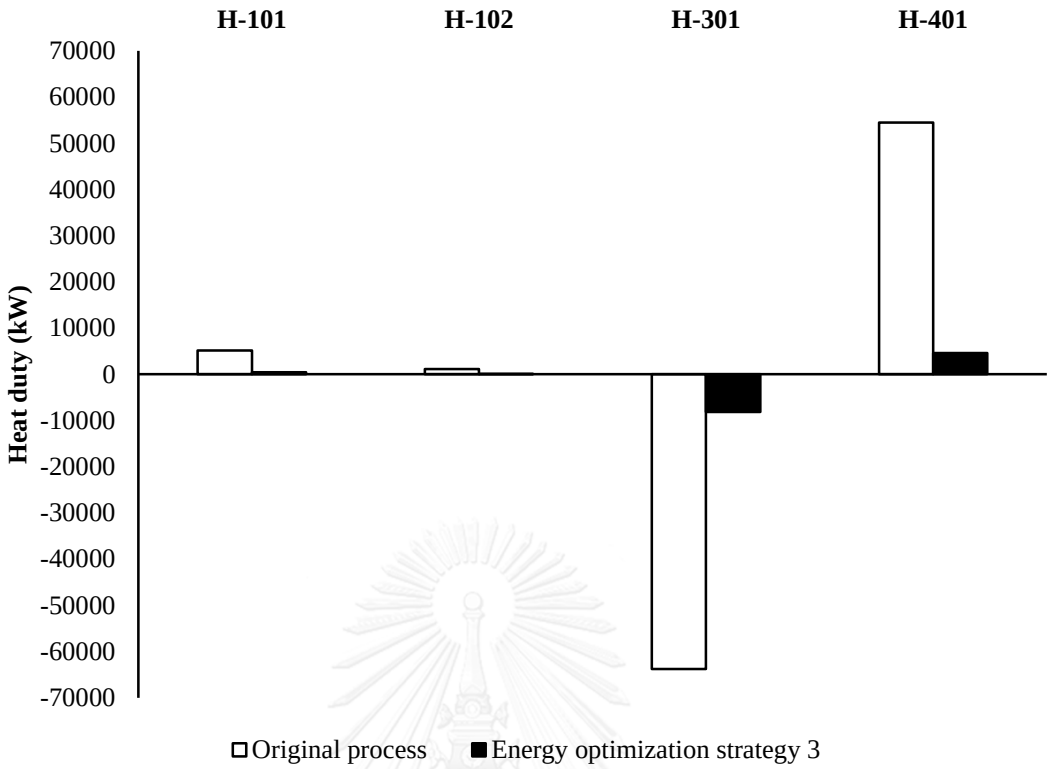

Figure 5.14 The energy requirement of
the original process and optimization strategy 3.

Table 5.7 Equipment summary for the energy optimization strategy 3.

Pump	**P-101A/B**	
Flow (kg/hr)	29399.70	
Volumetric flow (m^3/hr)	17.95	
Power (shaft) (kW)	28.66	
Efficiency	0.50	
Temperature (in) (°C)	30.00	
Temperature (out) (°C)	31.00	
Pressure (in) (bar)	1.01	
Pressure(out) (bar)	30.00	
Pressure reducing unit	**V-101**	**EP-301**
Pressure (in) (bar)	138.00	30.00
Pressure (out) (bar)	30.00	1.01
Power (kW)		-60.40
Reactor	**R-201**	
Temperature (°C)	300.00	
Pressure (bar)	30.00	
Duty (kW)	-6142.38	
Orientation	Vertical	
Type	Fixed bed isothermal reactor	

Table 5.7 Equipment summary for the energy optimization strategy 3. (Continued)

Heat exchanger	**E-101**	**E-102**	**E-301**	
Type	Shell & tube	Shell & tube	Shell & tube	
Area (m^2)	327.88	16.95	3067.65	
Duty (kW)	4703.04	1056.17	49838.50	
Temperature (°C)				
Hot stream (in)	300.00	300.00	300.00	
Hot stream (out)	52.81	217.188	71.23	
Cold stream (in)	30.96	34.36	50.00	
Cold stream (out)	280.00	280.00	280.00	
Heaters	**H-101**	**H-102**	**H-301**	**H-401**
Temperature (in) (°C)	280.00	280.00	77.3	280.00
Temperature (out) (°C)	300.00	300.00	50.00	300.00
Pressure (bar)	30.00	30.00	30.00	30.00
Duty (kW)	425.89	86.25	-8119.61	4622.13
Vessels	**D-301**	**D-302**	**D-303**	
Temperature (°C)	50.00	42.84	42.84	
Pressure (bar)	30.00	1.01	1.01	
Vapor fraction	0.99	0.16	-	
Orientation	Vertical	Vertical	Horizontal	

Table 5.8 The comparison of performance for green diesel production process with heat exchanger network (HEN).

	Original	**Strategy 1**	**Strategy 2**	**Strategy 3**
Hydrogen to oil feed volume ratio	1005.84	1011.24	1011.24	1003.71
Green diesel purity (wt%)	99.20	99.20	99.20	99.20
Green diesel yield (%)	88.25	88.25	88.25	88.25
H-101, heat duty (kW)	5128.93	4265.80	425.89	425.89
H-102, heat duty (kW)	1142.43	937.16	168.16	86.25
H-301, heat duty (kW)	-67341.3	-12815.30	-13481.40	-8119.61
H-401, heat duty (kW)	54496.9	4636.38	9912.09	4622.13
Cold utility requirement (kW)	63741.30	12815.30	13481.40	8119.61
Hot utility requirement (kW)	60768.26	9839.34	10506.14	5134.27
Heat recovery (kW)	-	102146.97	100813.40	111195.42
Total energy requirement (kW)	124509.56	22654.64	23987.54	13253.88
Heating requirement reduce (%)	-	83.81	82.71	91.55
Cooling requirement reduce (%)	-	80.97	78.85	87.26
Energy saving (%)	0	81.80	80.73	89.36
Productivity (kg green diesel/h)	25000	25000	25000	25000
Number of unit operation				
Pump	1	1	1	1
Valve	1	1	1	1
Reactor	1	1	1	1
Heat exchanger	4	7	7	7
Expansion	1	1	1	1
Flash drum	2	2	2	2
Decanter	1	1	1	1
Total unit operation	11	14	14	14

As summarized in Table 5.8, it can be seen that the heat integrated processes require lower energy consumption than the original process. The heating requirement are reduced by 84%, 83% and 92% and the cooling requirement are reduced by 81%, 79% and 87% for the energy optimization strategy 1, strategy 2 and strategy 3, respectively. The results show that the great strategy for minimum energy usage is the strategy 3. The strategy 3 can be reduced 111,195 kW of energy usage in the process. Thus, the heat exchanger network can be reduced heat of the process and improved the efficiency of energy usage.

5.2.4 The effect of minimum temperature difference (ΔT_{min})

The minimum temperature difference (ΔT_{min}) fixes the relative position of the hot and cold composite curves. Figures 5.15 to 5.18 show the composite curves of the process with the minimum temperature difference of 10°C, 15°C, 25°C and 30°C, respectively. (The composite curves of the process with the minimum temperature difference of 20°C is shown in Figure 5.5.)

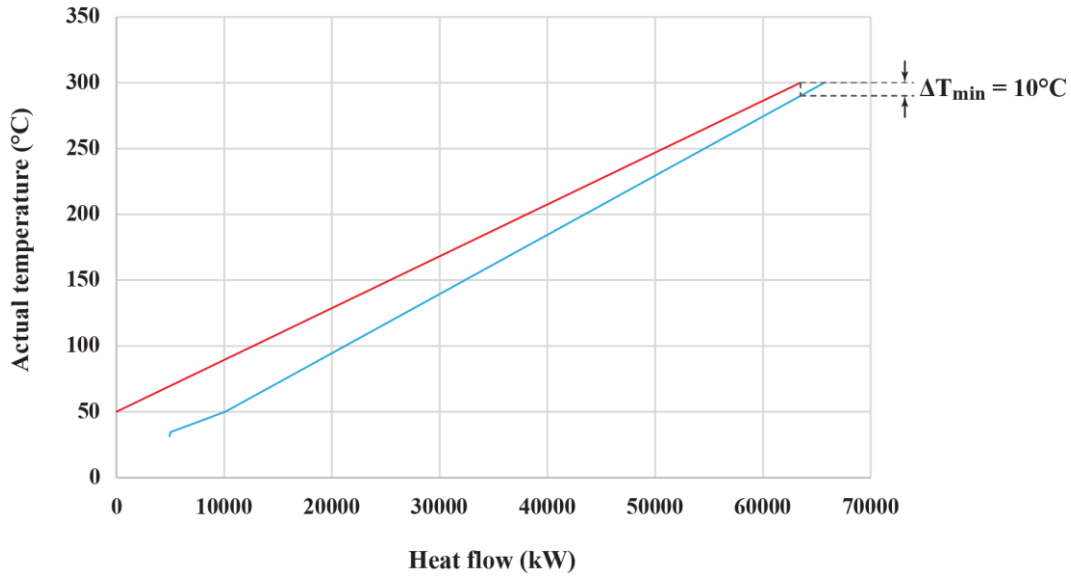

Figure 5.15 The composite curves for hot and cold streams at ΔT_{min} of 10°C.

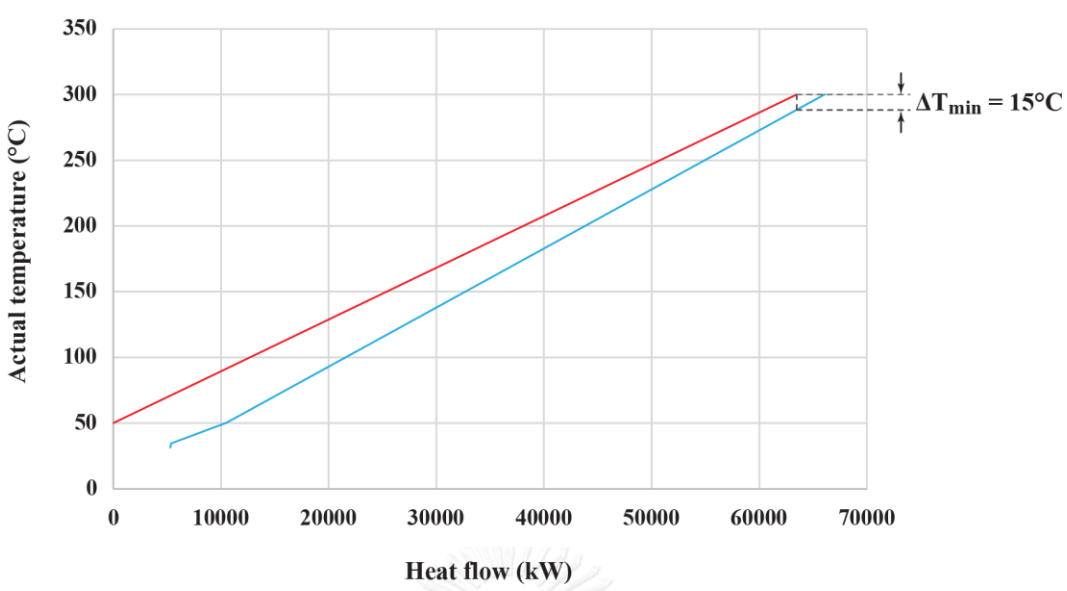

Figure 5.16 The composite curves for hot and cold streams at ΔT_{min} of 15°C.

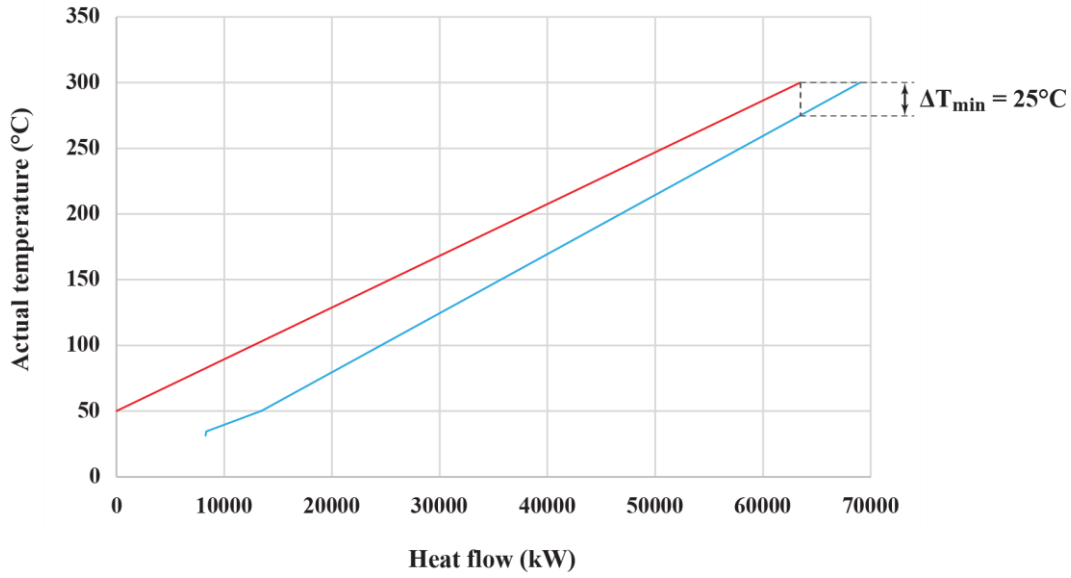

Figure 5.17 The composite curves for hot and cold streams at ΔT_{min} of 25°C.

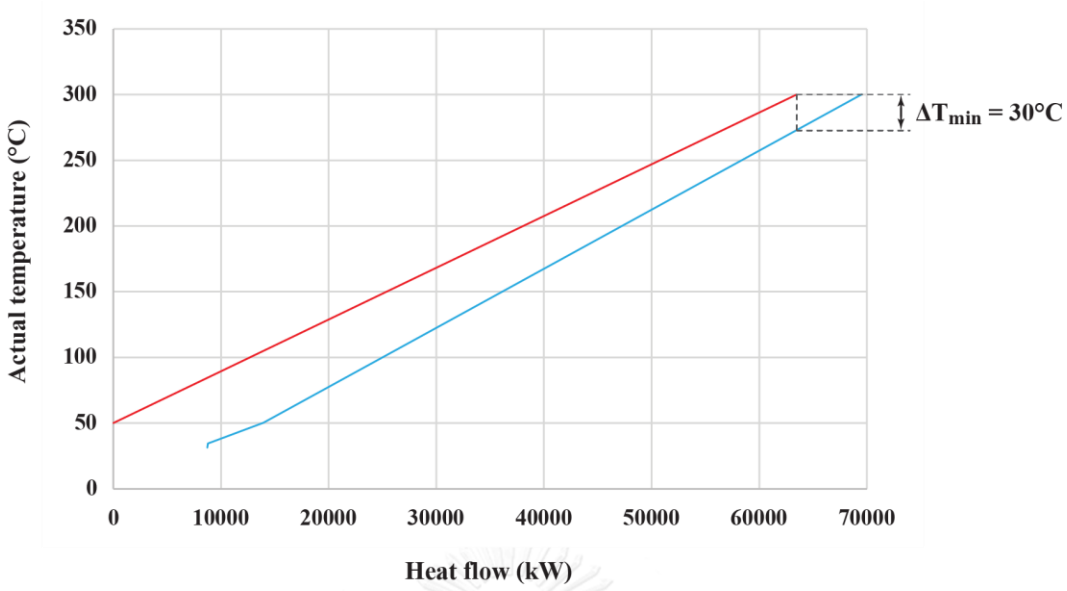

Figure 5.18 The composite curves for hot and cold streams at ΔT_{min} of 30°C.

The minimum temperature difference (ΔT_{min}) affects the utility requirement, heat recovery and area of heat exchanger. In this section, the effect of minimum temperature difference (ΔT_{min}) is considered under the greatest strategy, energy optimization strategy 3. The comparison between utility requirement, heat recovery and area of heat exchanger and the minimum temperature difference (ΔT_{min}) from 10°C to 30°C are shown in Figures 5.19 to 5.21, respectively.

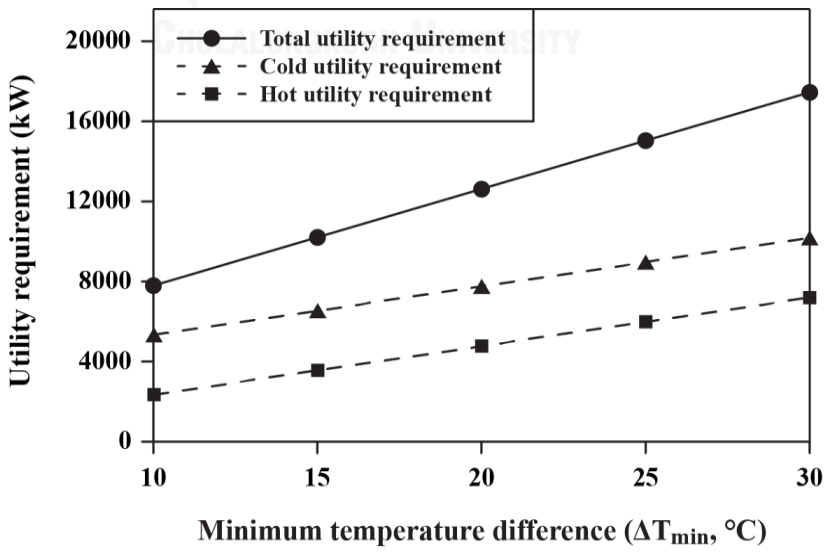

Figure 5.19 The comparison between utility requirement and the minimum temperature difference (ΔT_{min}).

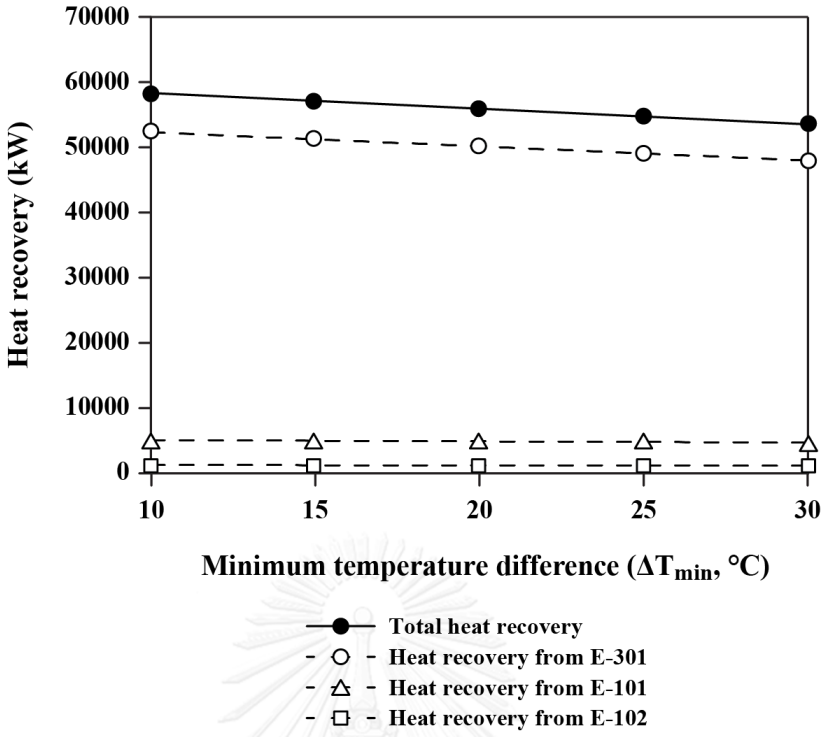

Figure 5.20 The comparison between heat recovery and the minimum temperature difference (ΔT_{min}).

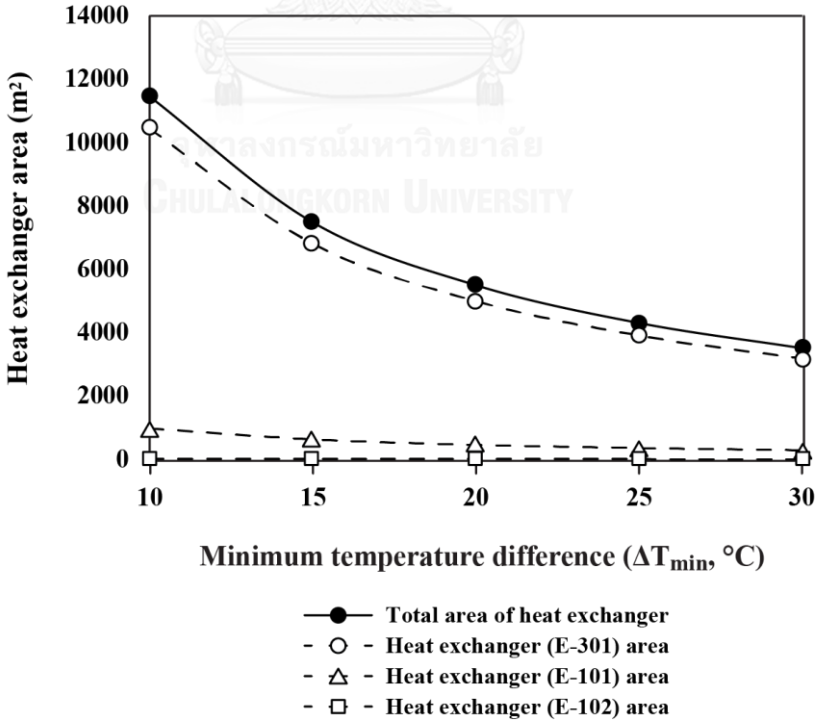

Figure 5.21 The comparison between area of heat exchanger and the minimum temperature difference (ΔT_{min}).

As illustrated in Figures 5.19 to 5.21, it can be seen that the increasing of minimum temperature difference (ΔT_{min}) from 10°C to 30°C affects to the utility requirement and heat recovery of the process linearly that can be expressed by Equations (5.1) and (5.2) with high coefficient of determination (R-square). The utility requirement increases and the heat recovery decreases when the minimum temperature difference (ΔT_{min}) increases. The area of heat exchanger network decreases exponentially when the minimum temperature difference (ΔT_{min}) increases from 10°C to 30°C that can be expressed by Equation (5.3).

$$Total\ utility\ requirement = 482.71\Delta T_{min} + 2973 \quad (5.1)$$

$$R^2 = 1.0000$$

$$Total\ heat\ recovery = 241.36\Delta T_{min} + 60768 \quad (5.2)$$

$$R^2 = 1.0000$$

$$Total\ heat\ exchanger\ area = 137127\Delta T_{min}{}^{-1.075} \quad (5.3)$$

$$R^2 = 0.9998$$

5.2.5 The cost estimation for heat exchanger network

The heat exchanger network can be reduced the energy consumption of the process. However, the reduced energy result in the increasing construction cost of heat exchanger network. In this part, the heat exchanger is made from carbon steel. The construction cost and operating cost of heat exchanger network are considered. The construction cost and operating cost of original process, energy optimization strategy 1, 2 and 3 are presented in Table 5.9.

Table 5. 9 The construction cost and operating cost of each strategy.

	Original	**Strategy 1**	**Strategy 2**	**Strategy 3**
Construction cost (Baht)				
Heat exchanger				
E-101	-	816,000	979,200	1,924,400
E-102	-	744,600	754,800	771,800
E-301	-	7,174,000	6,630,000	12,580,000
Heaters/Cooler				
H-101	907,800	897,600	754,800	754,800
H-102	181,560	179,520	153,680	132,600
H-401	2,437,800	1,278,400	1,734,000	1,247,800
H-301	3,236,800	2,206,600	2,240,600	1,924,400
Total construction cost	6,763,960	13,296,720	13,247,080	19,335,800
Operating cost (Baht/year)				
U-101	54,680,000	45,480,000	4,544,000	4,544,000
U-102	12,176,000	9,992,000	1,792,000	920,000
U-401	580,976,000	49,424,000	105,672,000	49,272,000
U-301	23,968,000	4,816,000	5,072,000	3,056,000
Total operating cost	671,800,000	109,712,000	117,080,000	57,792,000

As summarized in Table 5.9, it can be seen that the heat integrated processes require higher construction cost than the original process. However, the operating cost of heat integrated processes are lower than the original process. The highest construction cost is energy optimization strategy 3. However, the operating cost of energy optimization strategy 3 is less than other strategy. The comparison of construction cost and operating cost for are shown in Figures 5.22 and 5.23, respectively.

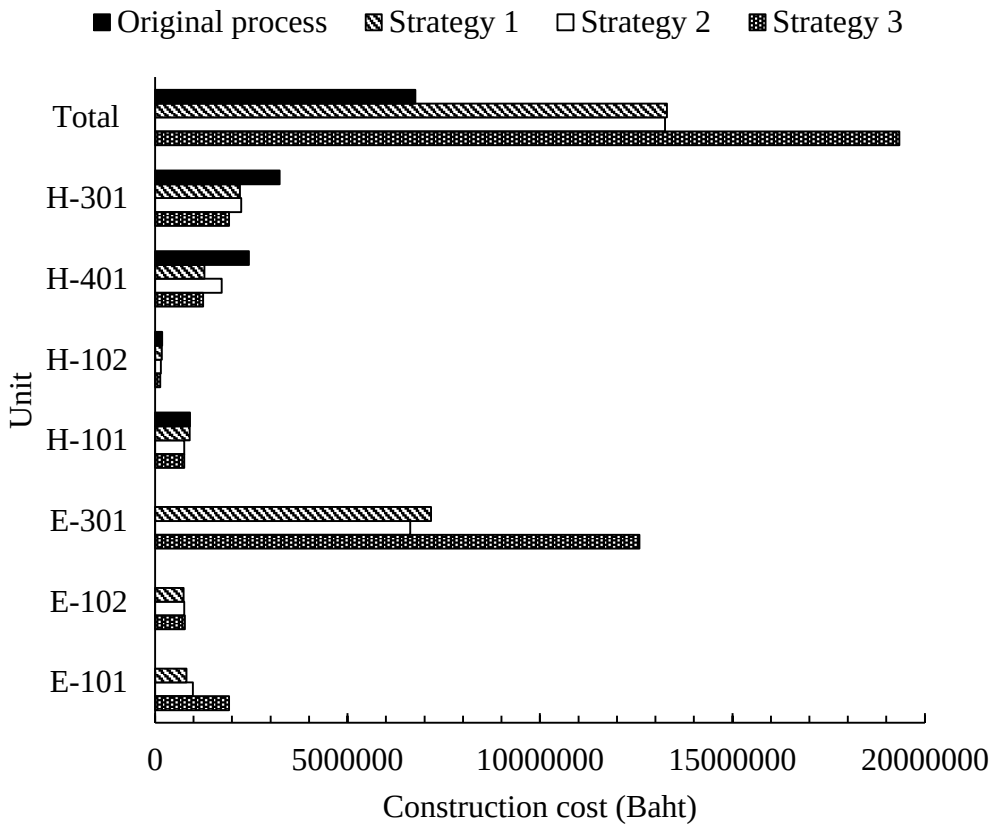

Figure 5. 22 The comparison of construction cost for each unit.

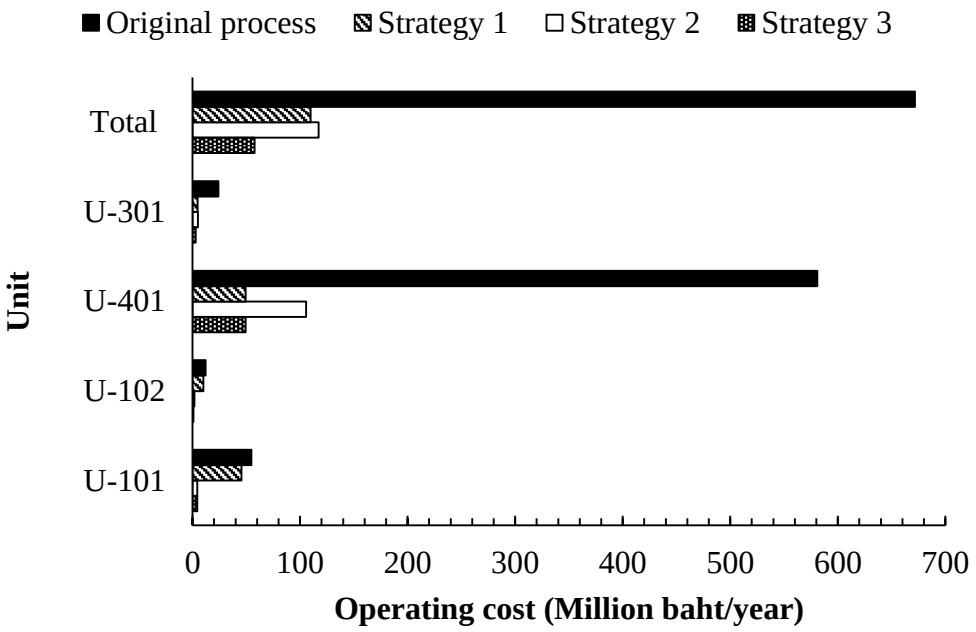

Figure 5. 23 The comparison of operating cost for each unit.

In case of 10 years plant life consideration, the average construction cost of original process, energy optimization strategy 1, 2 and 3 are 676,396, 1,329,672, 1,324,708 and 1,933,580 baht per year, respectively. The operating cost of original process, energy optimization strategy 1, 2 and 3 are constant at 671,800,000, 109,712,000, 117,080,000 and 57,792,000 baht per year, respectively. The total cost of heat exchanger network for 10-year plant life is presented in Figure 5.24.

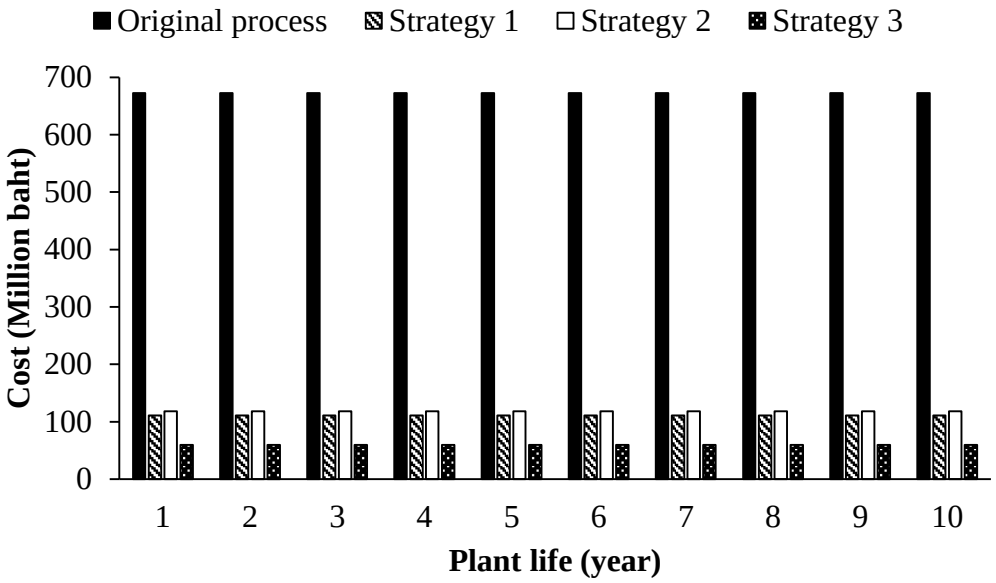

Figure 5. 24 The comparison of cost for heat exchanger network

As presented in Figure 4, it can be seen that the lowest cost is the energy optimization strategy 3. Therefore, the energy optimization strategy 3 is the most worthwhile investment.

5.2.6 Pressure drop consideration for the green diesel production process

In this part, the pressure drop in green diesel production process is considered. The pressure drop for each equipment is approximated in order to study the effect of pressure drop in the process. The pressure drop for each equipment is defined in Table 5.9.

The process flow diagram of the energy optimization strategy 1, 2 and 3 with pressure drop consideration are shown in Figures 5.22, 5.23 and 5.24, respectively. The comparison of total energy requirement between the energy optimization strategy 1, 2 and 3 with pressure drop consideration and the energy optimization strategy 1, 2 and 3 without pressure drop consideration are shown in Figures 5.25, 5.26 and 5.27, respectively. In this work, the compressor is added to the process in order to compress a recycled hydrogen to the required process condition. The energy of strategy 1, 2 and 3 with pressure drop consideration are increased around 7,217 kW, 4,381 kW and 11,241 kW when compared with the energy optimization strategy 1, 2 and 3, respectively. It can be seen that the pressure drop in the equipment result in the increasing energy of the process.

Table 5. 10 The pressure drop for each equipment.

Type		Pressure drop (ΔP),bar			Calculated method	Reference
		Strategy 1	Strategy 2	Strategy 3		
Reactor		8.85	8.85	8.85	Ergun's equation	(Silla 2003)
Heat exchanger					Kern's method	(Walas 1990)
E-101	Tube	0.48	0.73	0.04		
	Shell	0.014	0.02	0.06		
E-102	Tube	0.97	0.54	0.06		
	Shell	0.0004	0.0004	0.02		
E-301	Tube	0.27	0.33	0.30		
	Shell	0.39	0.40	0.52		
Flash drum		0.0025	0.0025	0.0025		(Sulzer-Chemtech)

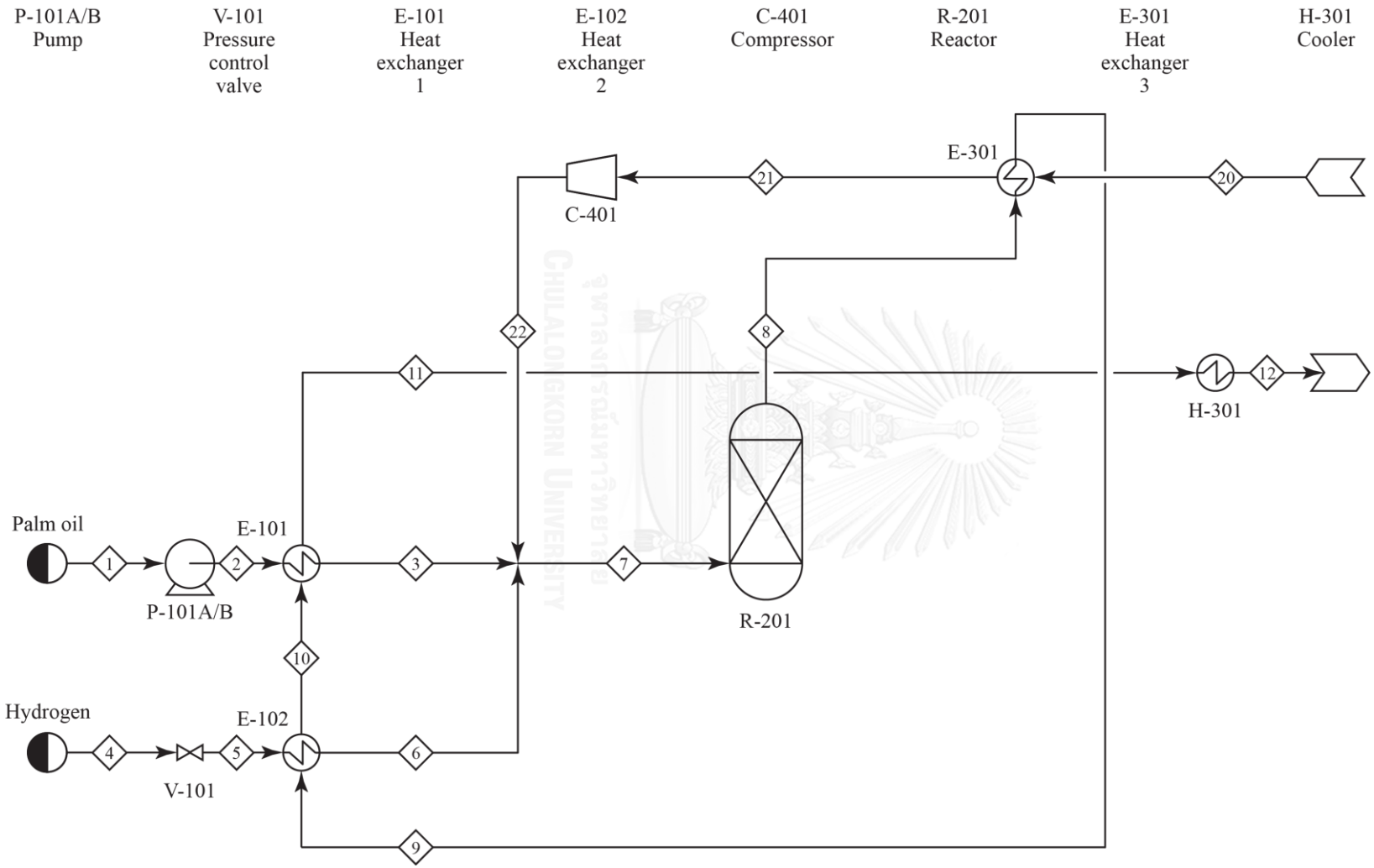

Figure 5.25 The process flow diagram for energy optimization strategy 1 with pressure drop consideration.

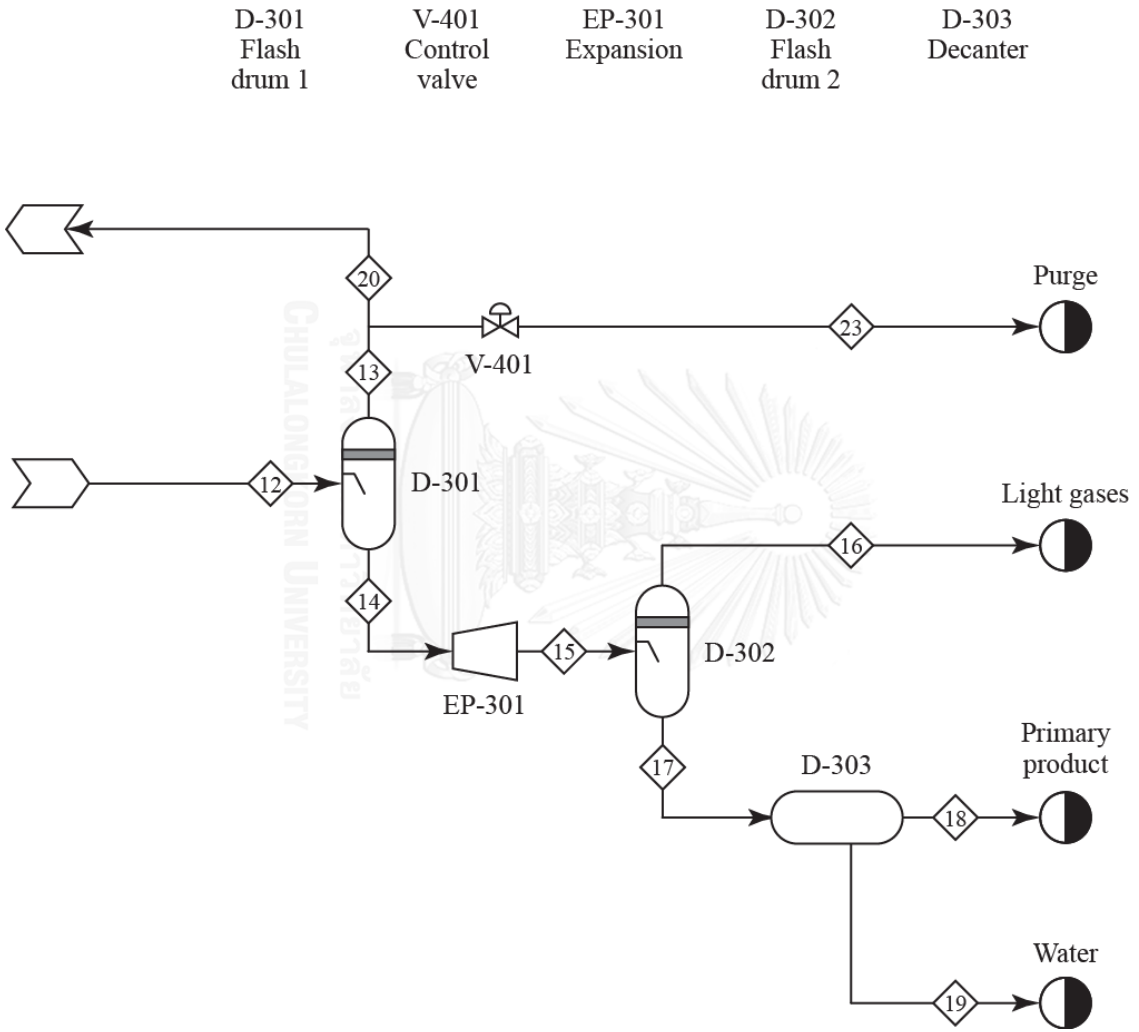

Figure 5.22 The process flow diagram for energy optimization strategy 1 with pressure drop consideration. (Continued)

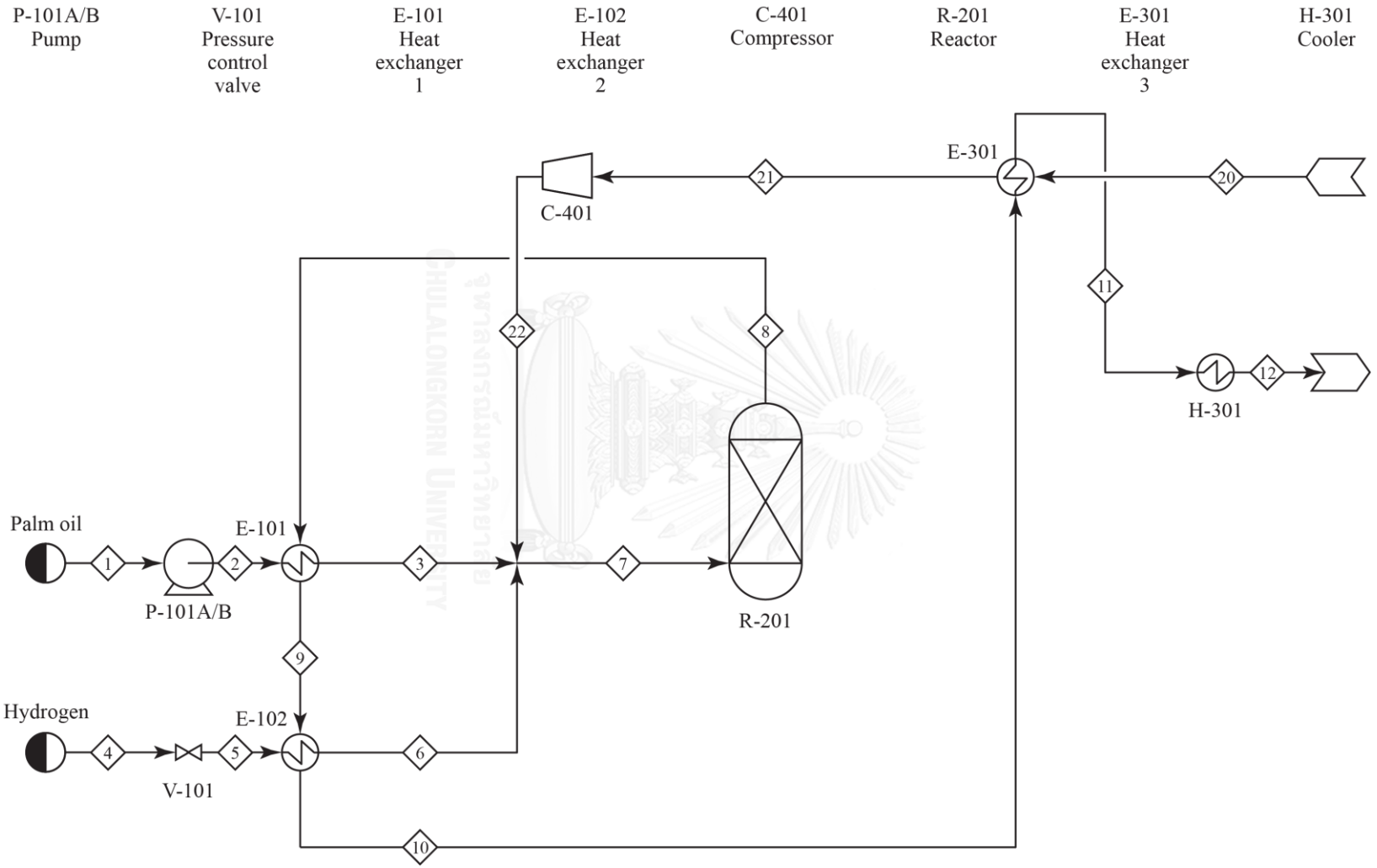

Figure 5. 26 The process flow diagram for energy optimization strategy 2 with pressure drop consideration.

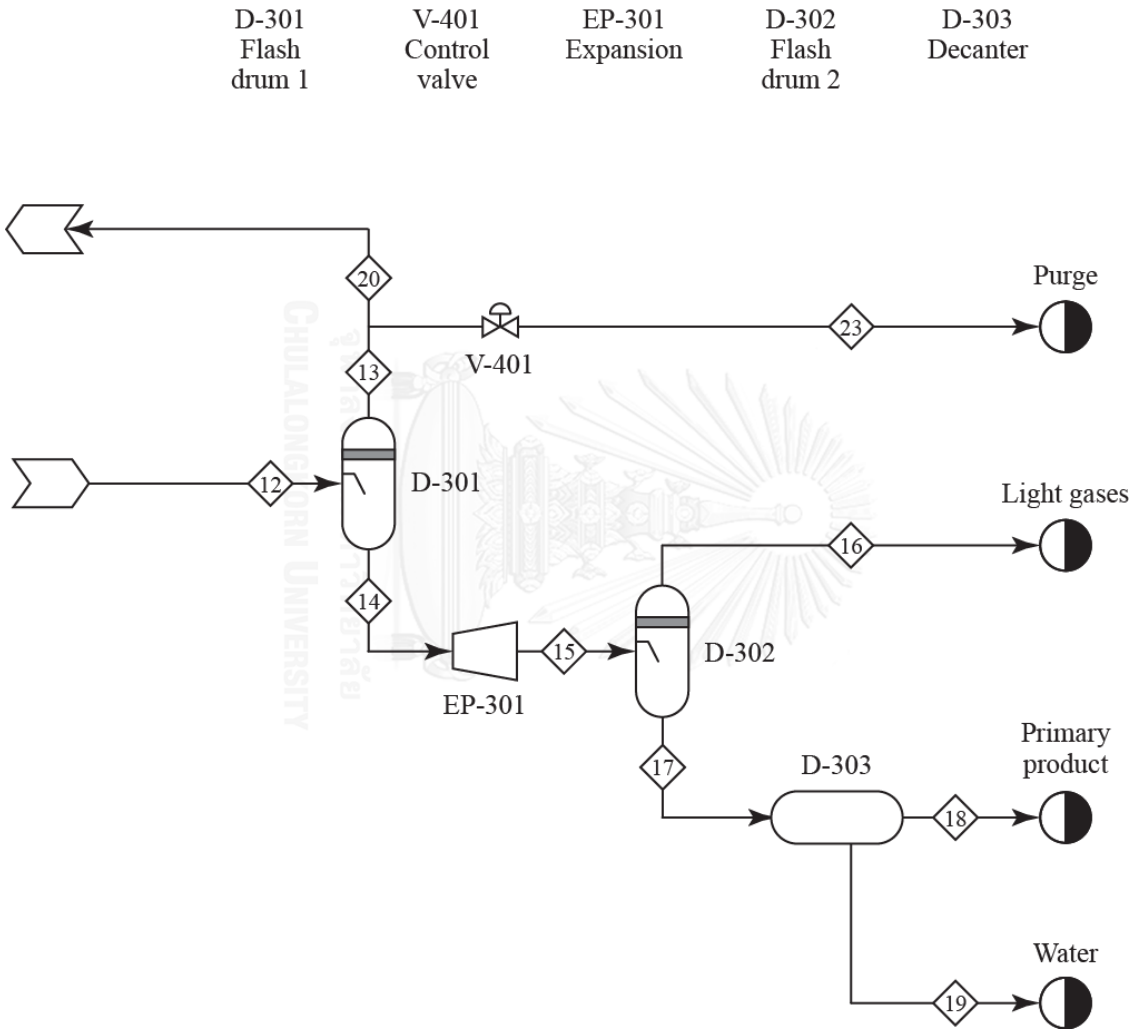

Figure 5.23 The process flow diagram for energy optimization strategy 2 with pressure drop consideration. (Continued)

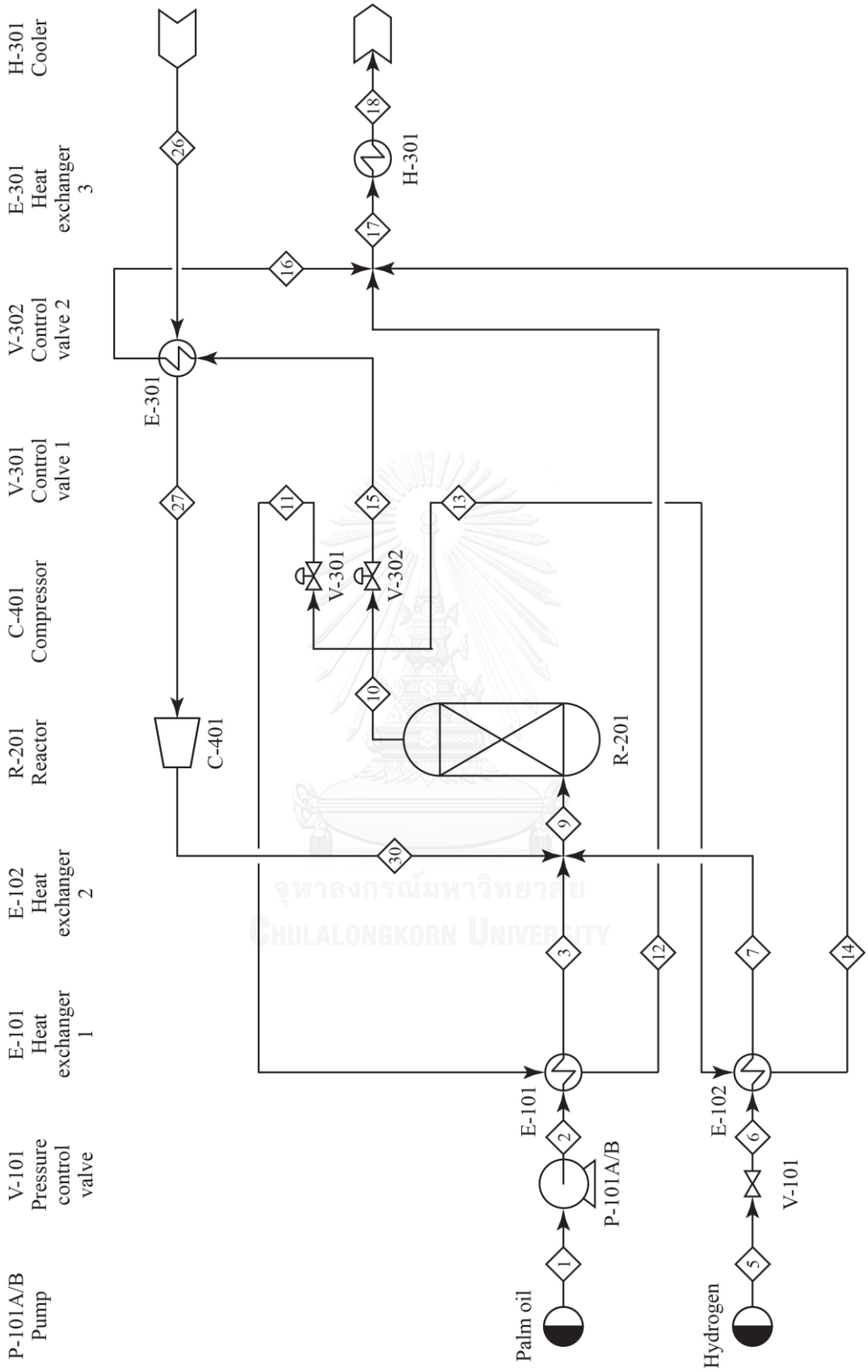

Figure 5. 27 The process flow diagram for energy optimization strategy 3 with pressure drop consideration.

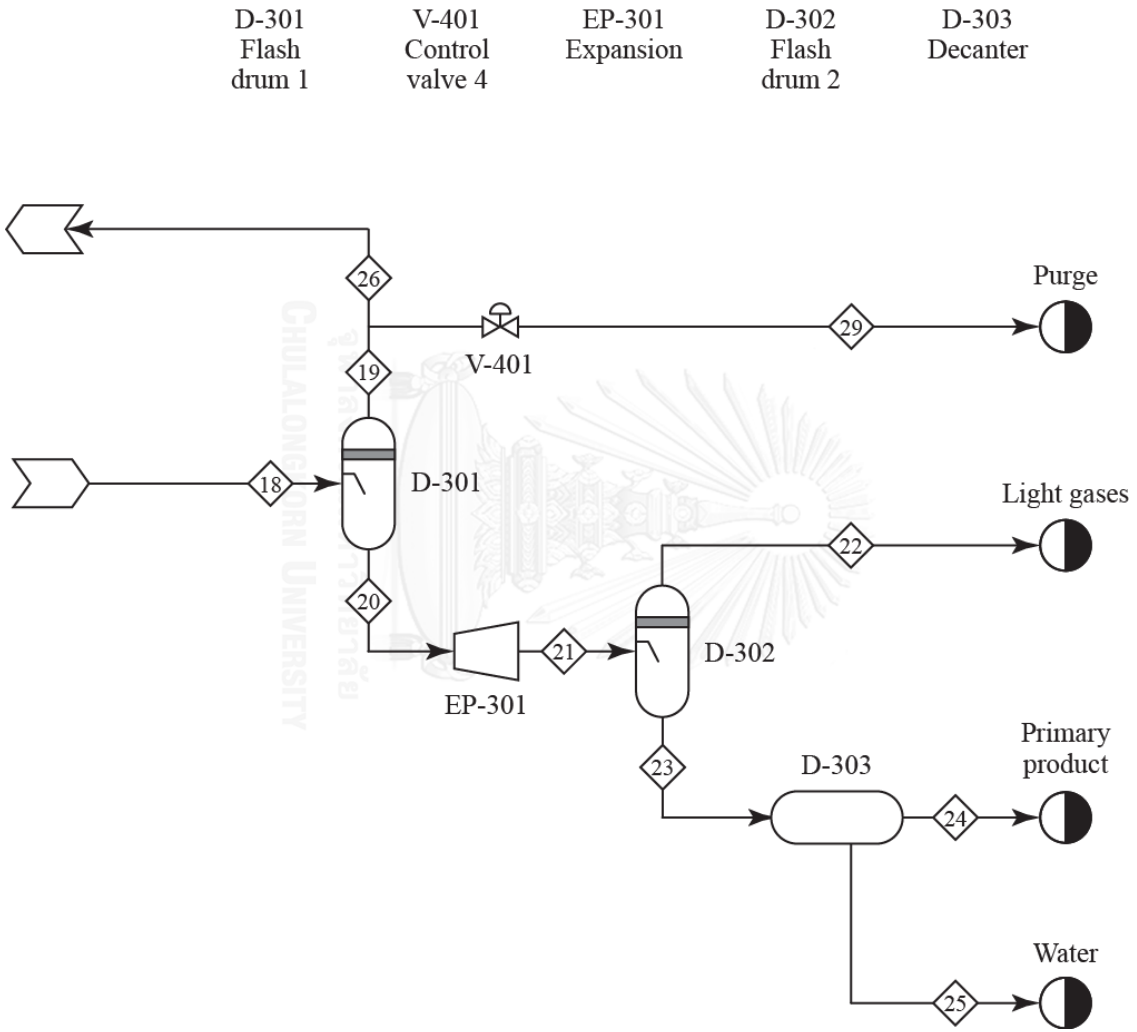

Figure 5.24 The process flow diagram for energy optimization strategy 3 with pressure drop consideration. (Continued)

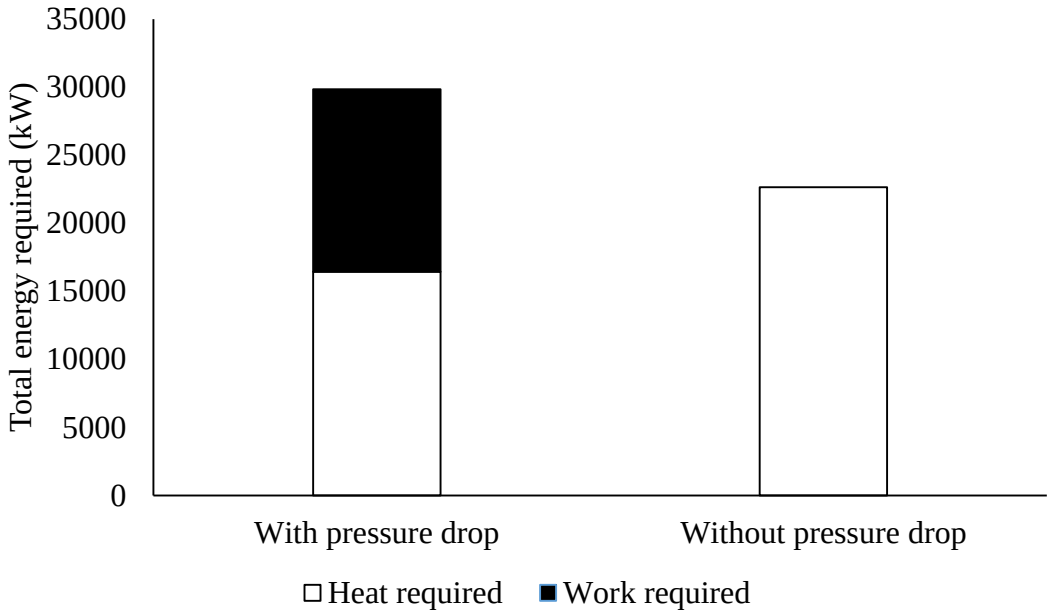

Figure 5. 28 The Comparison of energy between the energy optimization strategy 1 with and without pressure drop.

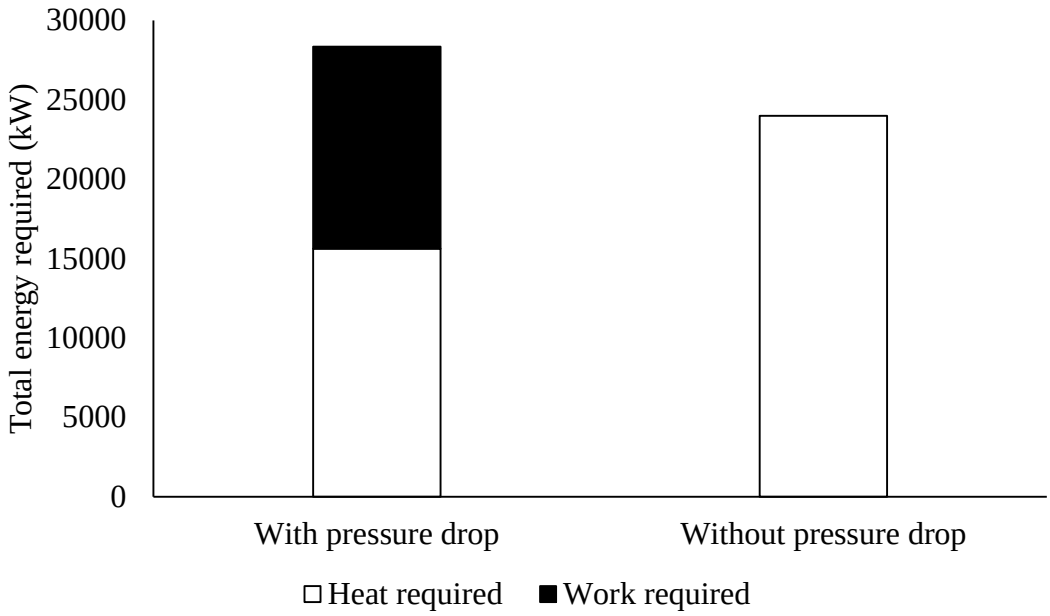

Figure 5. 29 The Comparison of energy between the energy optimization strategy 2 with and without pressure drop.

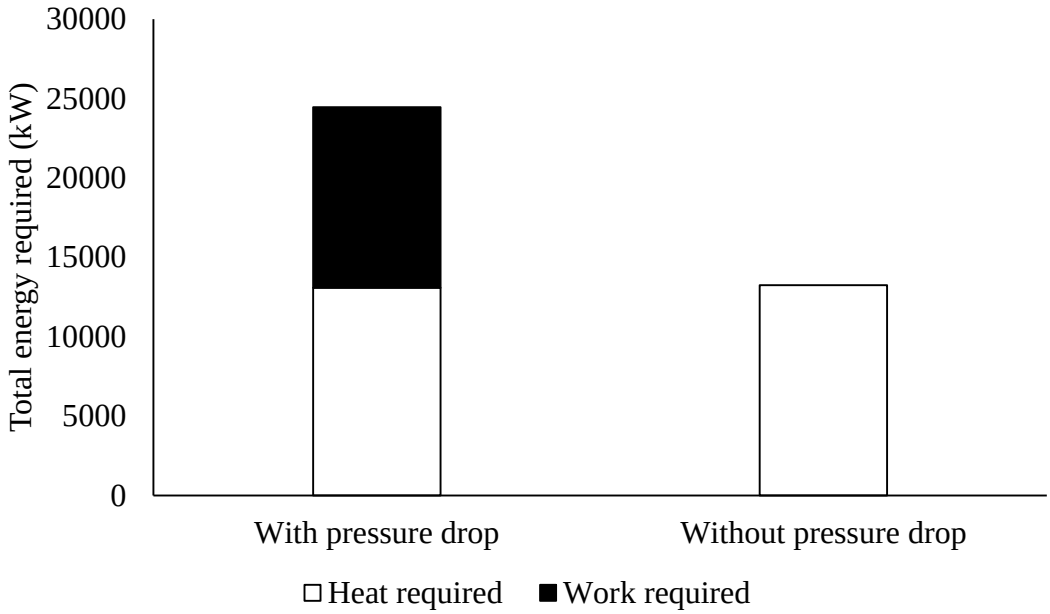

Figure 5. 30 The Comparison of energy between the energy optimization strategy 3 with and without pressure drop.

CHAPTER 6

CONCLUSION AND RECOMMENDATION

6.1 Conclusions

The green diesel production process by using $NiMoS_2/\gamma\text{-}Al_2O_3$ catalyst is simulated. A palm oil is used as a raw material that consists of trilinolein (11.5%), tripalmitin (42.2%) and triolein (46.3%). The condition for this process is 1000:1 of hydrogen to oil volume feed ratio, reaction temperature of 300°C and pressure of 30 bar. This condition provides the green diesel purity of 99.2 wt%, green diesel yield of 88.25%. The hydrodeoxygenation (HDO) and decarbonylation (DCO)/decarboxylation (DCO_2) distribution are 77.50% and 22.50%, respectively. The liquid product composition are 8.90%, 32.65%, 12.58% and 45.87% of n-C_{15}, n-C_{16}, n-C_{17} and n-C_{18}, respectively. The green diesel production capacity of this process is 200,000 metric tons per year with 8,000 of working hours per year. The results of this simulation study are good agreement with the experimental data. The tolerance allowed is not more than 2%. The energy consumption of 124,510 kW is used in this process.

To minimize the energy consumption of the green diesel production process, the heat exchanger network (HEN) is considered. The three energy optimization strategy are designed. All of the energy optimization strategies can keep the quality of green diesel product. The energy optimization strategy 1 and 2 can decrease the energy consumption of 81.80% and 80.73%, respectively. It indicated that the exchanged heat sequence affects on the energy saving. Based on the energy optimization strategy 3, the energy consumption of 89.36% is decreased. The energy saving of strategy 3 is greatest due to each split hot streams can be exchanged the energy with the maximum driving force. In this work, the construction and operating cost are considered. When considering the cost of construction and operation, it can be seen that the energy optimization strategy 3 is the most worthwhile investment.

The minimum temperature difference (ΔT_{min}) affects to the utility requirement, heat recovery and area of heat exchanger of the process. The utility requirement increases and the heat recovery decreases linearly when the minimum temperature difference (ΔT_{min}) increases. The area of heat exchanger network decreases exponentially when the minimum temperature difference (ΔT_{min}) increases. The pressure drop of each equipment results in the increasing energy requirement of the process.

6.2 Recommendations

In this work, the objectives only focus on the quality of green diesel product and energy consumption of the process. However, the economic feasibility, investment and operational costs and intensive equipment design should be considered.

All of the recommendations are provided the perfection of green diesel production process simulation.

REFERENCES

Alí, M. F., et al. (2005). Handbook of Industrial Chemistry, McGraw–Hill.

Anand, M. and A. K. Sinha (2012). "Temperature-dependent reaction pathways for the anomalous hydrocracking of triglycerides in the presence of sulfided Co–Mocatalyst." Bioresour Technol **126**: 148-155.

Ancheyta, J., et al. (2009). Asphaltenes: Chemical Transformation during Hydroprocessing of Heavy Oils. New York, CRC Press

Bezergianni, S. and A. Dimitriadis (2013). "Comparison between different types of renewable diesel." Renewable and Sustainable Energy Reviews **21**: 110-116.

Charusiri, W. and T. Vitidsant (2005). "Kinetic Study of Used Vegetable Oil to Liquid Fuels over Sulfated Zirconia." Energy & Fuels **19**: 1738-1789.

Charusiri, W., et al. (2006). "Conversion of used vegetable oils to liquid fuels and chemical over HZSM-5, sulfated zircinia and hybrid catalysts." Korean Journal of Chemical Engineering **23**: 349-355.

Chen, N., et al. (2013). "Effects of Si/Al ratio and Pt loading on Pt/SAPO-11 catalysts in hydroconversion of Jatropha oil." Applied Catalysis A: General **466**: 105-115.

Coker, A. K. (2015). "Process Integration and Heat Exchanger Networks." 491-622.

Donnis, B., et al. (2009). "Hydroprocessing of Bio-Oils and Oxygenates to Hydrocarbons, Understanding the Reaction Routes." Topics in Catalysis **52**: 229-240.

Evans, F. L. J. (1997). Equipment Design Handbook for Refineries and Chemical Plant. New York, Gulf Pub. Co.

Faungnawakij, K. and K. Suriye (2013). "Chapter 4 - current catalytic processes with hybrid materials and composites for heterogeneous catalysis.": 79-104.

Gong, S., et al. (2012). "Role of support in hydrotreatment of jatropha oil over sulfided NiMo catalysts." Industrial & Engineering Chemistry **51**: 13953-13960.

Guzman, A., et al. (2010). "Hydroprocessing of crude palm oil at pilot plant scale." Catalysis Today **156**(1-2): 38-43.

Hancsók, J., et al. (2007). "Investigation of the production of high cetane number bio gas oil from pre-hydrogenated vegetable oils over Pt/HZSM-22/Al2O3." Microporous and Mesoporous Materials **101**(1-2): 148-152.

Herskowitz, M., et al. (2013). "A commeicially-viable, one-step process for production of green diesel from soybean oil on Pt/SAPO-11." Fuel **111**: 157-164.

Huber, G. W. and A. Corma (2007). "Synergies between Bio- and Oil Refineries for the Production of Fuels from Biomass." Angewandte Chemie International Edition **46**: 7184-7201.

Jain, S. and M. P. Sharma (2010). "Stability of biodiesel and its blends, a review." Renewable and Sustainable Energy Reviews **14**: 667-678.

Kern, D. Q. (1965). Process Heat Transfer. New York, McGraw-Hill Book Co.

Kikhtyanin, O. V., et al. (2010). "Hydroconversion of sunflower oil on Pd/SAPO-31 catalyst." Fuel **89**: 3085-3092.

Kovacs, S., et al. (2011). "Fuel production by hydrotreating of triglycerides on NiMo/Al2O3/F catalyst." Chemical Engineering Journal **176-177**: 237-243.

Krár, M., et al. (2010). "Fuel Purpose Hydrotreating of Sunflower Oil on $CoMo/Al_2O_3$. Catalyst." Bioresour Technol **101**: 9287-9293.

Kubicˇka, D., et al. (2009). "Transformation of vegetable oils into hydrocarbons over mesoporous-alumina-supported CoMo catalysts." Topics in Catalysis **52**: 161-168.

Kubička , D. and L. Kaluža (2010). "Deoxygenation of vegetable oils over sulfided Ni, Mo and NiMo catalysts." Applied Catalysis A: General **372**: 199-208.

Lestari, S., et al. (2009). "Catalytic Deoxygenation of Stearic Acid in a Continuous Reactor over a Mesoporous Carbon Supported Pd Catalyst." Energy & Fuels **23**: 3842-3845.

Linnhoff, B. and E. Hindmarsh (1983). "The pinch design method for heat exchanger networks." Chemical Engineering Science **38**: 745-763.

Linnhoff, M. (1998). "Introduction to Pinch Technology." from www.ou.edu/class/che-design/a-design/Introduction%20to%20Pinch%20Technology-LinnhoffMarch.pdf.

Liu, C., et al. (2013). "A cleaner process for hydrocracking of jatropha oil into green diesel." Journal of the Taiwan Institute of Chemical Engineers **44**(2): 221-227.

Liu, Y., et al. (2011). "Hydrotreatment of Vegetable Oils to Produce Bio-Hydrogenated Diesel and Liquefied Petroleum Gas Fuel over Catalysts Containing Sulfided Ni–Mo and Solid Acids." Energy & Fuels **25**(10): 4675-4685.

Liu, Y., et al. (2012). "Production of Biohydrogenated Diesel by Hydrotreatment of High-Acid-Value Waste Cooking Oil over Ruthenium Catalyst Supported on Al-polyoxocation-Pillared Montmorillonite." Catalysts **2**: 171-190.

Ludwig, E. E. (1997). Applied Process Design for Chemical and Petrochemical Plants. Houston, Gulf Pub. Co.

Mandal, D., et al. (2013). "Void fraction and effective thermal conductivity of binary particulate bed." Fusion Engineering and Design **88**(4): 216-225.

Mikkonen, S. (2008). "Second-generation renewable diesel offers advantages." Hydrocarbon Processing **87**: 63-66.

Mikulec, J., et al. (2010). "Second Generation Diesel Fuel from Renewable Sources." Journal of Cleaner Production **18**: 917-926.

Morgan, T., et al. (2012). "Catalytic Deoxygenation of Triglycerides to Hydrocarbons over Supported Nickel Catalysts." Chemical Engineering Journal **189-190**: 346-355.

Murata, K., et al. (2010). "Production of Synthetic Diesel by Hydrotreatment of Jatropha Oils Using Pt−Re/H-ZSM-5 Catalyst." Energy & Fuels **24**(4): 2404-2409.

Naik, S. N., et al. (2010). "Production of first and second generation biofuels: A comprehensive review." Renewable and Sustainable Energy Reviews **14**: 578-597.

Nasikin, M., et al. (2009). "Biogasoline from Palm Oil by Simultaneous Cracking and Hydrogenation Reaction over NiMo/zeolite catalyst." World Applied Sciences Journal **5**: 74-79.

Nunes, P. P. (1984). Hydrocraquage de l'huile de soja sur des catalyseurs au rhodium et au ruthenium supportes. Paris, Université Pierre et Marie Curie

Nunes, P. P., et al. (1986). "Soybean Oil Hydrocracking under Pressure: Process and General Aspect of the Transformation." Revue de L'Institute Francais du Pétrole **41**: 421-431.

Raldov, W. (2005). Bio-Refining Workshop. Proceedings of the First International Conference, Washington D.C. .

Shin, H. Y., et al. (2011). "Thermal decomposition and stability of fatty acid methyl esters in supercritical methanol." Journal of Analytical and Applied Pyrolysis **92**: 332–338.

Silla, H. (2003). Chemical process engineering design and economics. New York, Marcel Dekker.

Simacek, P., et al. (2009). "Hydroprocessed rapeseed oil as a source of hydrocarbon-based biodiesel." Fuel **88**: 456-460.

Snåre, M., et al. (2006). "Heterogeneous catalytic deoxygenation of stearic acid for production of biodiesel." Industrial & Engineering Chemistry Research **45**: 5708-5715.

Sotelo-Boyás, R., et al. (2011). "Renewable Diesel Production from the Hydrotreating of Rapeseed Oil with Pt/Zeolite and NiMo/Al2O3Catalysts." Industrial & Engineering Chemistry Research **50**(5): 2791-2799.

Sotelo-Boyás, R., et al. (2012). "Hydroconversion of Triglycerides into Green Liquid Fuels." 187-216.

Srifa, A., et al. (2014). "Production of bio-hydrogenated diesel by catalytic hydrotreating of palm oil over NiMoS2/gamma-Al2O3 catalyst." Bioresour Technol **158**: 81-90.

Sulzer-Chemtech. "Gas/Liquid Seperation Technology." 2015, from http://www.sulzer.com/ms/-/media/Documents/ProductsAndServices/Separation_Technology/Mist_Eliminators/Brochures/Gas_Liquid_Separation_Technology.pdf.

Turton, R., et al. (2009). Analysis, Synthesis, and Design of Chemical Processes, Prentice hall.

Veriansyah, B., et al. (2012). "Production of renewable diesel by hydroprocessing of soybean oil: Effect of catalysts." Fuel **94**: 578-585.

Walas, S. M. (1990). Chemical process equipment selection and design. Boston, Butterworth-Heinemann.

Yang, Y., et al. (2013). "Hydrotreating of C18 fatty acids to hydrocarbons on sulphided NiW/SiO_2–Al_2O_3." Fuel Processing Technology **116**: 165-174.

APPENDIX

APPENDIX A

IDEAL HEAT CALCULATION FOR

HEAT EXCHANGER NETWORK

This section shows the ideal heat calculation for heat exchanger network with a constant heat capacity flow rate (CP). The heat exchange stream data for the green diesel production process is shown in Table 5.4. In this case, the hot stream of the process is split into 3 streams in order to exchange the maximum energy. The heat exchange stream data with split streams are presented in Table A.1.

Table A.1 The heat exchange stream data with split streams for the green diesel production process.

Stream	No.	Type	Supply temperature (°C)	Target temperature (°C)	Q (kW)	Heat capacity flow rate, CP* (kW/°C)
Hot	1	H-1	300.00	50.00	4766.78	19.07
Hot	2	H-2	300.00	50.00	55755.05	223.02
Hot	3	H-3	300.00	50.00	3220.68	12.88
Cold	4	C-1	31.00	300.00	5128.93	19.07
Cold	5	C-2	34.40	300.00	1142.43	4.30
Cold	6	C-3	50.00	300.00	54496.90	217.99

From the composition curves shown in Figure 5.5, the minimum temperature difference is set to 20°C. The pinch temperature, the hot pinch temperature and the cold pinch temperature are 290°C, 300°C and 280°C, respectively.

Conceptual network design (Linnhoff and Hindmarsh 1983)

Step 1: Stream 1 is matched with stream 4.

Stream 1 transfers the amount of heat to bring stream 4 to its pinch temperature. The amount of heat in stream 4 from the initial temperature to its pinch temperature is:

$$\Delta H_{ex} = CP\Delta T$$

$$= 19.07 \times (280 - 31)$$

$$= 4748.43\ kW$$

The amount of heat in stream 1 from the pinch temperature to its target temperature is:

$$\Delta H_{ex} = CP\Delta T$$

$$= 19.07 \times (300 - 50)$$

$$= 4767.50\ kW$$

A cooler is required in stream 1 as the remaining heat load is:

$$\Delta H_{Cold} = 4767.50 - 4748.43 = 19.07\ kW$$

The intermediate temperatures in the streams are:

In stream 1:

$$\Delta H_{ex} = CP\Delta T$$

$$\frac{4748.43}{19.07} = (300 - T)$$

$$T = 51℃$$

The cooler load is 19.07 kW. Thus, the target temperature is:

$$\Delta H_{ex} = CP\Delta T$$

$$\frac{19.07}{19.07} = (51 - T)$$

$$T = 50℃$$

The heater is required in stream 4 as the remaining heat load is:

$$\Delta H_{Hot} = 5128.93 - 4748.43 = 380.50\ kW$$

Thus, the target temperature is:

$$\Delta H_{ex} = CP\Delta T$$

$$\frac{380.50}{19.07} = (T - 280)$$

$$T = 300℃$$

Step 2: Stream 2 is matched with stream 6.

Stream 2 transfers the amount of heat to bring stream 6 to its pinch temperature. The amount of heat in stream 6 from the initial temperature to its pinch temperature is:

$$\Delta H_{ex} = CP\Delta T$$

$$= 217.99 \times (280 - 50)$$

$$= 50137.70\ kW$$

The amount of heat in stream 2 from the pinch temperature to its target temperature is:

$$\Delta H_{ex} = CP\Delta T$$

$$= 223.02 \times (300 - 50)$$

$$= 55755.00\ kW$$

A cooler is required in stream 2 as the remaining heat load is:

$$\Delta H_{Cold} = 55755.00 - 50137.70 = 5617.30\ kW$$

The intermediate temperatures in the streams are:

In stream 2:

$$\Delta H_{ex} = CP\Delta T$$

$$\frac{50137.70}{223.02} = (300 - T)$$

$$T = 75.19℃$$

The cooler load is 5617.30 kW. Thus, the target temperature is:

$$\Delta H_{ex} = CP\Delta T$$

$$\frac{5617.30}{223.02} = (75.19 - T)$$

$$T = 50℃$$

The heater is required in stream 6 as the remaining heat load is:

$$\Delta H_{Hot} = 54496.90 - 50137.7 = 4359.20\ kW$$

Thus, the target temperature is:

$$\Delta H_{ex} = CP\Delta T$$

$$\frac{4359.20}{217.99} = (T - 280)$$

$$T = 300℃$$

Step 3: Stream 3 is matched with stream 5.

Stream 3 transfers the amount of heat to bring stream 5 to its pinch temperature. The amount of heat in stream 5 from the initial temperature to its pinch temperature is:

$$\Delta H_{ex} = CP\Delta T$$

$$= 4.30 \times (280 - 34.4)$$

$$= 1056.08\ kW$$

The amount of heat in stream 3 from the pinch temperature to its target temperature is:

$$\Delta H_{ex} = CP\Delta T$$

$$= 12.88 \times (300 - 50)$$

$$= 3220\ kW$$

A cooler is required in stream 3 as the remaining heat load is:

$$\Delta H_{Cold} = 3220 - 1056.08 = 2163.92\ kW$$

The intermediate temperatures in the streams are:

In stream 3:

$$\Delta H_{ex} = CP\Delta T$$

$$\frac{1056.08}{12.88} = (300 - T)$$

$$T = 218.01℃$$

The cooler load is 2163.92 kW. Thus, the target temperature is:

$$\Delta H_{ex} = CP\Delta T$$

$$\frac{2163.92}{12.88} = (218.01 - T)$$

$$T = 50℃$$

The heater is required in stream 5 as the remaining heat load is:

$$\Delta H_{Hot} = 1142.43 - 1056.08 = 86.35\ kW$$

Thus, the target temperature is:

$$\Delta H_{ex} = CP\Delta T$$

$$\frac{86.35}{4.30} = (T - 280)$$

$$T = 300℃$$

It is noted that the results of this network is an ideal calculation with a constant heat capacity flow rate (CP). Thus, the calculated heat of this network is not equal to the network strategy that calculated from real physical properties by Aspen plus. However, the trend of ideal calculation is corresponding with the results from Aspen plus. This ideal calculation can be used to guild the further heat exchanger network design.

APPENDIX B

PRESSURE DROP CALCULATION OF THE PROCESS

In this work, the pressure drop calculation is divided into 2 parts. Firstly, the pressure drop in a reactor is considered. Secondly, the pressure drop on heat exchanger is considered.

1. Pressure drop calculation for the fixed bed reactor

In this section, the pressure drop calculation is divided into 8 steps as follows (Silla 2003):

Step 1: Calculate the bed volume (V_B) from equation (B.1).

$$V_B = \frac{V'_V}{S'_{CL}} \tag{B.1}$$

Where:

V'_V = Volumetric flow rate of fresh feed of limiting reactant (kg/m^3)

S'_{CL} = Space velocity (h^{-1})

$$V_B = \frac{17.945}{1}$$

$$V_B = 17.9450\ m^3$$

Step 2: Calculate bed area (A_B) from equation (B.2).

$$V_V = v'_s A_B \tag{B.2}$$

Where:

V_V = Volumetric flow rate of gas inlet (m^3/h)

v'_s = Superficial velocity, $v'_s \approx 1.0$ (m/s)

$$A_B = \frac{23434}{1}$$

$$A_B = 6.5094\, m^2$$

Step 3: Calculate the reactor diameter (D) from equation (B.3). Round off D in 6 inch (0.152 m) increments, starting at 30 inch (0.762 m). If D is less than 30 inch, use standard pipe.

$$A_B = \frac{\pi D^2}{4} \quad \text{(B.3)}$$

$$D = 2.8796\, m = 9.4450\, ft$$

Round off D = 9.5 ft = 2.8956 m

Step 4: After rounding off D, calculate the actual bed area from equation (B.3).

$$A_B = \frac{\pi(2.8956^2)}{4}$$

$$A_B = 6.5852\, m^2$$

Step 5: Calculate the actual superfacial velocity (V_S) from equation (B.2).

$$v_s = \frac{23434}{6.5852}$$

$$v_s = 0.9885\frac{m}{s} = 3.2430\frac{ft}{s} = 11675.2030\frac{ft}{h}$$

Step 6: Calculate the bed length (L_B) from equation (B.4).

$$L_B = \frac{V_B}{A_B} \tag{B.4}$$

(L_B minimum = 1/2D = 4.75 ft, L_B maximum = 25 ft)

$$L_B = \frac{17.945}{6.5852}$$

$$L_B = 2.7250\, m = 8.940\, ft$$

Step 7: Calculate the reactor length (L_R) from equation (B.5). Round off L_R in 3 inch (0.25 ft) increments (for example: 5.0, 5.25, 5.50, 5.75 etc.).

$$L_R = L_B + L'_I \tag{B.5}$$

Where:

$L'_I = 3\, ft$

$$L_R = 8.940 + 3$$

$$L_R = 11.940\, ft$$

Round off L_R = 12 ft = 3.6576 m

Step 8: Calculate the reactor pressure drop (ΔP) from equation (B.6).

$$\frac{\Delta P}{L} = 150\frac{\mu G}{kg\rho D^2}\frac{(1-\varepsilon)^2}{\varepsilon^3} + 1.75\frac{G^2}{kg\rho D}\frac{(1-\varepsilon)}{\varepsilon^3} \tag{B.6}$$

So,

$$\Delta P = 128.351\, psi = 8.85\, bar$$

Where:

ΔP = Pressure drop (lb/in^2, psi)

L = Depth of the packed bed (ft)

$G = \rho V$ = Mass velocity (lb/hr-ft^2) = 5165.11 lb/hr-ft^2

V = Superficial linear velocity (ft/hr) = 11675.203 ft/h

ρ = Fluid density (lb/ft^3) = 0.4424 lb/ft^3

μ = Fluid viscosity (lb/hr-ft) = 0.8891 lb/hr-ft

D = Effective particle diameter (ft) = 0.00328 ft

(Srifa, Faungnawakij et al. 2014)

ε = Interparticle void fraction (dimensionless) = 0.455

(Mandal, Sathiyamoorthy et al. 2013)

g = Gravitational constant (4.17 x 10^8 lb-ft/lb-hr^2)

k = Conversion factor (144 in^2/ft^2)

2. Pressure drop calculation for the heat exchanger

Type of heat exchanger: Shell and tube

Heat duty (Q): 1056.17 kW

Heat transfer area (A): 16.95 m^2

Heat transfer coefficient (U): 846.62 W/m^2-^oC

Shell side information:

Flow rate	W_{shell} = 1067.37 kg/h
Pressure (in)	P_1 = 3000 kPa (30 bar)
Temperature (in)	T_1 = 34.4 ^oC
Temperature (out)	T_2 = 280 ^oC
Fluid density	ρ_{shell} = 2.3239 kg/m^3
Fluid viscosity	μ_{shell} = 0.0091 cP

Tube side information:

Flow rate	W_{tube} = 12810.6 kg/h
Pressure (in)	P_2 = 3000 kPa (30 bar)
Temperature (in)	t_1 = 300 ^oC
Temperature (out)	t_2 = 217.19 ^oC
Fluid density	ρ_{tube} = 7.127 kg/m^3
Fluid viscosity	μ_{tube} = 0.0201 cP

Log Mean Temperature Difference (LMTD): 73.6 ^oC

In this case, the fixed tube sheet type of heat exchanger and Δ20X24 TEMA Steel tube is considered.

Identify the thickness of tube:

Safety working pressure P_s = 3x1.25 3.75 MPa

Safety working fiber stress S_s = 99.5 N/mm^2 (From Table B.1)

Corrosion Allowance C = 1.3 mm

Minimum safe thickness $t_m = \frac{d_0}{2.3}\left(\frac{P_s}{S_s} + \frac{1}{30}\right) + C = \frac{20}{2.3}\left(\frac{3.75}{99.5} + \frac{1}{30}\right) + 1.3$

$$t_m = 1.918\ mm$$

Thickness of tube t_m = 2.108 mm (From Table B.2)

Tube inside diameter (d_i) = 15.784 mm (From Table B.2)

Identify the length of tube:

Tube length L_T = 2000 mm

Effective tube length L_{eff} = 2000 – 75 = 1925 mm

Identify the total number of tubes:

Number of tube pass n_{TP} = 1

Number of tubes = $\frac{318310A}{d_o L_{eff}} = \frac{318310(16.95)}{(20)(1925)} = 140.139$

Number of tubes per pass $n_{TPP} = \frac{140.139}{1} = 141$

Total number of tubes n_T = 141

Identify the shell nominal diameter:

Shell diameter (D) = 400 mm (From Table B.3)

Check the ratio between tube length and shell diameter:

L_T/D = 2000/400 = 5 (between 2.5 – 8)

Identify the baffles detail:

Type: Segmental

Percent baffles cut (P_{BC}): 25

Baffle spacing (P_B) = 1xD = 400 mm

The tube side details are:

Tube side mass velocity (G_i) = $\frac{353.68W_{tube}}{n_{TPP}d_i^2} = \frac{(353.68)(12810.6)}{(141)(15.784^2)} = 128.98\frac{kg}{m^2}.s$

Tube side velocity (V_i) = $\frac{G_i}{\rho_{tube}} = \frac{128.98}{7.127} = 18.097\ m/s$

Tube side Reynolds' number (Re_i) = $\frac{d_i G_i}{\mu_{tube}} = \frac{(15.784)(128.98)}{0.0201} = 101138.169$

Tube side friction factor (j_f) = 0.0027 (From Figure B.1)

Thus, the tube side pressure drop (ΔP_i) is:

$$\Delta P_i = 10^{-3} n_{TP} \left[8 j_f \left(\frac{L_T}{d_i}\right) + 2.5\right] \left(\frac{\rho_i V_i^2}{2}\right)$$

$$\Delta P_i = 10^{-3}(1) \left[8(0.0027) \left(\frac{2000}{15.784}\right) + 2.5\right] \left(\frac{(7.127)(18.0977^2)}{2}\right)$$

$$\Delta P_i = 6.1122\ kPa$$

$$\Delta P_i = 0.06\ bar$$

The shell side details are:

Shell side mass velocity (G_o) = $\frac{277.8W_{shell}P_T}{DiP_BC'} = \frac{(277.8)(1067.37)(24)}{(400)(400)(4)}$

$$G_0 = 11.119\ \frac{kg}{m^2}.s$$

Where:

P_T = Tube pitch = 24 mm

C' = Tube clearance = P_T - d_o = 24 – 20 = 4 mm

d_o = Tube outside diameter (mm)

Shell side equivalent diameter (d_e) = $\frac{1.10}{d_0}(P_T^2 - 0.971d_0^2)$

$$d_e = \frac{1.10}{20}[(24^2 - 0.971(20^2)] = 10.32\ mm$$

Shell side velocity (V_0) = $\frac{G_0}{\rho_{shell}} = \frac{11.119}{2.3239} = 4.785\ m/s$

Shell side Reynolds' number (Re_o) = $\frac{d_e G_o}{\mu_{shell}} = \frac{(10.32)(11.119)}{0.0091} = 12609.679$

Shell side friction factor (J_f) = 0.048 (From Figure B.2)

Thus, the shell side pressure drop (ΔP_i) is:

$$\Delta P_i = 8 \times 10^{-3} J_f (\frac{D_i}{d_e})(\frac{L_T}{P_B})(\frac{\rho_{shell} V_0^2}{2})$$

$$\Delta P_i = 8 \times 10^{-3}(0.048)(\frac{400}{10.32})(\frac{2000}{400})(\frac{2.3239 \times 4.784^2}{2})$$

$$\Delta P_i = 1.979\ kPa$$

$$\Delta P_i = 0.02\ bar$$

Table B.1 The safety working fiber stress (S_s) of exchanger tube.

Tubing material	Temperature (°C)						
	50	100	150	200	250	300	350
Carbon steel	125.2	120	115	109.8	104.5	99.5	94

Table B.2 The tube size (TEMA Standard) (Kern 1965).

Size (mm)	BWG	Thickness (mm)	Inlet diameter (mm)
20	10	3.403	13.194
	12	2.768	14.464
	14	2.108	15.784
	16	1.651	16.698
	18	1.244	17.512
	20	0.889	18.222
22	10	3.403	15.194
	12	2.768	16.464
	14	2.108	17.784
	16	1.651	18.698
	20	0.889	20.222
25	8	4.191	16.618
	10	3.403	18.194
	12	2.768	19.464
	14	2.108	20.784
	16	1.651	21.698
	18	1.244	22.512
	20	0.889	23.222
32	8	4.191	23.618
	10	3.403	25.194
	12	2.768	26.464
	14	2.108	27.784
	16	1.651	28.698
	18	1.244	29.512
	20	0.889	30.222

Table B.3 The maximum tubes contained in shell side of heat exchanger (Evans 1997).

	Shell diameter (mm.)															
	950	900	850	800	750	700	650	600	550	500	450	400	350	300	250	200
								Δ20X24								
1-F	1240	1102	974	847	721	637	532	442	361	301	239	170	127	109	62	36
2-F	1200	1068	938	822	692	602	506	420	342	282	224	160	114	98	56	32
2-U	1126	1008	882	768	648	558	460	398	304	234	180	134	94	64	34	8
4-F	1144	1004	878	766	640	550	468	386	314	252	194	140	96	86	47	26
4-U	1092	976	852	740	622	534	438	378	286	218	166	122	84	56	28	
6-F	1104	988	852	722	620	536	446	378	306	244	188	136	90	82	42	24
6-U	1058	944	826	716	596	510	416	358	272	206	156	110	74			
8-F	1072	958	826	720	594	524	434	364	290	234	178	128	86	78	36	18
8-U	1032	916	796	688	578	490	398	342	254	190	142	102	68			
								Δ20X25								
1-F	1074	970	856	745	630	559	470	384	316	262	203	151	109	92	61	37
2-F	1044	938	830	728	604	534	452	376	302	250	196	138	106	82	52	30
2-U	1000	882	772	674	566	484	406	336	270	212	158	108	72	60	26	8
4-F	1012	882	774	678	556	488	422	352	278	226	178	122	86	76	40	24
4-U	968	852	744	648	542	462	386	318	254	198	146	98	64	52	20	
6-F	986	864	760	666	538	474	394	342	272	216	172	118	82	74	36	24
6-U	940	826	720	626	518	440	366	300	238	184	134	88	56			
8-F	870	848	732	640	508	464	382	328	260	210	166	110	74	70		
8-U	908	796	692	600	498	422	350	286	226	170	122	82	52			
								Δ25X32								
1-F	674	608	538	472	397	349	294	241	199	163	131	91	68	55	32	21
2-F	664	592	522	454	376	334	282	232	188	152	118	86	66	52	32	16
2-U	610	532	466	396	340	284	234	192	154	120	84	58	42	26	8	
4-F	632	562	486	430	338	302	256	212	170	140	106	80	58	48	26	16
4-U	584	508	444	376	322	266	218	178	142	110	74	50	36	20		
6-F	614	546	470	424	334	296	252	212	164	136	104	74	54	46	24	14
6-U	562	488	426	356	304	252	206	168	130	100	68	42	30			
8-F	598	532	454	400	316	286	242	202	160	128	94	72	50	44		
8-U	540	464	404	340	290	238	190	154	118	90	58	38	24			
								□20X24								
1-F	934	845	749	657	553	481	413	341	277	224	177	137	97	81	52	32
2-F	914	824	718	640	526	460	394	324	270	220	166	124	90	76	52	26
2-U	884	778	688	586	506	436	362	304	242	188	142	100	72	52	30	12
4-F	886	780	688	600	480	432	370	308	246	204	158	116	82	68	40	20
4-U	852	748	660	560	482	414	342	286	226	174	130	90	64	44	24	
6-F	866	766	676	580	468	420	356	302	240	192	150	108	76	68	36	20
6-U	820	718	632	534	458	392	322	268	210	160	118	80	56			
8-F	838	748	648	560	456	408	346	292	234	188	142	108	70	60		
8-U	792	692	608	512	438	374	306	254	194	146	106	70	48			
								□25X32								
1-F	596	522	465	406	341	300	260	213	177	138	112	81	61	48	32	21
2-F	574	518	460	398	326	288	252	208	166	132	112	76	56	45	32	16
2-U	526	464	406	356	304	256	214	180	134	100	76	58	38	22	12	
4-F	562	488	432	380	300	278	238	192	158	128	96	68	52	40	26	14
4-U	500	440	384	336	286	238	198	166	122	90	66	50	32	16		
6-F	544	484	420	368	294	268	226	184	152	122	90	68	48	38	24	
6-U	478	420	362	316	268	224	182	152	110	80	60	42				
8-F	532	472	414	358	286	260	222	184	148	116	82	64	44	36		
8-U	456	396	344	300	254	206	170	142	98	70	50	34				

*n-X: n = number of tube pass, X = F/fixed tube sheet, U/u-bend.

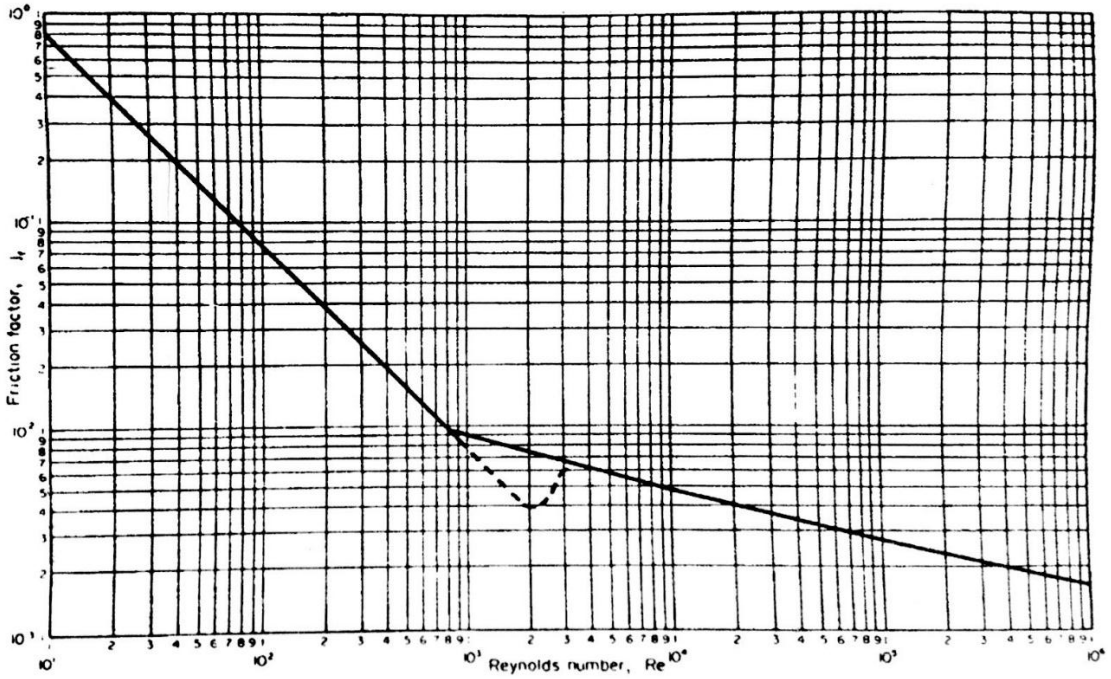

Figure B. 1 Friction factor of fluid in tube side (Ludwig 1997).

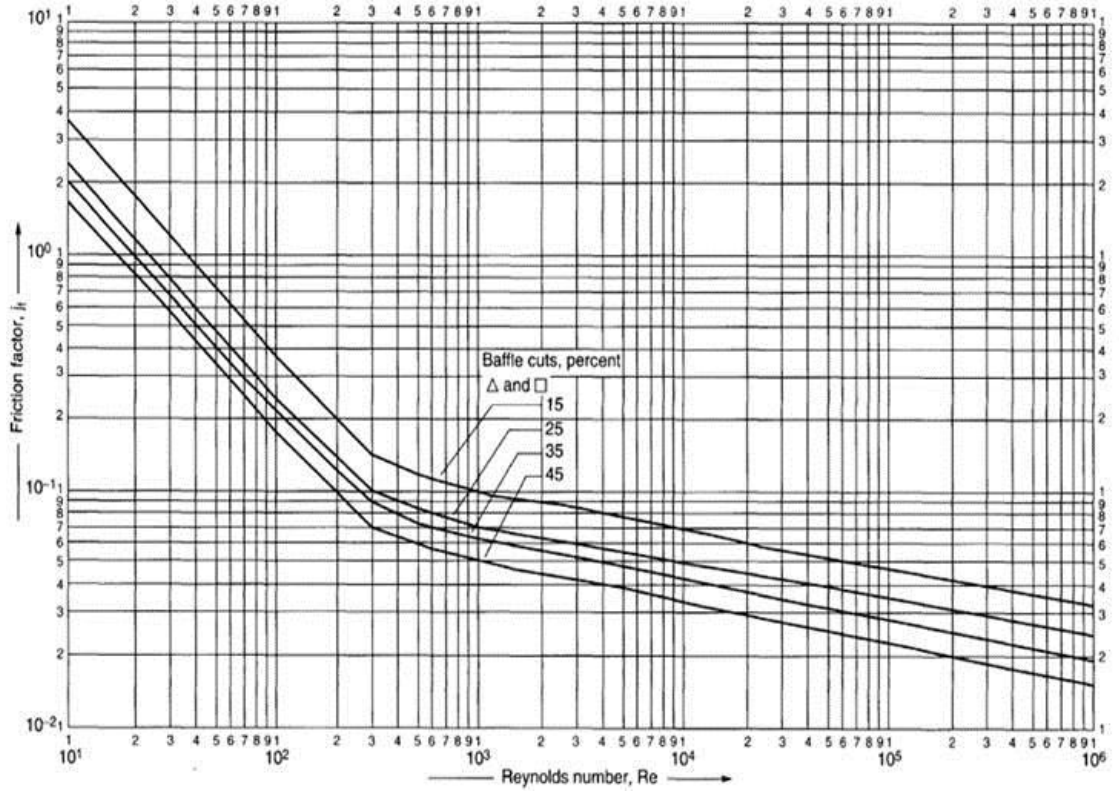

Figure B. 2 Friction factor of fluid in shell side (Ludwig 1997).

APPENDIX C

COST ESTIMATION FOR HEAT EXCHANGER NETWORK

In this part, the example of construction and operating cost for heat exchanger and utility are considered. The construction cost of heat exchangers are calculated by CAPCOST program (Turton, Bailie et al. 2009). The utilities supplement consist of Dowtherm-A and water that are circulated in the system. The natural gas is used as a fuel for thermal oil boiler.

In this case, the heat exchanger, H-101, of the energy optimization strategy 3 is considered. The Dowtherm-A is exchanged energy with palm oil feed stream (Stream no. 3). The cost estimation for heat exchanger can be calculated as follows:

1. The construction cost of heat exchanger

The data for the construction cost of the equipment, at ambient operating pressure and using carbon steel construction, C_p^0, were fitted to the following equation:

$$log_{10}C_p^0 = K_1 + K_2 log_{10}(A) + K_3[log_{10}(A)]^2 \qquad \text{(C.1)}$$

Where:

A = Heat transfer area (m^2)

K_1, K_2, K_3 = Construction cost factors (From Table C.1)

Table C.1 The construction cost factors for heat exchanger.

Exchanger Type	K_1	K_2	K_3
Double Pipe	3.3444	0.2745	-0.0472
Multiple Pipe	2.7652	0.7282	0.0783
Fixed tube, sheet, or U tube	4.3247	-0.303	0.1634
Floating Head	4.8306	-0.8509	0.3187
Bayonet	4.2768	-0.0495	0.1431
Kettle Reboiler	4.4646	-0.5277	0.3955

For H-101, the heat transfer area is 12.797 m^2 and K_1, K_2, K_3 are 4.3247, -0.303 and 0.1634, respectively.

Thus, the construction cost of the equipment on September, 2001 (CEPCI=397) is:

$$C_p^0 = \$15471.19$$

The pressure factor, F_p, for the remaining process equipment are given by the following form:

$$log_{10}F_p = C_1 + C_2 log_{10}(P) + C_3[log_{10}(P)]^2 \qquad \text{(C.2)}$$

Where:

P = Pressure (barg)

C_1, C_2, C_3 = Pressure correlations (From Table C.2)

Table C.2 The pressure factors for heat exchanger.

Exchanger Type	C_1	C_2	C_3
Double Pipe	13.1467	-12.6574	3.0705
40 barg < P < 100 barg	0.6072	-0.912	0.3327
P < 40 barg	0	0	0
Multiple Pipe	13.1467	-12.6574	3.0705
40 barg < P < 100 barg	0.6072	-0.912	0.3327
P < 40 barg	0	0	0
Fixed tube, sheet, or U tube	0.03881	-0.11272	0.08183
tubes only > 5 barg	-0.00164	-0.00627	0.0123
Floating Head	0.03881	-0.11272	0.08183
tubes only > 5 barg	-0.00164	-0.00627	0.0123

For H-101, the pressure correlations C_1, C_2, C_3 are -0.00164, -0.00627 and 0.0123, respectively.

Thus, the pressure factor is:

$$F_p = 1.0$$

The material factor, F_M, for heat exchanger is given in Figure C.1, with the appropriate identification number listed in Table C.3.

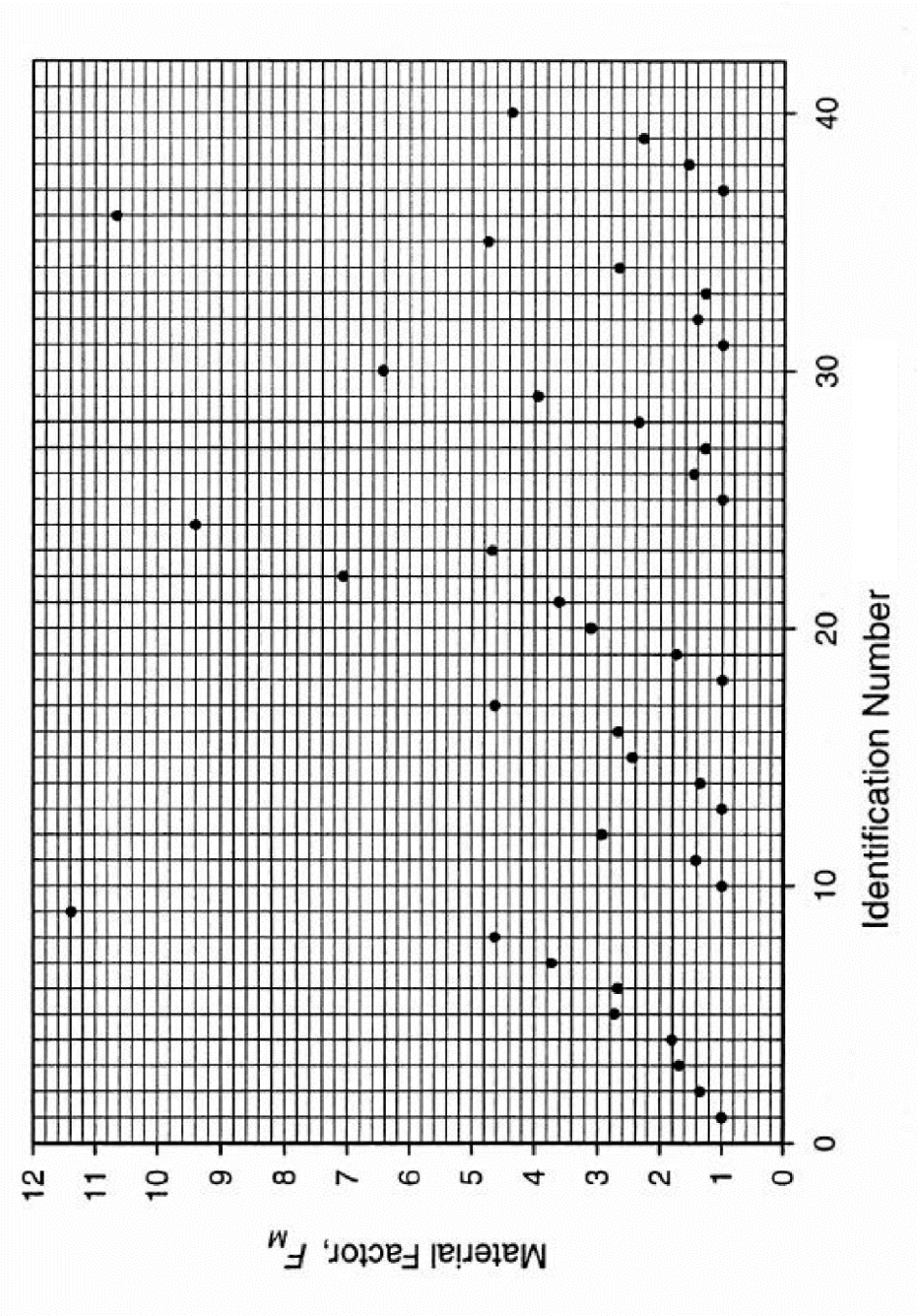

Figure C.1 The material factor for process equipment.

Table C.3 Identification numbers for material factor for heat exchanger.

Exchanger Type	Shell - CS Tube - CS	CS Cu	Cu Cu	CS SS	SS SS	CS Ni	Ni Ni	CS Ti	Ti Ti
Double Pipe	1.00	1.35	1.69	1.81	2.73	2.68	3.73	4.63	11.38
Multiple Pipe	1.00	1.35	1.69	1.81	2.73	2.68	3.73	4.63	11.38
Fixed tube sheet, or U tube	1.00	1.35	1.69	1.81	2.73	2.68	3.73	4.63	11.38
Floating Head	1.00	1.35	1.69	1.81	2.73	2.68	3.73	4.63	11.38
Bayonet	1.00	1.35	1.69	1.81	2.73	2.68	3.73	4.63	11.38
Kettle Reboiler	1.00	1.35	1.69	1.81	2.73	2.68	3.73	4.63	11.38
Scraped Wall	1.00	1.35	1.69	1.81	2.73	2.68	3.73	4.63	11.38
Spiral Tube	1.00	1.35	1.69	1.81	2.73	2.68	3.73	4.63	11.38

Thus, the material factor, F_M, is:

$$F_M = 1.0$$

The construction cost of heat exchanger, at operating pressure and using carbon steel construction, C_p^1, is:

$$C_p^1 = C_p^0 F_P F_M \quad \text{(C.3)}$$

Thus,

$$C_p^1 = \$15471.19$$

In 2015, the CEPCI is 568.7 (preliminary March, 2015). Thus, the construction cost of heat exchanger is:

$$Construction\ cost = \frac{CEPCI(2015)}{CEPCI(2001)} \times C_p^1 \quad \text{(C.4)}$$

The construction cost of heat exchanger, H-101, is around $22200.

Thus, the construction cost is 754,800 Baht (34 baht/$)

2. The utility cost of heat exchanger

2.1 Dowtherm-A supplement

From H-101, the input heat duty (Q) is:

Q = 1,453,196.305 Btu/h (425.89 kW)

A natural gas 1 m^3/h provides the energy of 35325.48 Btu/h.

In this heat exchanger, the required natural gas is 41.137 m^3/h.

The cost of natural gas is 13.7962 Baht/m^3.

Thus, the total cost of natural gas used in heat exchanger, H-101, is 568 Baht/h.

The process is operated 8,000 working hours per year.

Thus, the total cost of natural gas is 4,544,000 Baht per year.

2.2 Water supplement

The input heat duty of heat exchanger, H-301 (From energy optimization strategy 3), is:

Q = 29.2306 GJ/h (8,119.61 kW)

The cost of cooling water supplement is $0.384/GJ.

Thus, the total cost of utility requirement is $11.2245/h or 381.63 Baht/h.

The process is operated 8,000 working hours per year.

Thus, the total cost of cooling water is 3,056,000 Baht per year.

In this work, the data for cost calculation of heat exchanger network is presented in Table C.4.

Table C.4 The data for calculated cost of heat exchanger network.

	Energy optimization strategy 1			
	H-101	H-102	H-401	H-301
Heat duty (kW)	4265.80	937.16	4636.38	-12815.30
Area (m^2)	42.71	9.33	133.86	423.34
Type	Shell & Tube	Double pipe	Shell & Tube	Shell & Tube
Supplement	Dowtherm-A	Dowtherm-A	Dowtherm-A	Water
Tube side:				
Temperature (in) (°C)	81.43	82.31	280.00	97.70
Temperature (out) (°C)	300.00	300.00	300.00	50.00
Pressure (bar)	30.00	30.00	30.00	30.00
Shell side:				
Temperature (in) (°C)	350.00	350.00	350.00	30.00
Temperature (out) (°C)	310.00	312.99	312.40	39.90
Pressure (bar)	5.437	5.437	5.437	1.013

Table C.4 The data for calculated cost of heat exchanger network. (Continued)

	Energy optimization strategy 2			
	H-101	H-102	H-401	H-301
Heat duty (kW)	425.89	168.16	9912.09	-13481.40
Area (m^2)	12.80	4.31	266.89	434.89
Type	Shell & Tube	Double pipe	Shell & Tube	Shell & Tube
Supplement	Dowtherm-A	Dowtherm-A	Dowtherm-A	Water
Tube side:				
Temperature (in) (°C)	280.00	261.00	257.00	100.58
Temperature (out) (°C)	300.00	300.00	300.00	50.00
Pressure (bar)	30.00	30.00	30.00	30.00
Shell side:				
Temperature (in) (°C)	350.00	350.00	350.00	30.00
Temperature (out) (°C)	310.00	303.12	294.59	40.40
Pressure (bar)	5.437	5.437	5.437	1.013
	Energy optimization strategy 3			
	H-101	H-102	H-401	H-301
Heat duty (kW)	425.89	86.25	4622.13	-8119.61
Area (m^2)	12.80	2.25	125.21	327.72
Type	Shell & Tube	Double pipe	Shell & Tube	Shell & Tube
Supplement	Dowtherm-A	Dowtherm-A	Dowtherm-A	Water
Tube side:				
Temperature (in) (°C)	280.00	280.00	280.00	77.30
Temperature (out) (°C)	300.00	300.00	300.00	50.00
Pressure (bar)	30.00	30.00	30.00	30.00
Shell side:				
Temperature (in) (°C)	350.00	350.00	350.00	30.00
Temperature (out) (°C)	310.00	310.16	317.34	36.31
Pressure (bar)	5.437	5.437	5.437	1.013

VITA

Miss Suwisa Sae-ueng was born in May 28, 1991 in Betong, Yala, Thailand. She received the Bachelor's Degree in Chemical Engineering from Faculty of Engineering, Price of Songkla University in 2012. Afterward, she strated her Master's Degree in Chemical Engineering since October 2012.